Determination of Structure/Function Relationships of Bioactive Peptides

Reynold Giru Philip

M.Sc. Chemistry

For the degree of Doctor of Philosophy in Medical and Molecular Sciences

College of Public Health, Medical and Veterinary Sciences

James Cook University, Cairns, Australia

April 2023

Acknowledgments

First of all, I would like to acknowledge the Almighty God (Anutu) that I worship for making it possible for my PhD journey. Pursuing a PhD degree at James Cook University located at Cairns in the tropics is the best option for research in tropical diseases. My dream came through when awarded the Australia Awards Scholarships and I would like to thank the Australian Government through the Australian Department of Foreign Affairs and Trade (DFAT) for making my endeavour possible. My deepest gratitude also to my University and the College of Public Health and Veterinary Science for allowing me to undertake a PhD in Medicinal and Biological Science.

I would like to continue by expressing my immense gratitude to my primary supervisor Professor Norelle Daly who accepted me to do PhD under her mentorship and guided me with all her knowledge in sciences. I have known Professor Norelle at UQ since 2008 as a mentor in characterization of cyclotides from PNG plants and it is a great feeling doing a PhD in the Daly Group. This PhD work was made possible with her and I am extremely grateful for all her tireless support as a group leader.

I also would like to thank my secondary supervisor Professor Alex Loukas for his open door policy when I needed scientific advice/help for my vaccine project. His wealth of knowledge in immunological science, suggestions and organizational skills have helped me greatly. Thank you also to my co-supervisor Dr. David Wilson, who was always there when I needed help to run HPLC or Mass spectrometry (LCMS, MALDI-TOF) and every time when this two equipment are down, he is the group's key person to fix them that makes life stress free. I am also extremely grateful to Dr. Paramjit Bansal and Dr. Gaungzu Zhao who taught me peptide synthesis at different stages of my research.

I would like to thank the following people who were very helpful in the bioassays. Dr. Roland Ruscher, Kim Miles and Dr. Guangzu Zhao for assisting in cell assays on different cytokines and the statistical analysis. Dr. Paul Giacomin for providing relevant ethics for human blood collection and Dr. Yide Wong for fresh blood collection. In addition, I am grateful to Associate Professor Severine Navarro and Dr. Yan Lu at QIMR for carrying out allergic asthma assay using HDM model, cell analyses and statistics analysis of the results. This significantly added value to my research data in addition to the cytokine results.

I would like to thank Dr. Phurpa Wangchuk for sharing of light moments about small molecules and the interests of bridging with PNG plants, and Mr Karma Yesi for his assistance and friendship. My gratitude also to the following people in the Loukas Group who helped me with the human hookworm vaccine project. I would like to thank Dr. Bemnet Tedla for recombinant expression and isolation of protein, Mr. Luke Becker for helping with mice work and Darren Pickering for assisting in protein refolding assay. My special thank you to Dr. Vignesh Rathinasamy from Cooke's Group for the kind donations of specific reagents required for vaccine project and showing me how to purify antibodies. All your inputs and efforts have significantly helped me understand immunology.

I am extremely happy to be part of Daly's group, and although the group is small, we have the perfect combination of minds. My thank you to Dr. Rozita Takjoo Chelaras for the friendship and donations of kids toys to my little kid. To my other colleagues in Daly's Group, Mrs. Antin Widi, Mrs. Yoshimi Peck and Mr. Tiziano Raffaelli, your support and encouragement was invaluable. Special thank you the Daly's Group for the food vouchers and support in time of my need. In addition, I would like to thank the JCU International Student Support Service, Mr. Alex Salvador (Townsville) and Christine Martyn (Cairns) for the support in vouchers and food supplies during the Covid-19 pandemic. To Professor Norelle Daly and Dr. David Wilson, thank you for your sincere heartfelt donation of food during covid-19. Also,

I like to thank the following humanitarian organisations, Vinnies and Marlin Coast Neighbourhood Centre for food and fuel vouchers during the pandemic.

My deepest gratitude to the past and current administrative staff of AITHM for your assistance in my research studies. Mrs. Lynne Saunders for your help. I also would like to thank Mr. Phill Walsh for engaging me as a research assistant for a year and the technical staff Mr. Atik Susianto and Mr. Bjorn Hauge who helped me learn a lot while being employed as casual staff. You are the heart of AITHM. I also extend my thank you to Professor Norelle Daly and Alex Loukas of ParagenBio for a short engagement as research assistant in synthesising and characterisation of peptides.

Thank you very much for the help and opportunities from my College of Public Health, Medical and Veterinary Sciences. A special thank you to: Ms. Tina Cornell, A/Prof Kerrianne Watt, Mrs. Kerry Knight, A/Prof Zhaming Liang and Prof. Ted Whitten. Finally, I thank my family who accompanied me during my PhD journey, especially my spouse (Naomi) and four children (Elijah, Hadassah, Judy and Samuel) who stood by me with great patience. Special thanks to Mr. Peter Lambourne for his kind helping heart in many things and has become part of my family while in Cairns. To my late Mum (Perehulo Gosuve Philip), who inspired me so much to reach education at PhD level. I love you mum. Although you have passed on, I will always treasure your wisdom and pass it on to my children. To my dad (Philip Rupuve Ijaho), I only have you and will be here for you. To my siblings, thank you for representing me in the village in my absences. I like to thank all the Konos' Ijahos' and Giru families for your steadfast prayers. All glory belongs to Almighty God.

This thesis is dedicated to my late Mum, Dad and my beautiful family…

"*I can do all things through Christ Jesus who strengthens me*"-

1 Corinthians 2:28 (The Holy Bible)

Statement of the Contribution of Others

During my PhD candidature my thesis work has included:

1) Synthesis of the peptides (synthesis, purification, mass analysis, oxidation)

2) Structural analysis of peptides using NMR spectroscopy

3) Biological assays (cell assay, mouse assays, tissue collection, antioxidant assay, immunological assays, allergic asthma assay).

4) Thesis write up. I have had great support from the AITHM team, an Australia Awards scholarship, internal scholarship and writing grants. I have attached a list outlining the contributions from others in the following table.

Nature of Assistance	Contribution	Name and Affiliations
Intellectual Support	Project Plan and Development	1) Prof Norelle Daly, AITHM 2) Prof Alex Loukas, AITHM
	Data Analysis	Prof. Norelle Daly, AITHM Prof. Alex Loukas, AITHM Dr. David Wilson, AITHM Dr. Roland Rusher, AITHM Dr. Guangzu Zhao, AITHM A/Prof Severine Navarro, QIMR Dr. Yan Lu, QIMR
	Editorial Support	Prof Norelle Daly Prof. Alex Loukas Dr. David Wilson A/Prof Severine Navarro
Financial Support	Research Costs	1) Australian Research Council and National Health and Medical Research Council via a Future Fellowship (110100226)

		2) Fellowship (1117504)
	Stipend	Australia Awards Scholarship (AAS) James Cook University
	Conference Assistance	Student Research funds
	Write-Up Grants	Doctoral Completion Grant, College of Public Health, Medical and Veterinary Science, James Cook University
Data Collection	Research Assistance	Dr. David Wilson (mass spectrometry) Dr. Paramjit Bansal (peptide synthesis) Dr. Guangzu Zhao (ELISA)
	Cell assays	Dr. Roland Ruscher Kim Miles Dr. Guangzu Zhao
	Allergic Asthma House Dust Mice (HDM) assay	Dr. Yan Lui A/Prof Severine Navarro

	Vaccine Antibody generation and Protein Expression	Luke Becker Dr. Bemnet Tedla Dr. Guangzu Zhao Darren Pickering
Technical **Support**	Peptide Synthesis	Dr. Paramjit Bansal
	Fresh Blood collection	Dr. Yide Wong
	HDM sample collections	Dr. Yan Lui, QIMR
	Mice bleeding and sample collection	Luke Becker

Unpublished Works by The Author Incorporated Into The Thesis

Chapter 2 and Chapter 3 contain unpublished data, that will be submitted for publication following IP protection.

Chapter 2. Immunomodulatory Activity of a Lunasin Fragment.

Author contributions: RP, AL and NLD designed the study and wrote the paper. RP and PSB synthesized and purified the peptides. RP and DW carried out the mass spectrometry analyses. RP and NLD determined the structure of the peptide. RP, KY and PW did the antioxidant assay. KM, GZ and RR carried out the cell assays. SN and YL assisted in the animal experiments. All authors analysed the results and approved the final version of the manuscript.

Chapter 3. Characterisation of an anti-inflammatory motif based on the soybean protein lunasin.

Author contributions: RP, AL and NLD designed the study and wrote the paper. RP and PSB synthesized and purified the peptides. RP and DW carried out the mass spectrometry analyses. RP and NLD determined the structure of the peptide. KM, GZ and RR carried out cell assays. SN and YL conducted the animal experiments and histological evaluation. All authors analysed the results and approved the final version of the manuscript

Chapter4. Effects of cyclization on an anti-inflammatory peptide

Author contributions: RP, AL and NLD designed the study and wrote the paper. RP, GZ and PSB synthesized and purified the peptides. RP and DW carried out the mass spectrometry analyses. RP and NLD determined the structure of the peptide. KM and RR carried out different cell assay.

Chapter 5. Characterization of an *Na*-APR-2 derived peptide as a vaccine target

Author contributions: RP, AL and NLD designed the study and wrote the paper. RP, GZ and PSB synthesized and purified the peptides. RP and DW carried out the mass spectrometry analyses. RP and NLD determined the structure of the peptide. RP and LB carried out animal experiment. RP and GZ screened antibodies using ELISA. RP and BT did protein recombinant expression and purification. RP and DP carried out protein refolding and cleavage assay.

Abstract

The focus of this thesis was on peptides with anti-inflammatory activity, and exploring their potential as drug leads against autoimmune and chronic inflammatory diseases. Such diseases, which include inflammatory bowel disease (IBD), and allergic asthma, have impacted the health and economics of countries globally. To date, there is no cure for IBD and other systematic autoimmune induced inflammatory diseases. Peptides have potential in the development of new therapeutics due to properties such as high potency and specificity, low immunogenicity and being cheaper to manufacture compared to protein-based drugs/biologics.

The peptides studied in this thesis were generally small, unconstrained with disordered structures. Interest in intrinsically disordered peptides has increased recently and Chapter 2 of this thesis describes an intrinsically disordered region of a soybean peptide, lunasin. Cytokine and allergic asthma assays demonstrated anti-inflammatory properties indicating that this region could be a possible lead molecule in drug design.

In addition, Chapter 3 characterized another region of the lunasin peptide which was found to have a conserved motif (E/DXXXXXEK) to that present in hookworm derived peptides recently described by Cobos et al, 2022. *In vitro* and *in vivo* assays indicated the presence of anti-inflammatory activity. Interestingly the peptide inhibits neutrophil cell production in an allergic asthma assays, which indicates a potential histone interaction and potential as a lead molecule for chronic asthma peptide drug development.

Following on from the link identified in Chapter 3 between lunasin and hookworm derived peptides, Chapter 4 explores anti-inflammatory peptides (AIPs) in Excretory/Secretory (ES) products of hookworm parasites. Cobos et al, 2022, identified peptides, including ES2-10, that

alleviated colitis symptoms in a mouse model but the peptides lacked stability in serum. Chapter 4 describes engineered analogues of ES2-10 with enhanced stability achieved through head-tail disulfide cyclisation and extension of the peptide. Cyclisation was effective in improving the stability but the native conformation of ES2-10 was altered and it appears that this correlates with a decrease in bioactivity. However, the extended version of ES2-10 formed a stable helical structure in solution with serum stability and looks promising as a drug lead.

In addition to the AIPs found in ES products of hookworm parasites, this work also explores a potential antigen against human hookworm infection. Hookworm infection is a neglected tropical disease that causes devastating morbidity and mortality in developing countries, yet there are no vaccines against these complex multicellular pathogens. Chapter 5 describes a potential antigen ($G_{350}Y$) downsized from the *Na*-APR2 protein from the hookworm *Necator americanus*. Antibodies were generated through intraperitoneal injection but not in orally administered mice, most likely due to the unstable peptide structure. The recombinant *Na*-APR-2 displayed no neutralization activity with antibodies indicating that a different recombinant protein expression system is required to produce active recombinant protein which can subsequently be used to further explore the potential of the $G_{350}Y$ peptide as a vaccine candidate.

Overall, the studies in this thesis highlight soybean derived peptides with potential in the development of allergic asthma, a conserved sequence motif associated with anti-inflammatory activity and insight into future studies aimed at developing a hookworm vaccine.

Table of Contents

CHAPTER 1: Introduction

1.1. Protein and Peptide Therapeutics

Proteins and peptides have been a valuable resource for the development of therapeutics (1, 2). More than 200 pharmaceutical protein products have been marketed since the early 1980s (3). The first protein therapeutic was initially discovered in 1889 by two German scientists – Oskar Minkoski and Joesph vab Mering from their animal experimental work, where they described a substance responsible for metabolic control secreted by the pancreas (4). Further study led to this substance being referred to as "insuline" by a Belgian investigator (de Meye) and British researcher (Schaefer) in 1909 and 1916 respectively (5). In 1921, insulin was successfully administered to a human as a therapeutic for diabetes (4). Using DNA recombinant technology, human insulin was developed to a product called Humulin® as the first protein therapeutic (6). Humulin® has been further re-engineered to produce various analogues of insulin that last longer and better mimic properties of endogenous insulin (7).

Since the early studies on insulin, protein engineering through rational design and molecular evolution has dramatically improved the understanding of structure/function relationships of proteins and subsequent drug development efforts (8).The field of protein therapeutics has also been advanced through approaches such as glycoengineering, Fc fusion (3) or polyethylene glycol conjugation (9, 10) and antibody based drugs (11). In particular, antibody-based drugs are the largest and fastest growing class of protein therapeutics (11). More than 24 antibody-based drugs have been marketed (11) with over 240 in clinical development (12). Despite the advances in protein therapeutics, there are still issues surrounding efficacy, safety, immunogenicity and effective delivery platforms.

Although occupying a smaller niche than protein-based therapeutics, peptide-based drugs are experiencing renewed interest. Peptides occupy the chemical space between the two major therapeutics - small molecules and biologics (13). Early studies involved the development of the drug cyclosporine, a 12 amino acid, natural cyclic peptide, which is currently used as an immunosuppressant during organ transplant, and was originally isolated from a fungus (14). From 2012-2016, more than 60 peptide-drugs were approved by the FDA, and the majority of approved peptide drugs have ten residues or less (15, 16). The number of approved peptide-drugs increased to more than 100 in 2020 (17), with more than 170 peptides in clinical development and preclinical studies (18, 19). Peptides also have potential in the development of vaccines, such as GV100 (Riavaxtm, Tertomotide) which is currently authorised for use in Korea for pancreatic cancer, and is undergoing clinical trials in other countries to gain approval for use (20). This peptide vaccine is derived from human enzyme telomerase reverse transcriptase (TERT), and contains 16 residues that can directly activate the immune cells (21). TERT is highly expressed in a range of cancer cells, making GV100 of interest in other types of cancer (22). Overall, the increasing interest in peptides has been attributed to their molecular properties such as high binding affinity to specific sites, selectivity, low toxicity effects and permeability across tissues unlike the major therapeutics (15).

Several approaches are being used in the development of new peptide and protein-based treatments. In particular, plants and animals are valuable sources of novel peptides and proteins with diverse biological activities and potential therapeutic applications (23, 24, 25). These biological activities include hormone signalling, communication and host defence (26, 27). In addition, a range of naturally occurring proteins and peptides have been shown to have anticancer (28), anti-inflammatory (29, 30, 31), anti-HIV (32), anti-microbial (33), anti-fungal and insecticidal activities (34) among others. This thesis explores the potential of peptides

derived from soybean and helminth proteins in the development of novel therapies or vaccines. The key theme of the thesis was exploring the therapeutic potential of small bioactive regions within peptides/proteins. This "downsizing" approach was primarily used to identify bioactive-regions with potential as anti-inflammatory agents but was also applied to the development of an epitope from an aspartic protease (*Na*-APR-2) identified in human hookworm as a potential vaccine candidate against human hookworm (*Necator americanus*).

An overview of the disease states and proteins of interest for this thesis is given in section 1.2.

1.2. Inflammatory diseases – development of therapeutics

Inflammatory diseases have become a major health concern in developed, and many developing, countries. In particular, autoimmune conditions/diseases such as inflammatory bowel disease (IBD) - Crohn's diseases (CD) and Ulcerative colitis (UC), have a significant burden on health systems and affect quality of life resulting in reduction of work ability, social stigma and restriction in career choices (35). Multiple factors have been linked to the origin of IBD including genetic, environmental, hormonal, and immunological factors (36). However, the exact pathogenesis mechanism that triggers IBD still remains unknown and there is currently no cure. Current therapies for IBD rely on antibiotics, steroids, and the use of immunomodulators targeting the TNF pathway or the gut-homing integrin α4β7 to relieve inflammation (37, 38). Recently, monoclonal antibodies were used to target the subunit receptors of IL-12/IL-23 pathway inducing anti-inflammatory effects in the intestine (39). For instance, Ustekinumab was approved for treating UC and CD (40), while others such as Mirikizumab (41), Risankizumab (42), Brazikumab, and Guselkumab (43) are in clinical trials. In addition, small molecules also displayed inhibitory effects in Janus kinase (JAK) - a family of pro-inflammatory enzymes that activate multiple immune pathways instead of a single cytokine or receptor (44). A small molecule drug, facitinib has been approved as JAK inhibitor but effective only in UC while some small molecules are still in clinical trials as JAK inhibitors (45). Despite new promising therapeutics, IBD relapse becomes inevitable (46) and surgery is often required as the last option. There are emerging novel therapy such as apheresis therapy(47), improved intestinal microecology (48), cell therapy (49), and exosome therapy (50), but requires more studies to provide insights into new treatment options for IBD.

It is estimated that over 100,000 Australians are living with IBD based on the 2021 annual report sponsored by Crohns and Colitis Australia (51). Based on findings released in 2013 by PricewaterhouseCoopers, the costs associated with IBD in Australia were estimated to be $100 million for the major hospitals and $380 million in productivity losses in addition to the annual $2.7 billion financial and economic costs associated with management of IBD (52). Similarly, IBD has been estimated to cost $2.8 billion ($12,000 per IBD patient) per year in Canada (35). A study in selected developing countries showed lower prevalence of IBD compared to developed countries, but it was observed that when a society transits to a developed status, there is higher IBD prevalence (53). These are indications that IBD prevalence is evolving at a faster rate in the developed nations and gradually developing nations will be impacted by this burden in their health systems.

Allergic asthma is another serious inflammatory condition that creates a burden to health systems and has significant social costs. According to the Australian Bureau of Statistics using the National Health Survey data, 2.7 million people had asthma in 2020-2021 (54) and in 2015 the estimated yearly cost of treating asthma in Australia was $28 billion. Allergic asthma is caused by inappropriate responses to inhaled allergens that is often characterized by eosinophilic airway inflammation, mucus hypersecretion and airways hyperresponsiveness (55). Specifically, allergen-specific IgE, Th1/Th2-mediated cytokines, interleukins (IL-4, IL-5, IL-13, IL-8), TNF and various chemokines are over expressed in the airway structural cells (56). The mechanism that links airway structural cells and the induced inflammatory responses still remains unclear. Asthma associated with increased neutrophils is also emerging as a particular type of asthma (57) .

The current treatments available for inflammatory diseases generally only provide temporary relief, and the need for new drugs is great due to repetitive occurance of acute inflammation after treatment, that can lead to serious side effects (37, 38). With the on-going search for new drugs, exploiting natural sources for anti-inflammatory drug candidates is a promising approach. This thesis focuses on two sources of drug leads for treating inflammatory diseases based on proteins from parasitic worms and soybeans. Although they might seem like quite divergent sources, a conserved sequence motif in the peptides/proteins found in hookworms and the soybean protein lunasin was identified in this thesis. To place this work into context, an introduction to soybean proteins and hookworms is given in sections 1.2.1 and 1.2.2 respectively.

1.2.1. Soybean proteins and peptides

Soybean (*Glycine max*) is a legume with wide a range of applications in agriculture, and the food industry, but also has significant health benefits (58). In 2020, soybean was the 42nd most traded product with a net trade of 64 billion USD (59). Soybean is used in infant formulas, flours, protein concentrates and isolates, and textured fibres in addition to other different soybean derived products such as cheese, soybean milk, dairy substitutes, miso, soy sauce, tofu, tofu skin, tempeh, vegan salami, and meat substitutes (58). Many new soybeans products are also being developed (60, 61) and their demand is increasing due to their documented beneficial effects on nutrition and health (62).

Soybean is generally composed of 30-40% protein, 30% carbohydrate, 20% lipids and 10% dietary fibre (63, 64). The protein component comprises two major storage proteins namely,

11S globulin (also known as glycinin) and 7S globulin (also known as β-conglycinin) (65, 66). Other minor proteins include 2S-albumin, lectin, Kunitz and Bowman–Birk protease inhibitors (BBI), β-amylase, lipoxygenase, oleosin, basic 7S protein, and urease (62, 67, 68, 69, 70, 71). Several soybean proteins are converted to peptides by various processes through human digestion, enzymatic hydrolysis, food processing or fermentation (72, 73, 74, 75). The bioactive peptides from soybean have been reported to have several activities including hypocholesterolemic, anti-diabetic, hypotensive, phagocytosis and immunstimulation, anti-inflammatory, chemopreventive, and antioxidative properties (72, 75, 76).

Among the compounds found in soybean, lunasin has been identified as a unique bioactive soy peptide. Lunasin belongs to the 2S-albumin family, has 43 residues and contains three different domains/regions with different activities/functions. Several studies have demonstrated that lunasin has effects against cancer (77, 78), cardiovascular (79), and anti-inflammatory diseases (80, 81). The effects of lunasin observed in different *in vivo* and *in vitro* models of cancer cell studies demonstrated inhibition of cancer cell cycle and anti-mitotic process that leads to apoptosis (82, 83, 84, 85). However, the structure/function relationships of lunasin with respect to the suppression of pro-inflammatory cytokines induced by cancer forming cells is unclear.

Another interesting property of lunasin is its intrinsically disordered nature. Attempts to solve the 3-D structure of lunasin have been unsuccessful due to its highly intrinsically disordered nature (86). The intrinsically disordered character of lunasin has been attributed to its high composition of hydrophilic residues, creating a dynamic equilibrium that causes the peptide to remain unstructured but upon binding to a biological target it could potentially become structured. Although intrinsically disordered proteins (IDPs) are less preferred over

conventional proteins and peptides in therapeutic development due to the disordered character and non-conserved sequences, the potential of harnessing IDPs as anticancer therapeutics has increased over the last decade (87). This was made possible with improved scientific technologies such as NMR spectroscopy analysis and various computational biology tools that enabled studies into the complexity of IDPs' nature (87).

One of the main aims of my thesis was to provide insight into the bioactive regions of lunasin. Interestingly, one of the bioactive regions studied as part of this thesis has a similar sequence to a conserved region in the anti-inflammatory proteins (AIPs) from hookworms, which have been shown to alleviate systems in colitis (88). It appears that this conserved sequence is not restricted to parasite proteins but could be a key motif in anti-inflammatory proteins.

1.2.2. Hookworm proteins as drug leads

Proteins derived from parasitic worms have attracted interest in the development of novel drug leads. In particular, hookworm-derived proteins have potential in treating immune related diseases despite the negative impacts of hookworm infections. Hookworm infections affect almost 500 million people worldwide, predominantly in the tropical regions of South America, Africa and Asia (89). Most of these infections are caused by *Necator americanus*, *Ancylostoma ceylancium* and *A. duodenale* species (90), and can result in growth retardation, psychological impairment and iron deficiency anaemia, which is a clinical hallmark of hookworm infection (91, 92). Treatment with anti-helminth drugs does not stop reinfection occurring.

Although deworming activity in developed nations has eradicated human hookworm infections, this action correlates with increased autoimmune diseases/conditions such as IBD, asthma and other life-style related inflammatory diseases compared to hookworm infested developing countries (93, 94, 95). Several studies have shown the co-existence of hookworm in humans has reduced autoimmune diseases (93, 95). This implies that worms are producing molecules to protect themselves but are also beneficial to humans by developing a parasite-human relationship.

Analysis of secretomes produced at different life stages of the hookworm have provided insights into harnessing bioactive molecules produced by hookworms as drug leads as well as vaccine development. Hookworms secrete Excretory/Secretory (ES) products that contains a cocktail of proteins among other molecules such as lipids, carbohydrates and secondary metabolites to sustain their existence in their hosts. A study showed that hookworms secrete deoxyribonuclease (Nb-DNase II) to degrade the DNA backbone of neutrophils to evade the host immune response (96). Analysis of the secretomes also showed the presence of anti-inflammatory proteins (AIPs) such as *Ac*-AIP-1 and *Ac*-AIP-2 derived from *Ancylostoma caninum* hookworm responsible for anti-inflammatory activity in colitis (30, 97) and asthma respectively (31).

1.2.3. Vaccine development using hookworm proteins

Despite the potential of hookworm derived proteins as drug leads there is still a clear need to develop methods for treating hookworm infections. Infections with human hookworm cause devastating morbidity and mortality in developing countries. More than a half a billion people have been affected in developing tropical countries (98). The hookworm parasites primarily feed on intestinal blood and establish chronic infections that can last for decades. Heavy intensity infections can led to iron-deficiency anaemia, which drastically affects intellectual development and weakens the neurological functions in children, can reduce productivity in adults and have a significant impact during pregnancy (99, 100). Although, application of chemotherapy have treated adult parasites with benzimidazoles drugs such as albendazoles, reinfection occurs rapidly after treatment (101, 102). The only approach for effectively controlling hookworm infection is to develop a vaccine for inducing immunological resistance to hookworm infections.

Several vaccine antigens have been identified in different developmental stages of mammalian hookworms (103, 104). Among them is *Na*-APR-1 (105), a 45 kDa cathepsin-D-like aspartic protease found in the gut of adult *N. americanus* and is responsible for initiating the haemoglobin digestive cascade (106). Inhibiting *Na*-APR-1 proteolytic activity kills the parasites by preventing it from obtaining nutrients but there is no indication that it causes initiation of a different pathway. Studies have been shown that antibodies generated from the recombinant form of *Na*-APR-1 inhibit the ability of the hookworm parasite to digest haemoglobin and confers protection in canine and hamster models of human hookworm

infection (107, 108). For example, recombinant *Na*-APR-1 used in vaccination trials in dogs effectively reduced the adult parasite loads and blood loss compared to unchallenged dogs (control) (105, 107). However, expressing this protein on a large scale has been challenging (109) as low yields have been obtained following purification, which is likely to limit its potential as a subunit vaccine.

Elucidating the epitopes involved in the protective antibody response might provide an alternative source of vaccine candidates, and this approach has been applied to *Na*-APR-1. Using a series of overlapping fragments from *Na*-APR-1, Pearson and co-workers (110) mapped an epitope region which corresponds to residues 291 to 303 in *Na*-APR-1. This peptide was termed $A_{291}Y$, and is the target of monoclonal antibodies that neutralise the proteolytic activity of *Na*-APR-1, consequently inhibiting its ability to cleave synthetic and natural substrates (110).

$A_{291}Y$ requires adjuvants to induce an antibody response, but Skwarczynski *et al*., 2012 (109), introduced a self-adjuvating lipid core (LCP) system that effectively triggered a strong immune response when incorporated with the $A_{291}Y$ peptide. Upon vaccination of mice, the new chimeric LCP construct induced effective production of antibodies that inhibit the proteolytic activity of *Na*-APR-1. The LCP system has also been used in a recent study involving three chimeric peptides (p1, p2 and p3) derived from the $A_{291}Y$ epitope. A β sheet peptide conjugated to LCP was developed that demonstrated the potential of inducing antibodies that blocked the enzymatic activity of the native hookworm protease (111, 112). These studies show that the LCP system has potential for subunit vaccine development and can drive protective antibody responses (113, 114).

Given that helminths have several developmental stages expressing unique antigens, it is of interest to explore epitopes from a range of antigens. *Na*-APR-2 is a pepsin-like aspartic protease from *N. americanus* that is distinct from *Na*-APR-1 and is primarily expressed in the L3 stage of development in contrast to *Na*-APR-1 which is more abundant in the adult stage (115). The sequences of *Na*-APR-1 and *Na*-APR-2 have only 30% sequence identity and distinct activities (115). *Na*-APR-1 can neutralise haemoglobin proteolysis at an optimum pH of 5.5. It is regarded as an upstream protease because it can cleave and expose other sites to cascading proteolysis by other proteases such as cystine proteases, metalloproteases or aspartic proteases (106, 115). However, recombinant *Na*-APR-2 is capable of digesting complete haemoglobin *in vitro* and is most active at a much lower pH, and cleaves at multiple distinct sites compared to *Na*-APR-1 (115). This means *Na*-APR-2 is not upstream of *Na*-APR-1 but operate independently (115). Therefore, it is of interest to explore epitopes from *Na*-APR-2 as potential vaccine candidates.

1.3. Scope of thesis

Identification of bioactive regions within peptides and proteins can provide fundamental information useful in the development of therapeutics and vaccines. A primary reason for this is that small synthetic peptides can be ideally suited to mimic protein-protein interactions, which play a major role in numerous biological processes (116). A range of techniques and approaches have been used to identify bioactive sequences within proteins and peptides, including analysis of sequence conservation and structure-based design. The latter approach is based on the importance that three-dimensional structures of proteins and peptides often play in biological functions. However, intrinsically disordered proteins and peptides can still be biologically active (117, 118). This thesis describes studies that have used a combination of sequence conservation and structure-based design in the characterisation of the clinical potential of proteins of peptide/protein fragments. These studies are inclusive of disordered and well-structured regions of proteins.

Chapter 2 reports on an intrinsically disordered N-terminal region of the soybean peptide lunasin. Although a range of bioactivities had been attributed to the C-terminal regions of lunasin, the role of the N-terminal has not been well studied. However, it had been suggested that the N-terminal might have redox properties based on the presence of free cysteine residues (86). Based on this suggestion, and the link between antioxidation activity and inflammation (119), we hypothesized that the anti-inflammatory effects might be related to the N-terminal region of lunasin. To explore this hypothesis, we tested the effects of the peptide on inflammatory cytokine levels in cell assays, the effect of the peptide in a HDM assay for

allergic asthma in mice, and the effect of the peptide in an *in vitro* antioxidant assay (DPPH). Overall, the peptide appears to show anti-inflammatory effects. This chapter contains unpublished data, written in a paper format ready for submission.

Chapter 3 continues on from the initial studies on lunasin in Chapter 2, through the analysis of a sequence motif in lunasin with similarity to chromatin binding proteins. Homology searches revealed this motif has similarity to a bioactive region within hookworm anti-inflammatory proteins (88). The anti-inflammatory activities were analysed using cytokine assays in PBMCs and macrophages M1-cells. Cytokines were reduced in some and not in other donors, indicating that the peptide effects could be donor specific. Although there was variation in the assays results, cytokine reduction observed in some donors is an indication the peptide has anti-inflammatory activity. Analysis of the effects of the peptide in an *in vivo* allergic asthma mouse model did not show any effect in eosinophil cell reduction, but showed significant reduction of neutrophils, indicating the disease effects were decreased consistent with anti-inflammatory activity. This chapter contains unpublished data, written in a paper format ready for submission.

Chapter 4 explores the stabilization of the bioactive motif identified in Chapter 3 and in the previous hookworm protein studies. The peptide chosen for study is referred to as ES2-10, and is derived from the hookworm *Aes*ES2 protein (120). Although ES2-10 has anti-inflammatory activity in an *in vivo* assay (TNB colitis) and pro-inflammatory cytokine assay, it degraded in human plasma in less than 4 hours. The main objective was to determine if cyclization via disulfide bonds, or helical extension stabilized the ES2-10 peptide and enhanced its potential as a therapeutic agent. Both approaches significantly improved the stability of the peptide, but

at the expense of bioactivity shown based on *in vitro* cytokine assays. This chapter contains unpublished data.

Parasite-derived compounds can be useful in the treatment of disease as outlined in Chapter 4, however, they might also have potential in alleviating the detrimental effects of parasite infection. The final experimental chapter of my thesis addresses this alternative perspective. In search of potential vaccine antigens from hookworm parasite proteins, Chapter 5 describes an epitope ($G_{350}Y$) derived from aspartic protease – (*Na*-APR-2) as a potential antigen against human hookworm. The aim was to identify an epitope that could induce antibodies against hookworm infection. An epitope ($G_{350}Y$) was designed based on previous studies on an epitope from the aspartic protease - *Na*-APR-1 (110). This chapter also involved the expression of *Na*-APR-2 to allow testing of the bioactivity of the epitope. Promising results were obtained in terms of antibody production, but further study is required to produce a bioactive version of *Na*-APR-2. This chapter contains some unpublished data and requires additional data for publication in the future.

1.4. References

1. Mathur S, Hoskins C. Drug development: Lessons from nature. Biomedical reports. 2017;6(6):612-4.

2. Phillipson JD. Human medicinal agents from plants, edited by AD Kinghorn and MF Balandrin, American Chemical Society, Washington, DC, 1993 No. of pages: 356, price US $89.95. ISBN 0-8412-2705-5. Wiley Online Library; 1994.

3. Walsh G. Biopharmaceutical benchmarks 2010. Nat Biotechno. 2010;28(9):917-24.

4. Bliss M. The history of insulin. Diabetes care. 1993;16(Supplement_3):4-7.

5. Wilcox G. Insulin and insulin resistance. Clinical biochemist reviews. 2005;26(2):19.

6. Goeddel DV, Kleid DG, Bolivar F, Heyneker HL, Yansura DG, Crea R, et al. Expression in Escherichia coli of chemically synthesized genes for human insulin. Proceedings of the National Academy of Sciences. 1979;76(1):106-10.

7. Vigneri R, Squatrito S, Sciacca L. Insulin and its analogs: actions via insulin and IGF receptors. Acta diabetologica. 2010;47(4):271-8.

8. Carter PJ. Introduction to current and future protein therapeutics: a protein engineering perspective. Experimental cell research. 2011;317(9):1261-9.

9. Jevševar S, Kunstelj M, Porekar VG. PEGylation of therapeutic proteins. Biotechnology Journal: Healthcare Nutrition Technology. 2010;5(1):113-28.

10. Veronese FM, Mero A. The impact of PEGylation on biological therapies. BioDrugs. 2008;22(5):315-29.

11. Reichert JM, editor Metrics for antibody therapeutics development. MAbs; 2010: Taylor & Francis.

12. Reichert JM, editor Antibodies to watch in 2010. MAbs; 2010: Taylor & Francis.

13. Northfield SE, Wang CK, Schroeder CI, Durek T, Kan M-W, Swedberg JE, et al. Disulfide-rich macrocyclic peptides as templates in drug design. European Journal of Medicinal Chemistry. 2014;77:248-57.

14. Ito C, Ribeiro RC, Behm FG, Raimondi SC, Pui CH, Campana D. Cyclosporin A induces apoptosis in childhood acute lymphoblastic leukemia cells. Blood. 1998;91(3):1001.

15. Fosgerau K, Hoffmann T. Peptide therapeutics: current status and future directions. Drug discovery today. 2015;20(1):122-8.

16. Usmani SS, Bedi G, Samuel JS, Singh S, Kalra S, Kumar P, et al. THPdb: Database of FDA-approved peptide and protein therapeutics. PLoS One. 2017;12(7):e0181748.

17. D'Aloisio V, Dognini P, Hutcheon GA, Coxon CR. PepTherDia: Database and structural composition analysis of approved peptide therapeutics and diagnostics. Drug Discovery Today. 2021;26(6):1409-19.

18. Henninot A, Collins JC, Nuss JM. The current state of peptide drug discovery: back to the future? Journal of medicinal chemistry. 2018;61(4):1382-414.

19. Lau JL, Dunn MK. Therapeutic peptides: Historical perspectives, current development trends, and future directions. Bioorganic & medicinal chemistry. 2018;26(10):2700-7.

20. Research and Markets. Global peptide cancer vaccine market & clinical trials insight 2026 2002-2022 [Available from:https://www.researchandmarkets.com/reports/5317366/global-peptide-cancer-vaccine-market-and-clinical.

21. Jafri MA, Ansari SA, Alqahtani MH, Shay JW. Roles of telomeres and telomerase in cancer, and advances in telomerase-targeted therapies. Genome medicine. 2016;8(1):1-18.

22. Staff C, Mozaffari F, Frödin J-E, Mellstedt H, Liljefors M. Telomerase (GV1001) vaccination together with gemcitabine in advanced pancreatic cancer patients. International journal of oncology. 2014;45(3):1293-303.

23. Henriques ST, Craik DJ. Cyclotides as templates in drug design. Drug discovery today. 2010;15(1-2):57-64.

24. Akondi KB, Muttenthaler M, Dutertre S, Kaas Q, Craik DJ, Lewis RJ, et al. Discovery, synthesis, and structure-activity relationships of conotoxins. Chemical reviews. 2014;114(11):5815-47.

25. Arnison PG, Bibb MJ, Bierbaum G, Bowers AA, Bugni TS, Bulaj G, et al. Ribosomally synthesized and post-translationally modified peptide natural products: overview and recommendations for a universal nomenclature. Natural product reports. 2013;30(1):108-60.

26. W Gruber C, Muttenthaler M, Freissmuth M. Ligand-based peptide design and combinatorial peptide libraries to target G protein-coupled receptors. Curr Pharm Des. 2010;16(28):3071-88.

27. Jennings C, West J, Waine C, Craik D, Anderson M. Biosynthesis and Insecticidal Properties of Plant Cyclotides: The Cyclic Knotted Proteins from Oldenlandia affinis. Proceedings of the National Academy of Sciences of the United States of America. 2001;98(19):10614-9.

28. Svangård E, Göransson U, Hocaoglu Z, Gullbo J, Larsson R, Claeson P, et al. Cytotoxic cyclotides from Viola tricolor. Journal of natural products. 2004;67(2):144.

29. Yang Y-L, Hua K-F, Chuang P-H, Wu S-H, Wu K-Y, Chang F-R, et al. New cyclic peptides from the seeds of Annona squamosa L. and their anti-inflammatory activities. J Agric Food Chem. 2007;56(2):386-92.

30. Ferreira IB, Pickering DA, Troy S, Croese J, Loukas A, Navarro S. Suppression of inflammation and tissue damage by a hookworm recombinant protein in experimental colitis. Clinical & translational immunology. 2017;6(10):e157.

31. Navarro S, Pickering DA, Ferreira IB, Jones L, Ryan S, Troy S, et al. Hookworm recombinant protein promotes regulatory T cell responses that suppress experimental asthma. Science translational medicine. 2016;8(362):362ra143-362ra143.

32. Gustafson KR, McKee TC, Bokesch HR. Anti-HIV cyclotides. Current Protein and Peptide Science. 2004;5(5):331-40.

33. Tam JP, Lu Y-A, Yang J-L, Chiu K-W. An Unusual Structural Motif of Antimicrobial Peptides Containing End-to-End Macrocycle and Cystine-Knot Disulfides. Proceedings of the National Academy of Sciences of the United States of America. 1999;96(16):8913-8.

34. Pinto MF, Fensterseifer IC, Migliolo L, Sousa DA, de Capdville G, Arboleda-Valencia JW, et al. Identification and structural characterization of novel cyclotide with activity against an insect pest of sugar cane. J Biol Chem. 2012;287(1):134-47.

35. Rocchi A, Benchimol EI, Bernstein CN, Bitton A, Feagan B, Panaccione R, et al. Inflammatory bowel disease: a Canadian burden of illness review. Canadian Journal of Gastroenterology. 2012;26(11):811-7.

36. Shoenfeld Y, Isenberg DA. The mosaic of autoimmunity. Immunology today. 1989;10(4):123-6.

37. Coskun M, Vermeire S, Nielsen OH. Novel targeted therapies for inflammatory bowel disease. Trends in pharmacological sciences. 2017;38(2):127-42.

38. Furfaro F, Bezzio C, Ardizzone S, Massari A, de Franchis R, Maconi G. Overview of biological therapy in ulcerative colitis: current and future directions. Journal of Gastrointestinal & Liver Diseases. 2015;24(2).

39. Neurath MF. IL-23: a master regulator in Crohn disease. Nature medicine. 2007;13(1):26-7.

40. Almradi A, Hanzel J, Sedano R, Parker CE, Feagan BG, Ma C, et al. Clinical trials of IL-12/IL-23 inhibitors in inflammatory bowel disease. BioDrugs. 2020;34:713-21.

41. Sandborn WJ, Ferrante M, Bhandari BR, Berliba E, Feagan BG, Hibi T, et al. Efficacy and safety of mirikizumab in a randomized phase 2 study of patients with ulcerative colitis. Gastroenterology. 2020;158(3):537-49. e10.

42. Feagan BG, Sandborn WJ, D'Haens G, Panés J, Kaser A, Ferrante M, et al. Induction therapy with the selective interleukin-23 inhibitor risankizumab in patients with moderate-to-

severe Crohn's disease: a randomised, double-blind, placebo-controlled phase 2 study. The Lancet. 2017;389(10080):1699-709.

43. Hanžel J, D'Haens GR. Anti-interleukin-23 agents for the treatment of ulcerative colitis. Expert opinion on biological therapy. 2020;20(4):399-406.

44. Fernández-Clotet A, Castro-Poceiro J, Panés J. JAK inhibition: the most promising agents in the IBD pipeline? Current Pharmaceutical Design. 2019;25(1):32-40.

45. D'amico F, Parigi TL, Fiorino G, Peyrin-Biroulet L, Danese S. Tofacitinib in the treatment of ulcerative colitis: efficacy and safety from clinical trials to real-world experience. Therapeutic advances in gastroenterology. 2019;12:1756284819848631.

46. Ruffolo C, Scarpa M, Faggian D, Basso D, D'Incà R, Plebani M, et al. Subclinical intestinal inflammation in patients with Crohn's disease following bowel resection: a smoldering fire. Journal of Gastrointestinal Surgery. 2010;14(1):24-31.

47. Naganuma M, Yokoyama Y, Motoya S, Watanabe K, Sawada K, Hirai F, et al. Efficacy of apheresis as maintenance therapy for patients with ulcerative colitis in an open-label prospective multicenter randomised controlled trial. Journal of gastroenterology. 2020;55:390-400.

48. Ocansey DKW, Wang L, Wang J, Yan Y, Qian H, Zhang X, et al. Mesenchymal stem cell–gut microbiota interaction in the repair of inflammatory bowel disease: an enhanced therapeutic effect. Clinical and Translational Medicine. 2019;8:1-17.

49. Jin J. Stem cell treatments. Jama. 2017;317(3):330-.

50. Peng Q, Zhang J, Zhou G. Differentially circulating exosomal microRNAs expression profiling in oral lichen planus. American Journal of Translational Research. 2018;10(9):2848.

51. Crohn's and Colitis Australia. 2021 annual report of Crohn's & Colitis Australia 2022 [Available from: https://crohnsandcolitis.org.au/wp-content/uploads/2022/05/CCA-2021-Annual-Report-FINAL.pdf.

52. PricewaterhouseCoopers. Improving inflammatory bowel disease care across Australia. 2013.

53. Wong SH, Ng SC. What can we learn from inflammatory bowel disease in developing countries? Current Gastroenterology Reports. 2013;15(3):1-9.

54. Statistics ABo. 2008 Year Book Australia No. 90: Aust. Bureau of Statistics; 2008.

55. Locksley RM. Asthma and allergic inflammation. Cell. 2010;140(6):777-83.

56. Corry DB. Emerging immune targets for the therapy of allergic asthma. Nature Reviews Drug Discovery. 2002;1(1):55-64.

57. Wigerblad G, Kaplan MJ. Neutrophil extracellular traps in systemic autoimmune and autoinflammatory diseases. Nature Reviews Immunology. 2022:1-15.

58. Cabanos C, Matsuoka Y, Maruyama N. Soybean proteins/peptides: A review on their importance, biosynthesis, vacuolar sorting, and accumulation in seeds. Peptides. 2021;143:170598.

59. OEC World. Soybeans - The observatory of economic complexcity 1995-2020 [Available from: https://oec.world/en/profile/hs/soybeans?redirect=true.

60. Singh P, Kumar R, Sabapathy S, Bawa A. Functional and edible uses of soy protein products. Comprehensive reviews in food science and food safety. 2008;7(1):14-28.

61. Chen K-I, Erh M-H, Su N-W, Liu W-H, Chou C-C, Cheng K-C. Soyfoods and soybean products: from traditional use to modern applications. Applied microbiology and biotechnology. 2012;96(1):9-22.

62. Friedman M, Brandon DL. Nutritional and health benefits of soy proteins. J Agric Food Chem. 2001;49(3):1069-86.

63. Wang W, Dia VP, Vasconez M, De Mejia EG, Nelson RL. Analysis of soybean protein-derived peptides and the effect of cultivar, environmental conditions, and processing on lunasin concentration in soybean and soy products. J AOAC Int. 2008;91(4):936-46.

64. Sanjukta S, Rai AK. Production of bioactive peptides during soybean fermentation and their potential health benefits. Trends in Food Science & Technology. 2016;50:1-10.

65. Maruyama N, Mikami B, Utsumi S. The development of transgenic crops to improve human health by advanced utilization of seed storage proteins. Bioscience, biotechnology, and biochemistry. 2011;75(5):823-8.

66. Mori T, Maruyama N, Nishizawa K, Higasa T, Yagasaki K, Ishimoto M, et al. The composition of newly synthesized proteins in the endoplasmic reticulum determines the transport pathways of soybean seed storage proteins. The Plant Journal. 2004;40(2):238-49.

67. Hirano H. Basic 7S globulin in plants. Journal of Proteomics. 2021;240:104209.

68. Jiang Y, Li L, He F, Yan W, Tang Y, Yang R, et al. Highly effective inactivation of anti-nutritional factors (lipoxygenase, urease and trypsin inhibitor) in soybean by radio frequency treatment. International Journal of Food Science & Technology. 2021;56(1):93-102.

69. Hirata A, Adachi M, Sekine A, Kang Y-N, Utsumi S, Mikami B. Structural and enzymatic analysis of soybean β-amylase mutants with increased pH optimum. J Biol Chem. 2004;279(8):7287-95.

70. Palavalli MH, Natarajan SS, Wang TT, Krishnan HB. Imbibition of soybean seeds in warm water results in the release of copious amounts of Bowman–Birk protease inhibitor, a putative anticarcinogenic agent. J Agric Food Chem. 2012;60(12):3135-43.

71. Ebisawa M, Brostedt P, Sjölander S, Sato S, Borres MP, Ito K. Gly m 2S albumin is a major allergen with a high diagnostic value in soybean-allergic children. J Allergy Clin Immunol. 2013;132(4):976-8. e5.

72. Chatterjee C, Gleddie S, Xiao C-W. Soybean bioactive peptides and their functional properties. Nutrients. 2018;10(9):1211.

73. De Mejia E, Ben O. Soybean bioactive peptides: A new horizon in preventing chronic diseases. Sexuality, Reproduction and Menopause. 2006;4(2):91-5.

74. Fernández-Tomé S, Hernández-Ledesma B. Current state of art after twenty years of the discovery of bioactive peptide lunasin. Food Res Int. 2019;116:71-8.

75. Singh BP, Vij S, Hati S. Functional significance of bioactive peptides derived from soybean. Peptides. 2014;54:171-9.

76. Jayachandran M, Xu B. An insight into the health benefits of fermented soy products. Food chemistry. 2019;271:362-71.

77. Shidal C, Al-Rayyan N, Yaddanapudi K, Davis KR. Lunasin is a novel therapeutic agent for targeting melanoma cancer stem cells. Oncotarget. 2016;7(51):84128-41.

78. Jiang Q, Pan YU, Cheng Y, Li H, Liu D, Li HUI. Lunasin suppresses the migration and invasion of breast cancer cells by inhibiting matrix metalloproteinase-2/-9 via the FAK/Akt/ERK and NF-κB signaling pathways. Oncol Rep. 2016;36(1):253-62.

79. Hubert HB, Feinleib M, McNamara PM, Castelli WP. Obesity as an independent risk factor for cardiovascular disease: A 26-year follow-up of participants in the Framingham Heart Study. Circulation. 1983;67(5):968-77.

80. Cruz-Huerta E, Fernández-Tomé S, Arques MC, Amigo L, Recio I, Clemente A, et al. The protective role of the Bowman-Birk protease inhibitor in soybean lunasin digestion: the effect of released peptides on colon cancer growth. Food Funct. 2015;6(8):2626-35.

81. Cam A, de Mejia EG. RGD-peptide lunasin inhibits Akt-mediated NF-κB activation in human macrophages through interaction with the αVβ3 integrin. Mol Nutr Food Res. 2012;56(10):1569-81.

82. McConnell EJ, Devapatla B, Yaddanapudi K, Davis KR. The soybean-derived peptide lunasin inhibits non-small cell lung cancer cell proliferation by suppressing phosphorylation of the retinoblastoma protein. Oncotarget. 2015;6(7):4649-62.

83. Odani S, Koide T, Ono T. Amino acid sequence of a soybean (Glycine max) seed polypeptide having a poly(L-aspartic acid) structure. J Biol Chem. 1987;262(22):10502-5.

84. Dia VP, De Mejia EG. Lunasin induces apoptosis and modifies the expression of genes associated with extracellular matrix and cell adhesion in human metastatic colon cancer cells. Mol Nutr Food Res. 2011;55(4):623-34.

85. Davis KR, Devapatla B, Shidal C, Yaddanapudi K. Validation of syngeneic mouse models of melanoma and non-small cell lung cancer for investigating the anticancer effects of the soy-derived peptide Lunasin. F1000Research. 2017;5:2432.

86. Aleksis R, Jaudzems K, Muceniece R, Liepinsh E. Lunasin is a redox sensitive intrinsically disordered peptide with two transiently populated α-helical regions. Peptides. 2016;85:56-62.

87. Santofimia-Castaño P, Rizzuti B, Xia Y, Abian O, Peng L, Velázquez-Campoy A, et al. Targeting intrinsically disordered proteins involved in cancer. Cellular and Molecular Life Sciences. 2020;77(9):1695-707.

88. Cobos C, Bansal PS, Wilson DT, Jones L, Zhao G, Field MA, et al. Peptides derived from hookworm anti-inflammatory proteins suppress inducible colitis in mice and inflammatory cytokine production by human cells. Frontiers in Medicine. 2022:2743.

89. Pullan RL, Smith JL, Jasrasaria R, Brooker SJ. Global numbers of infection and disease burden of soil transmitted helminth infections in 2010. Parasites & vectors. 2014;7(1):37.

90. Farthing MJ, Keusch GT. Enteric Infection: Mechanisms, Manifestations, and Management: Chapman & Hall; 1989.

91. Traub RJ. Ancylostoma ceylanicum, a re-emerging but neglected parasitic zoonosis. International journal for parasitology. 2013;43(12-13):1009-15.

92. George S, Levecke B, Kattula D, Velusamy V, Roy S, Geldhof P, et al. Molecular identification of hookworm isolates in humans, dogs and soil in a tribal area in Tamil Nadu, India. PLoS neglected tropical diseases. 2016;10(8).

93. Weinstock JV, Elliott DE. Helminths and the IBD hygiene hypothesis. Inflammatory bowel diseases. 2009;15(1):128-33.

94. To T, Stanojevic S, Moores G, Gershon AS, Bateman ED, Cruz AA, et al. Global asthma prevalence in adults: findings from the cross-sectional world health survey. BMC public health. 2012;12(1):204.

95. Helmby H. Human helminth therapy to treat inflammatory disorders-where do we stand? BMC immunology. 2015;16(1):12.

96. Bouchery T, Moyat M, Sotillo J, Silverstein S, Volpe B, Coakley G, et al. Hookworms evade host immunity by secreting a deoxyribonuclease to degrade neutrophil extracellular traps. Cell host & microbe. 2020;27(2):277-89. e6.

97. Mulvenna J, Hamilton B, Nagaraj SH, Smyth D, Loukas A, Gorman JJ. Proteomics analysis of the excretory/secretory component of the blood-feeding stage of the hookworm, Ancylostoma caninum. Molecular & Cellular Proteomics. 2009;8(1):109-21.

98. Loukas A, Hotez PJ, Diemert D, Yazdanbakhsh M, McCarthy JS, Correa-Oliveira R, et al. Hookworm infection. Nature Reviews Disease Primers. 2016;2:16088.

99. Tolentino K, Friedman JF. An update on anemia in less developed countries. The American journal of tropical medicine and hygiene. 2007;77(1):44-51.

100. Jones BF, Cappello M. Hookworm infection: molecular mechanisms of disease and targets for control. Drug Discovery Today: Disease Mechanisms. 2004;1(2):217-22.

101. Albonico M, Smith PG, Ercole E, Hall A, Chwaya HM, Alawi KS, et al. Rate of reinfection with intestinal nematodes after treatment of children with mebendazole or albendazole in a highly endemic area. Transactions of the Royal Society of Tropical Medicine and Hygiene. 1995;89(5):538-41.

102. Keiser J, Utzinger J. Efficacy of current drugs against soil-transmitted helminth infections: systematic review and meta-analysis. Jama. 2008;299(16):1937-48.

103. Hotez PJ, Bethony JM, Diemert DJ, Pearson M, Loukas A. Developing vaccines to combat hookworm infection and intestinal schistosomiasis. Nature Reviews Microbiology. 2010;8(11):814.

104. Seid CA, Curti E, Jones RM, Hudspeth E, Rezende W, Pollet J, et al. Expression, purification, and characterization of the Necator americanus aspartic protease-1 (Na-APR-1 (M74)) antigen, a component of the bivalent human hookworm vaccine. Human vaccines & immunotherapeutics. 2015;11(6):1474-88.

105. Pearson MS, Bethony JM, Pickering DA, de Oliveira LM, Jariwala A, Santiago H, et al. An enzymatically inactivated hemoglobinase from Necator americanus induces neutralizing antibodies against multiple hookworm species and protects dogs against heterologous hookworm infection. The FASEB Journal. 2009;23(9):3007-19.

106. Williamson AL, Brindley PJ, Abbenante G, Prociv P, Berry C, Girdwood K, et al. Cleavage of hemoglobin by hookworm cathepsin D aspartic proteases and its potential contribution to host specificity. The FASEB Journal. 2002;16(11):1458-60.

107. Loukas A, Bethony JM, Mendez S, Fujiwara RT, Goud GN, Ranjit N, et al. Vaccination with recombinant aspartic hemoglobinase reduces parasite load and blood loss after hookworm infection in dogs. PLoS medicine. 2005;2(10):e295.

108. Xiao S, Zhan B, Xue J, Goud GN, Loukas A, Liu Y, et al. The evaluation of recombinant hookworm antigens as vaccines in hamsters (Mesocricetus auratus) challenged with human hookworm, Necator americanus. Experimental parasitology. 2008;118(1):32-40.

109. Skwarczynski M, Dougall AM, Khoshnejad M, Chandrudu S, Pearson MS, Loukas A, et al. Peptide-based subunit vaccine against hookworm infection. PLoS One. 2012;7(10):e46870.

110. Pearson MS, Pickering DA, Tribolet L, Cooper L, Mulvenna J, Oliveira LM, et al. Neutralizing Antibodies to the Hookworm Hemoglobinase Na-APR-1: Implications for a Multivalent Vaccine against Hookworm Infection and Schistosomiasis. The Journal of Infectious Diseases. 2010;201(10):1561-9.

111. Fuaad AAHA, Pearson MS, Pickering DA, Becker L, Zhao G, Loukas AC, et al. Lipopeptide Nanoparticles: Development of Vaccines against Hookworm Parasite. ChemMedChem. 2015;10(10):1647-54.

112. Skwarczynski M, Dougall AM, Khoshnejad M, Chandrudu S, Pearson MS, Loukas A, et al. Peptide-based subunit vaccine against hookworm infection. PloS one. 2012;7(10):e46870-e.

113. Zhong W, Skwarczynski M, Toth I. Lipid core peptide system for gene, drug, and vaccine delivery. Australian journal of chemistry. 2009;62(9):956-67.

114. Moyle PM, Toth I. Self-adjuvanting lipopeptide vaccines. Current medicinal chemistry. 2008;15(5):506-16.

115. Williamson AL, Brindley PJ, Abbenante G, Datu BJ, Prociv P, Berry C, et al. Hookworm aspartic protease, Na-APR-2, cleaves human hemoglobin and serum proteins in a host-specific fashion. The Journal of infectious diseases. 2003;187(3):484-94.

116. Groß A, Hashimoto C, Sticht H, Eichler J. Synthetic peptides as protein mimics. Frontiers in bioengineering and biotechnology. 2016;3:211.

117. Wright PE, Dyson HJ. Intrinsically unstructured proteins: re-assessing the protein structure-function paradigm. Journal of molecular biology. 1999;293(2):321-31.

118. Peti W, C Nairn A, Page R. Folding of intrinsically disordered protein phosphatase 1 regulatory proteins. Current physical chemistry. 2012;2(1):107-14.

119. Majumder K, Chakrabarti S, Davidge ST, Wu J. Structure and activity study of egg protein ovotransferrin derived peptides (IRW and IQW) on endothelial inflammatory response and oxidative stress. J Agric Food Chem. 2013;61(9):2120-9.

120. Kucera K, Harrison LM, Cappello M, Modis Y. Ancylostoma ceylanicum excretory–secretory protein 2 adopts a netrin-like fold and defines a novel family of nematode proteins. Journal of molecular biology. 2011;408(1):9-17.

CHAPTER 2: Immunomodulatory Activity of a Lunasin Fragment

Reynold Philip, David T. Wilson, Roland Ruscher, Kim Miles, Karma Yeshi, Phurpa Wangchuk, Paramjit S. Bansal, Guangzu Zhao, Severine Navarro, Yan Lu, Alex Loukas and Norelle L. Daly*

2.1. Abstract

Lunasin is a bioactive soy peptide with potential in the treatment of cancer and obesity related diseases. Although the peptide is only 43 residues in length, it contains three regions with different proposed activities/functions and appears to have oral bioavailability, albeit in the presence of other proteins. The full-length peptide suppresses the production of inflammatory cytokines and although truncated versions have been studied, the N-terminal region has not been fully characterized due to its intrinsically disordered character. Here we have identified a 10-residue peptide from the N-terminal of lunasin, that reproducibly suppressed TNF in a human cell line-based assay. In addition, the peptide displayed antioxidant activity based on a DPPH free radical scavenging assay and suppressed neutrophils in an asthma mouse model. Taken together these properties suggest potential roles for this region in the anti-inflammatory and antioxidant effects of lunasin.

2.2. Introduction

The consumption of soy products has been correlated with low mortality from different types of cancers, anti-inflammatory diseases and cardiovascular diseases (1). Lunasin is a 43-residue soybean derived peptide with a range of bioactivities, and is thought to be responsible, in part, for the beneficial effects of soybean consumption (2, 3). Amongst the many bioactivity studies on lunasin, it has been shown to have effects against a range of cancers (4), has improved efficacy for lowering plasma low density lipoprotein cholesterol when used in combination with simvastatin (5), and recent data have also shown antipsychotic/anti-schizophrenic effects in the central nervous system (6). In addition, lunasin has displayed immuno-modulatory effects (7, 8) by activating the innate immune system. For instance, dendritic cell studies have indicated higher levels of CD86 and CD40, that indirectly increased the production of cytokines, chemokines and proliferation of CD4+ T cells, following exposure to lunasin (9, 10).

Despite being a relatively small protein, lunasin appears to be orally bioavailable when administered as a soy protein extract (11). It has been suggested that two cysteine-rich protease inhibitors from the Bowman-Birk inhibitor and Kunitz trypsin inhibitor families occur naturally in complex with lunasin and provide protection against digestive proteases (12). Transgenic application for lunasin has already shown promising results in genetically modified food, and it has been suggested that transgenic soybean has potential as a functional food for treating cancer and obesity (13, 14).

The importance and potential applications of lunasin has led to numerous studies on the origin of the peptide, as well as elucidation of structure/function relationships (4, 5, 6, 7, 8, 10, 15, 16, 17, 18, 19, 20, 21, 22, 23, 24, 25, 26, 27, 28, 29). Lunasin is encoded within a soybean 2S albumin gene (30, 31). Although other plants such as wheat, rye and barley reportedly contain lunasin (32, 33, 34), genomic sequencing analyses indicate that they lack the gene encoding the peptide and therefore it has been suggested that lunasin might have a microbial origin to account for its presence in these plants (35, 36).

In terms of the peptide primary structure, lunasin contains three distinct regions (Figure 2.1), including a cell adhesive motif comprising an arginine-glycine-aspartic acid (RGD) sequence that is responsible for cell internalization, residues spanning from Glu23-Ile30 which are homologous to chromatin binding proteins with immunomodulatory function, and a chain of nine aspartic acid residues at the C-terminal end which are involved with histone binding (4, 9, 22, 26, 27, 30, 37). Based on NMR analyses, lunasin appears to be intrinsically disordered with a propensity to form two helical regions comprising residues 3-12 and 21-30 for the reduced form of the peptide (38). Oxidation of two cysteine residues does not have a significant effect on the structure presumably because of the lack of well-defined structure, and a similar propensity for helical regions was also observed for the oxidized form (38).

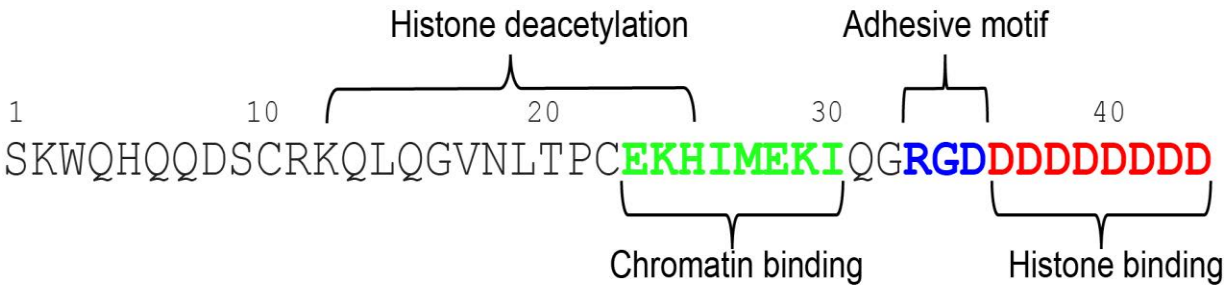

Figure 2.1: Primary sequence of lunasin, highlighting the proposed bioactive regions. Residues 12-25 appear to be involved in histone deacetylation; Residues 23-30 involved in chromatin binding (green); Residues 33-35 correspond to an RGD adhesive motif involved in cell internalization (blue); Poly-aspartic acid tail (residues 35-43) appears to be involved with core histone (H3 and H4) binding (red).

Several truncated forms of lunasin have previously been studied (4, 5, 6, 7, 8, 10, 15, 16, 17, 18, 19, 20, 21, 22, 23, 24, 25, 26, 27, 28, 29) but limited studies have been carried out on the N-terminal region. Here we have characterised a 10-residue peptide (Trp3-Lys12) derived from the N-terminal region of lunasin. The peptide, termed LN10, did not display a well-defined structure in solution, but we show that the peptide appears to have a role in suppressing inflammation.

2.3. Experimental Procedures

2.3.1. Peptide synthesis and purification

Peptides were synthesised manually using solid-phase peptide synthesis with Fmoc chemistry on a 0.1 mmole scale. A H-Lys (Fmoc)-2-chlorotrityl chloride resin was mixed in dimethylformamide (DMF) prior to assembly of the amino acid chain. The amino acids were activated with 0.5 M O-(1H-6-chlorobenzotriazole-1-yl)-1,1,3,3 tetramethyluronium hexafluorophosphate (HCTU) and 10% diisopropylethylamine (DIPEA) and coupled to the resin followed by washing with 20% piperidine in DMF. Peptides were cleaved from the resin using trifluoroacetic acid (TFA)/water/trisisopropylsilane (95:2.5:2.5) for 2-3 hours, precipitated with diethyl ether, dissolved in 50% acetonitrile, 0.05% TFA and subsequently lyophilized. The resulting crude peptides were purified with an Agilent HPLC using a C18 preparative column (Phenomenex Jupiter 10 µm, 300 Å, 250 x 21.2 mm) using a 1% gradient of solvent B (solvent A: 0.05% TFA; solvent B: 90% acetonitrile, 0.05% TFA). Masses were analysed using a 5800 MALDI TOF-TOF (SCIEX) mass spectrometer. The sequence of LN10 given is WQHQQDSCRK and the sequences of scrambled and control peptides (S1 and S2) were IMEKQHIEK and GVLDGGDP respectively. These peptides correspond to a scrambled version of LN9 (Chapter 3) and a peptide previously used as a negative control in in allergic house dust mice (HDM) studies (39).

2.3.2. NMR spectroscopy and Structural analyses

Lyophilized LN10 was resuspended with H_2O: D_2O (500 µL:50 µL), pH 4.5 to acquire 1D and 2D (TOCSY, NOESY, DQF-COSY and ^{13}C HSQC) spectra at 290 K using a 600 MHz AVANCE III NMR spectrometer (Bruker, Karlsruhe, Germany). Secondary shifts were determined by subtracting random coil chemical shifts (40) from the alpha proton shifts. Slowly exchanging amide protons were detected from a series of one-dimensional and TOCSY spectra recorded over 24 hours after dissolution of the peptide in 100% D_2O. The peptide solution was at pH 4.5 prior to lyophilisation for the exchange experiment.

2.3.3. LN10 Dimerization

Purified LN10 peptide (1 mg) was dissolved in 1 mL of 20 mM sodium phosphate buffer at pH 6.8 and left at room temperature for 24 hours. The solution (40 µL) was analysed through a 1% gradient of solvent B (solvent A: 0.05% formic acid, and solvent B: 90% acetonitrile, 0.05% formic acid) on a column (Phenomenex Aeris 150 x 2.1 mm, 3.6 µm PEPTIDE XB-C18 100 Å at 30 ℃) using a Shimadzu Liquid Chromatography Mass Spectrometer (LCMS)-2020, and using an Agilent HPLC with a C-12 analytical column (Phenomenex Jupiter 150 x 2.0 mm, 4 µm 90 Å). A 50 µL injection using a 1% gradient of solvent B (solvent A: 0.05% TFA; solvent B: 90% acetonitrile, 0.05% TFA) was used for the HPLC analysis and the eluent was monitored at 214 nm.

2.3.4. Antioxidant assay- 2,2-Diphenyl-1-picrylhydrazyl (DPPH)

The DPPH free radical scavenging activity of LN10 was analysed using a method based on protocols published in Brand-Williams *et al*. (41) and Yeshi *et al*. (42). Peptide or gallic acid

(200 µL) was incubated with 800 µL of methanolic solution of DPPH (0.1 mM) and transferred into a deep well plate (2 mL). The peptide concentrations used were 50 µg/mL, 100 µg/mL, 250 µg/mL and 500 µg/mL and were prepared from a LN10 stock (1 mg/mL). An equivalent weight concentration of gallic acid was prepared as a positive control, including negative control (Milliq water + DPPH), and an additional lunasin-derived peptide containing nine residues (Chapter 3) was also used in the experiment. The reaction mixture was shaken and left in the dark at room temperature for 30 mins. After 30 mins of incubation, 250 µL aliquots were transferred to a 96-well flat-bottom plate (Falcon®, Corning, USA). The absorbance was then measured at 517 nm using a Polarstar Omega microplate reader (BMG Labtech). All sample extracts and controls were evaluated in triplicate. The percentage of DPPH-free radical scavenged was calculated using the equation below:

$$\%\ \text{DPPH free radical scavenging activity} = \left(\frac{\text{ODc} - \text{ODs}}{\text{ODc}}\right) * 100,$$

where ODc is the absorbance value of the control, and ODs is the absorbance value of the tested sample or positive control.

2.3.5. Cytokine assay (THP-1 derived M1 macrophages)

M1 macrophages derived from the human THP-1 monocyte cell line were obtained from Sigma as described elsewhere (43) with some modifications. THP-1 cells were resuspended in R-10 (RPMI 10% FBS + Pen/Strep) medium containing 200 nM phorbol 12-myristate 13-acetate (PMA) (Sigma) and cultured at 1×10^5 cells per 100 µL in flat-bottom 96-well plates. After 48 hours the cells were washed with PBS and the medium was replaced with R-10 (without PMA). After 24 hours of PMA starvation, the resulting M0 macrophages were polarized by replacing

the medium with R-10 containing 20 ng/mL human recombinant IFNγ and 2 ng/mL human recombinant TNF (PeproTech). Forty-eight hours later the cells were washed, and the media replaced with R-10 containing either 100 μg/mL LN10 or an equivalent volume of PBS (vehicle control). The cells were stimulated with 10 ng/mL LPS (Sigma) and supernatants were collected 24 hours later and analysed using an ELISA kit as per the manufacturer's instructions. The data generated were analysed using the unpaired T-test Statistical methods in Prism 9.

2.3.6. Allergic asthma house dust mite (HDM) model

HDM extract (Citeq Biologics, Groningen, Netherlands) was resuspended in a sterile Dulbecco's phosphate-buffered saline (DPBS) with Ca^{2+} Mg^{2+} purchased from ThermoFisher Scientific (catalogue # 14040141) and administered via intratracheal instillation (i.t.) in 23 male BALB/c mice. The treatment groups contained five mice and three mice were placed in the naïve group. Mice were treated with 10 μg HMD *(D. pteronyssinus*) dissolved in 30 μL DPBS+Ca^{2+} Mg^{2+} buffer saline on days 0-7 and day 14, 15 and 16. No treatment was given for days 8-11. On day 12 and 13, 20 μg of the peptides (LN10 or scrambled peptides), dissolved in 200 μL DPBS+Ca^{2+} Mg^{2+} saline, was administered with intraperitoneal (i.p) injection. On days 14, 15 and 16, the negative control mice continued to receive the HDM dose, while the peptide treated mice received HDM in the morning and peptide in the evening. On day 17 mice were culled. Mice were euthanized with ketamine (K)/xylazine (X) to reduce red blood cells (RBC) in the bronchoalveolar lavage fluid (BALF). Blood was collected from inferior vena cava, put in the z-gel serum tube, spun at 10,000 *g* for 10 min, and stored at -80°C. BALF from trachea was collected after flushing the lungs with 1 mL DPBS 3 times at room temperature and placed immediately on ice. Lung tissue was snap frozen in liquid nitrogen, the superior lobe in a separate tube for RNA extraction and the rest with trachea and mediastinal lymph

node (MdLN) in nitrogen for cytokine analysis. The BALF tubes were spun at 360 g for 5 minutes at 4°C. Supernatants were removed and ammonium chloride potassium (ACK) pellets collected and those that appeared red were neutralized with DPBS and centrifuged again and the supernatant subsequently removed. Cells were counted during the staining process and 5 µL of cells from each purified cell sample tubes was taken as control tube for voltage/gating setup. The cells were stained with a monoclonal antibody (mAb) cocktail for 30 minutes at 4°C in the dark (5 µl x 25 =125 µL = 37.5 mAb +87.5 FACS). Cells were further washed with FACS buffer and reading were acquired on the flow cytometry.

The experiment was repeated once in dose response at 20 µg/mL, 100 µg/mL and 200 µg/mL of LN10 peptide.

2.4. Results

2.4.1. Peptide Design and Synthesis

The modelled structure of lunasin generated using PEP Fold 3 (44, 45, 46) is shown in Figure 2.2A. The two helical regions (Lys2-Gln13, Pro21-Gln31) are consistent with previous NMR studies which have suggested a propensity for helical structure (38, 47), despite lunasin being considered a largely disordered peptide. Although the N-terminal region has propensity to form helical structure, it has not been reported to have a specific bioactivity. This is in contrast to other regions of lunasin which have been studied in isolation and have been shown to contribute to various bioactivities (4, 5, 6, 7, 8, 10, 15, 16, 17, 18, 19, 20, 21, 22, 23, 24, 25, 26, 27, 28, 29). To explore the structure/function relationships of the N-terminal region of lunasin, a peptide corresponding to residues 3-12 (referred to as LN10) was synthesised using Fmoc chemistry and purified using RP-HPLC. The peptide was obtained in high yield >95% for subsequent studies. About 4 milligram of purified peptide was obtained after purification.

2.4.2. NMR Spectroscopy

The structure of LN10 was analysed in aqueous solution using NMR spectroscopy. The peptide displayed sharp peaks in the one-dimensional proton spectra. Resonance assignments were primarily done using two-dimensional TOCSY and NOESY spectra (48). Analysis of the proton secondary chemical shifts is shown in Figure 2.2B. Consecutive secondary shifts more positive than 0.1 are indicative of β-sheet structures, whereas consecutive secondary shifts more negative than 0.1 are indicative of helical structures. However, the majority of the

secondary shifts in LN10 are within +/- 0.1 ppm indicating the peptide is unstructured in aqueous solution. The NOESY spectra for LN10 had limited medium or long-range NOEs and lacked characteristic NOEs of helical structures. The majority of the amide protons were in fast exchange, consistent with the lack of regular secondary structure suggested by the secondary shifts.

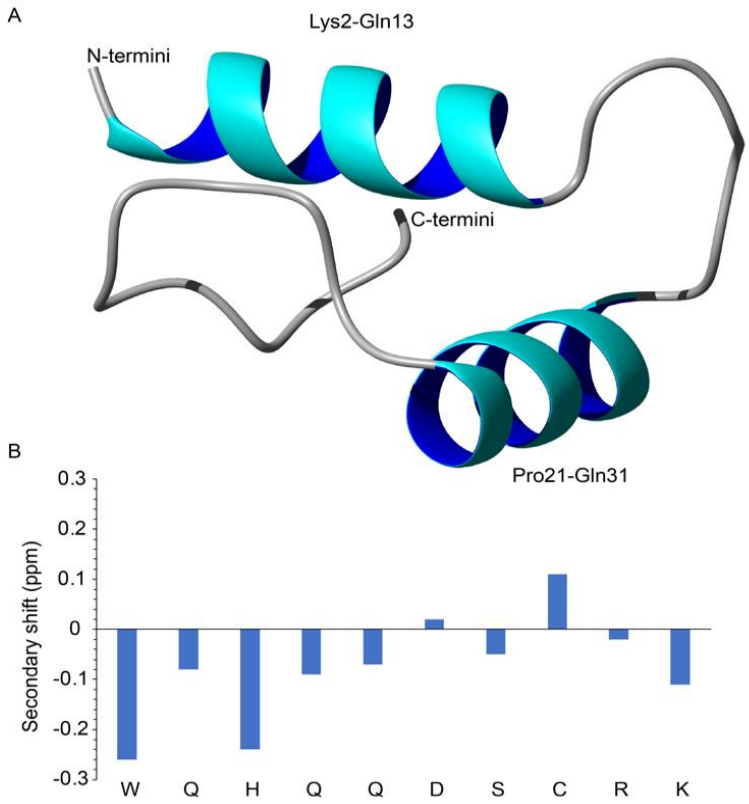

Figure 2.2: Structural analysis of truncated lunasin. (A) Three-dimensional structure of lunasin generated using molecular modelling with PEP Fold 3. The model indicates two helical regions (residues 2-13, and 21-31), consistent with previous studies (38, 47). Figure generated/viewed in MOLMOL (49). **(B)** Secondary chemical shifts of LN10. The secondary shifts were determined by subtracting the random coil shifts from the alpha proton shifts. The random coil shifts were taken from Wishart et al (1995) (40).

2.4.3 Cytokine Bioassay

The effect of LN10 on cytokine suppression was assessed with an ELISA based THP-1 M1-macrophage cell assay (Figure 2.3). Analyses carried out with fresh M1-macrophage cells showed a significant reduction of tumour necrosis factor (TNF) compared to the controls (Figure 3). Suppressive effects were also observed with frozen M1-macrophage cells, although not to the same extent as fresh M1-macrophage cells. The consistent reduction of the multifunctional cytokine (TNF) by LN10 is indicative of the peptide having anti-inflammatory properties.

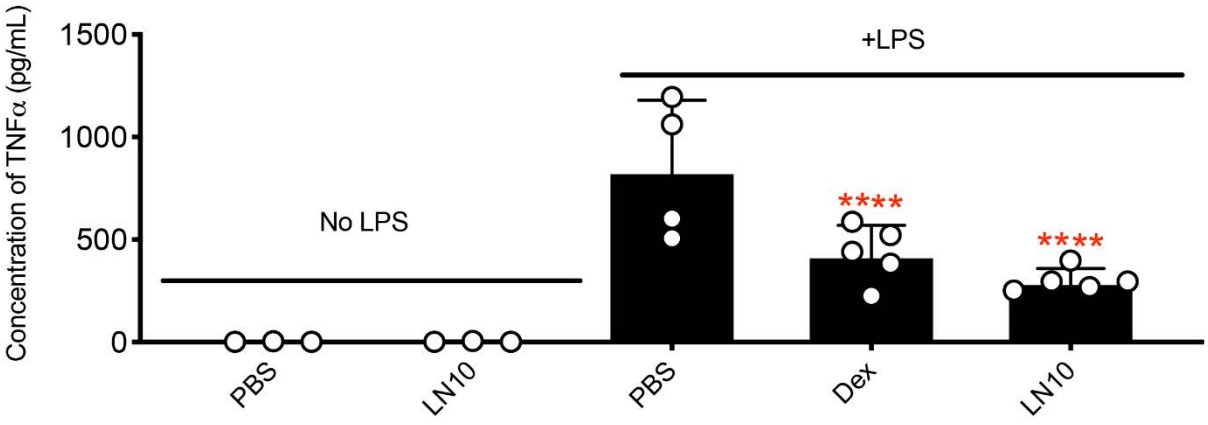

Figure 2.3: Suppressive effects of LN10 on TNF. The cell line used was human M1-macrophage cells derived from THP-1 monocytes**.** A final concentration of 10 µg/mL of LN10 showed no production of cytokine in M1-macrophages without lipopolysaccharide (LPS) stimulation, whereas LPS induced TNF was consistently reduced in the two repetitive assays, highlighting LN10 as a potential anti-inflammatory agent. Dexamethasone (Dex) was used as positive control.

2.4.4 Sequence Homology and Alignment of LN10

The LN10 sequence was searched across the NCBI protein repository database using BLAST/p. High sequence homology was found to several proteins from *Microbiospora* bacteria species, with two examples shown in Figure 2.4. Despite the sequence homology with the N-terminal region of lunasin, the sequences do not represent homologues of lunasin as there is no homology with the remainder of the lunasin sequence. The role of the LN10 sequence has not been elucidated in these bacterial proteins.

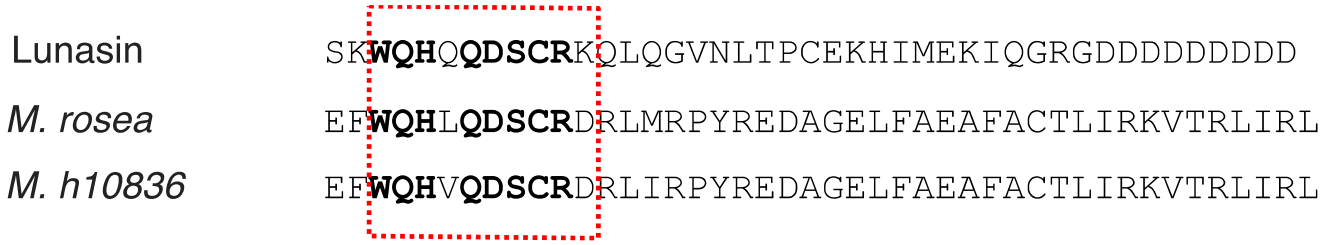

Figure 2.4: Sequence alignment of lunasin with bacterial proteins. The sequences corresponding to LN10 are boxed in red dotted lines, while the conserved residues are in bold and indicates the similarities between LN10 and the bacterial proteins. The codes for the bacterial proteins from *M. rosea* and *M.h10836* are WP_076440832.1 and WP_169986856.1 respectively.

2.4.5 Dimerization of LN10

LN10 contains a single cysteine residue (Cys 10) and consequently has the potential to form a disulfide-linked dimer. A previous study (Aleksis *et al*) on a truncated version of lunasin comprising residues 16-43, which also includes a single cysteine residue (Cys 22), showed the peptide did not form a dimer and that Cys 22 was in a reduced state at pH 6.5 (38). To determine the propensity of LN10 to form a dimer through Cys 10, we incubated LN10 in 20 mM sodium

phosphate at pH 6.5 at room temperature. These conditions were chosen as they are the same conditions used in the Aleksis *et al*, 2016 study, and consequently allowed a direct comparison. After 24 hours the majority of the peptide was still in a monomeric form based on LC/MS; a shoulder on the peak corresponding to the monomeric mass indicates dimer formation at a very slow rate at room temperature as shown in Figure 2.5. LN10 was prepared fresh for the bioassays indicating that the monomeric form is likely to be present during the course of the assay, which takes less than 24 hours. However, the pH and environment in the cells will be distinct from the *in vitro* assay carried out here and therefore we cannot conclusively determine the state of the peptide in the bioassays.

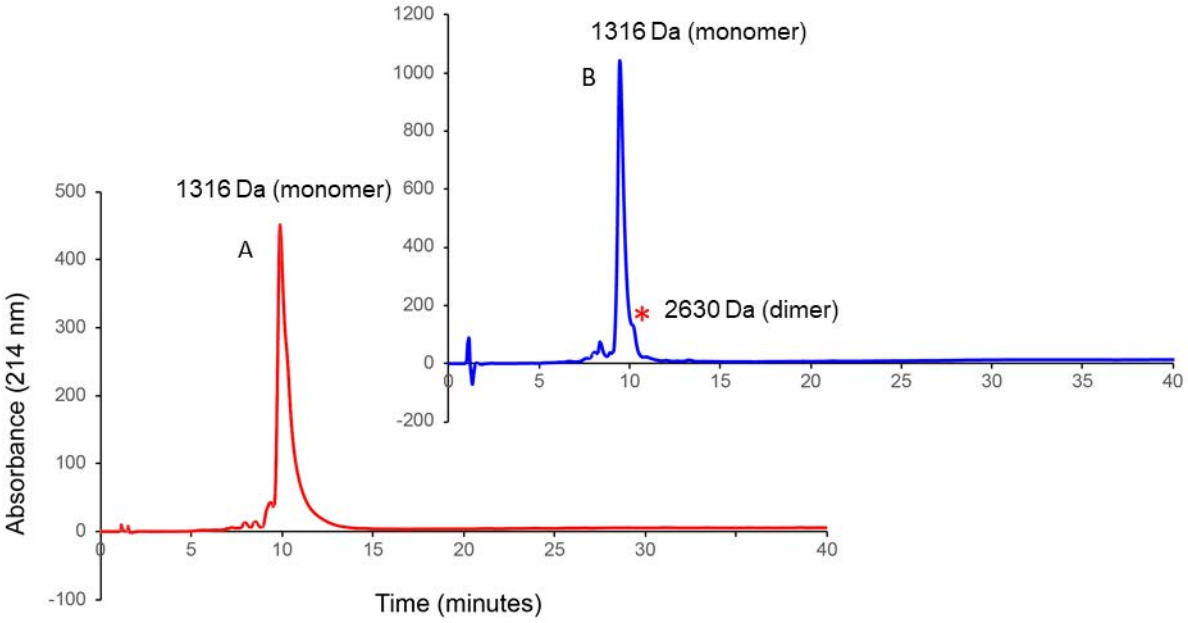

Figure 2.5: LN10 dimer formation. HPLC chromatograms of purified LN10 before and after incubation with phosphate buffered sodium at room temperature**.** Profile (A) shows the purified native LN10, while profile (B) displays a dimer formation after 24 hours of incubation in phosphate buffer. The shoulder on the monomer peak, marked with red asterisk, indicates the dimer product, while LN10 exists predominantly as a monomer throughout the incubation period.

2.4.6 DPPH Antioxidant assay

LN10 shows a dose response effect for DPPH-free radical scavenging (Figure 2.6), indicating that it has antioxidant effects. Gallic acid was chosen as a standard, despite the differences in molecular weights between it and LN10, to enable comparison with previous studies in the laboratory. A recent study using different antioxidant assays on sulfur containing amino acids (methionine, cystine and taurine) showed that only cysteine residues inhibited free radicals due

to the reactive nucleophilic thiol (50). The presence of the single cysteine in LN10 could be responsible for the antioxidant effects observed in this assay. The correlation between antioxidant effects and anti-inflammatory activity has recently been shown in proteins and peptides derived from egg white (51).

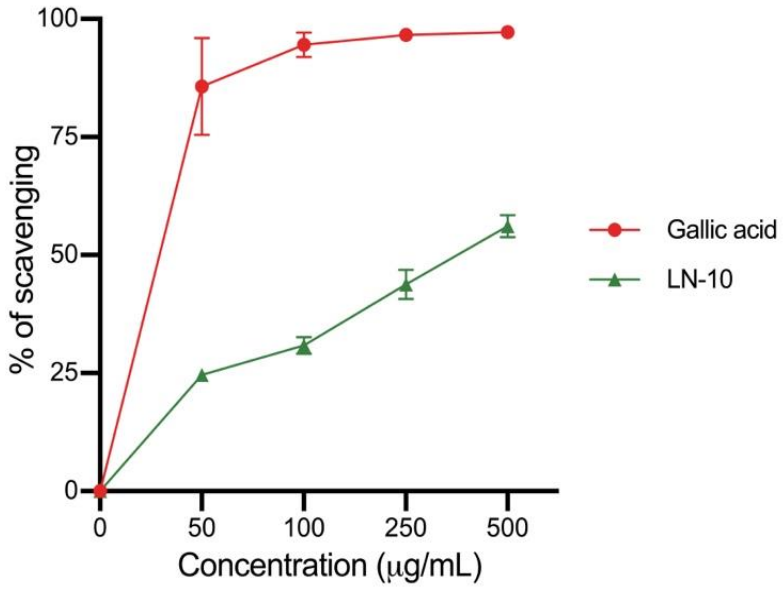

Figure 2.6: Percentage DPPH-free radical scavenging of LN10 at different concentrations (µg/mL). Gallic acid was used as standard due to its high free-radical scavenging property. The increase in free radical inhibition shows LN10 as a potential antioxidant agent. Results displayed using Prism 9.

2.4.7 Allergic Asthma HDM model

In addition to the *in vitro* assays, LN10 was tested in an *in vivo* house dust mite induced allergic asthma mouse model. This assay showed significant suppression of neutrophil cells in the presence of LN10, but not in eosinophils cells or lymphocytes (Figure 2.7). However, there is a trend across all three datasets for suppression of eosinophils and lymphocytes. Interestingly, a lunasin derived control peptide (S1, IMEKIQHIEK) initially used as control, displayed reduction against neutrophils and therefore another control peptide (S2, GVLDGGDP) was used in a repeat assay. The S2 control did not have an influence on the cell numbers indicating

that the difference observed for LN10 was not related to the injection regime chosen for the peptides.

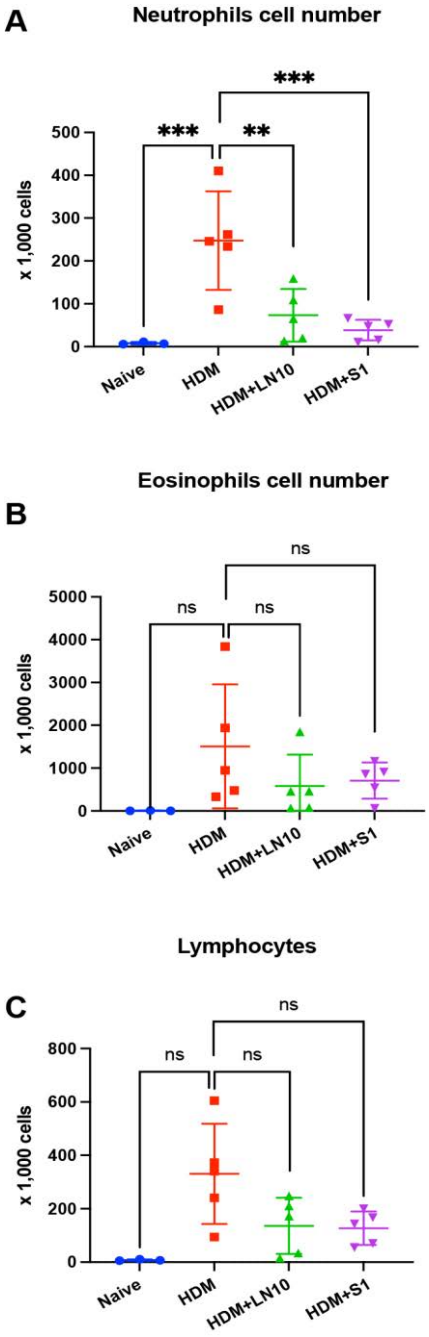

Figure 2.7. Effects of LN10 in a house dust mite induced allergic asthma assay in mice. (A) Neutrophils were decreased in the presence of 20 μg/mL of LN10 and lunasin derived scrambled peptide (S1). No significant effects observed in (B) eosinophils or (C) lymphocytes.

Results are shown as mean±SD in GraphPad Prism9. Differences between groups were analysed by one-way ANOVA with multiple comparison (* $p<0.05$, ** $p<0.01$, ***$p<0.0007$).

Repetition of the asthma assay using multiple doses of LN10 showed consistency with neutrophil reduction at 20 μg/mL and 100 μg/mL. The new control peptide (S2) showed no activity in contrast to the lunasin derived scrambled peptide (S1) (Figure 2.8). The consistent reduction of LN10 observed in the two assays suggests that LN10 is a potential therapeutic agent for neutrophil-cell related asthma.

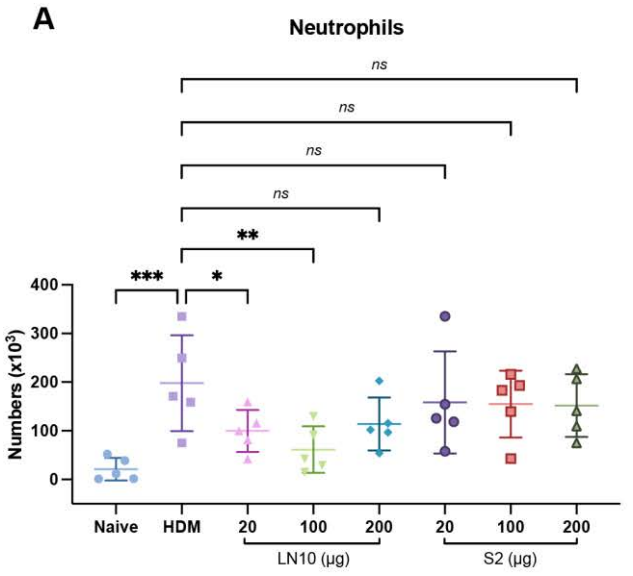
A
Neutrophils
ns
ns
ns
ns
**
***
*
Numbers (x10³)
400
300
200
100
0
Naive
HDM
20
100
200
20
100
200
LN10 (µg)
S2 (µg)

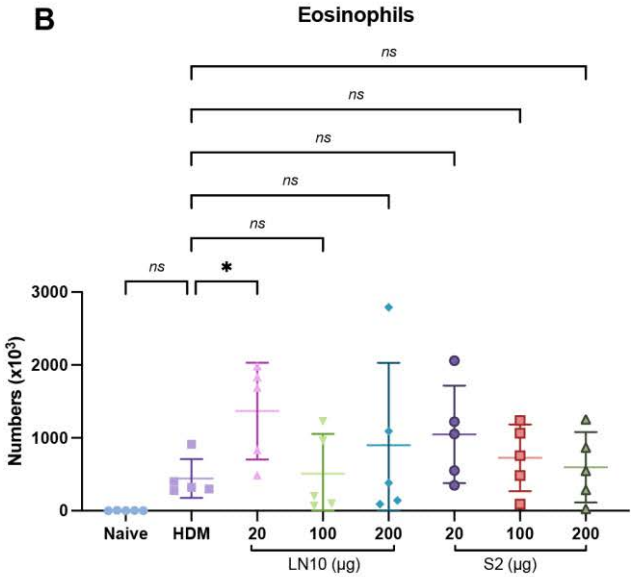
B
Eosinophils
ns
ns
ns
ns
ns
ns
*
Numbers (x10³)
3000
2000
1000
0
Naive
HDM
20
100
200
20
100
200
LN10 (µg)
S2 (µg)

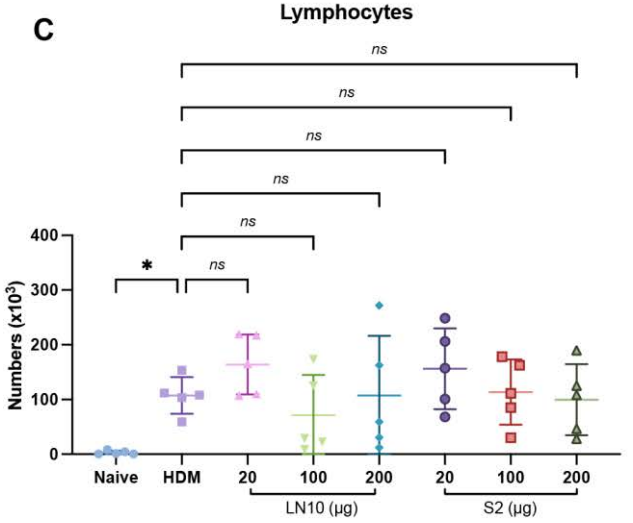
C
Lymphocytes
ns
ns
ns
ns
ns
ns
*
Numbers (x10³)
400
300
200
100
0
Naive
HDM
20
100
200
20
100
200
LN10 (µg)
S2 (µg)

Figure 2.8: Dose response effects of LN10 in a house dust mite induced allergic asthma assay in mice. (A) Neutrophil cells were reduced in the presence of LN10 at 20 μg/mL and 100 μg/mL but at 200 μg/mL there was no significant reduction. Further study is required to determine the reason for this effect. No statistical difference was observed between LN10 treated mice for (B) eosinophils cell or (C) lymphocytes and the HDM treated mice. The S2-scrambled peptide (control) displayed no significant differences in any of the cell types tested compared to HDM treated mice. No significant difference was observed between the HDM and naïve mice with respect to the eosinophils, indicating that this cell type does not have a significant impact in this model. Data displayed as mean±SD in GraphPad Prism 9. Differences between groups are analysed by one-way ANOVA with multiple comparison (* $p<0.05$, ** $p<0.01$).

2.5. Discussion

Lunasin has a range of potential applications for treating chronic disorders but there is limited understanding of the structure/function relationships related to the N-terminal region. Here we show that a peptide corresponding to residues 3-12 in lunasin can suppress secretion of a pro-inflammatory multifunctional cytokine (TNF) from a human monocyte-derived macrophage cell line, but does not form a well-defined structure in solution. Full-length lunasin has previously been shown to have anti-inflammatory activity (4, 5, 6, 7, 8, 10, 15, 16, 17, 18, 19, 20, 21, 22, 23, 24, 25, 26, 27, 28, 29) and our study suggests that the N-terminal region is, at least in part, responsible for this bioactivity (52).

Sequence homology analysis on LN10 indicated 89% sequence identity to a segment in a 22 kDa *Microbiospora* protein. Although the function of this protein is not known, it is conceivable that the fragment in *Microbiospora* protein displays similar bioactivity to LN10. Further study will be required to explore this hypothesis and indicate if the suppressive activity observed for LN10 is displayed in a much larger protein. The sequence similarity to *Microbiospora* proteins is intriguing given the proposed bacterial origin of lunasin (35, 36) and might provide insight into the evolution of the soybean peptide. Many *Microbiospora* bacterial species are involved in biodegradation and are excellent producers of secondary metabolites (antibiotic, enzymatic inhibitors, antidiabetic and antiatherogenic agents) that suppress plant pathogens in the soil (53, 54, 55, 56).

The lack of a well-defined structure for LN10 based on NMR analyses is not surprising for a 10-residue peptide in solution. Although the region corresponding to LN10 has previously been

suggested to have a propensity to form helical structure, in general the full-length lunasin peptide sequence is consistent with intrinsically disordered proteins (IDPs) (38, 47). IDPs are known to lack bulky hydrophobic (I, L and V) residues responsible for hydrophobic cores in folded globular proteins (57), however have aromatic amino acids (W, F and Y) that occur in low frequency and are highly conserved (57). IDPs are also generally rich with hydrophilic residues (A, R, G, Q, S, P, E, and K) that can promote disorder in peptides (57, 59, 60, 61). Although IDPs have dynamic conformational ensembles that are in constant structural exchange (57, 62, 63, 64, 65), they can fold into a well-defined structure when exposed to binding partners (66, 67, 68, 69). It is possible that both the full-length lunasin peptide and LN10 may adopt a defined structure upon binding to biological targets.

LN10 contains a single cysteine residue. Studies have revealed that free cysteine residues can act as catalytic residues for metabolism of various biochemicals (70) and at the cellular level they can be involved in protecting cells from oxidative damage (71). We have shown that the cysteine residue in LN10 does not readily oxidise in phosphate buffer. This is similar to studies on a truncated lunasin peptide comprising residues 16-43, which did not form a disulfide bond containing dimer, despite the presence of Cys 22 (38), prompting the authors to suggest that Cys 10 might be responsible for anti-inflammatory effects that could be mediated by the redox properties of lunasin (38, 52). However, we suggest that further study would be required to determine if Cys 10 is involved in the redox properties. In particular incubation at pH 7.4 and pH 5.5 which mimic the cytosol and late endosomes respectively. It appears more likely that the lack of inter-molecular disulfide bond formation for the peptides containing either Cys 10 or Cys 22 results from the higher propensity of the lunasin forming an intramolecular disulfide bond rather than inter-molecular disulfide bonds.

The inhibitory effect of LN10 observed on DPPH-free radicals has implications for the antioxidant and anti-inflammatory effects of lunasin. Free radicals are unstable compounds that can damage cells and overrun existing antioxidant systems within the human body and induce oxidative stress (72). They can cause inflammatory responses mediated via nuclear factor kappa B (NF-*k*B) (73), and have been linked to multiple diseases such as cancer, atherosclerosis, hypertension, diabetes, acute respiratory diseases, chronic obstructive pulmonary diseases and asthma (74). Several studies have shown that small peptides are capable of displaying antioxidant and/or anti-inflammatory effects including peptides derived from ovostransferrin (75, 76) and dipeptides (CR, FL, HC, LL, and MK) which displayed anti-inflammatory effects, and the tripeptides (IRW and IQW) that displayed both antioxidant and anti-inflammatory activities (77). Our results from the current study suggest that the LN10 sequence might be responsible for both the antioxidant and anti-inflammatory properties demonstrated in the native lunasin peptide but further study is required to assess the effects of the full-length peptide.

The allergic asthma assay indicated that LN10 produced a significant reduction in neutrophils. Asthma associated with neutrophils is rare and chronic, and commonly occurs in adults when bacteria accumulate in airways as a result of non-effective actions of neutrophils to kill bacteria (78). This action causes more neutrophils released into airways that causes remodelling of airways in patients that can affect airflow, eventually leading to death. In future studies the use of full-length lunasin peptide as a control in HDM assays might provide further insights into the bioactivities.

The mode of action of LN10 is not clear at this stage, but from cytokine studies it is generally found that LPS can activate the NFκB pathway which in turn will activate the transcription factors that control many cytokine genes and their subsequent release (79, 80, 81). These cytokines can be down regulated in the presence of anti-inflammatory agents. Consequently, we postulate that LN10 might be down-regulating the NFκB pathway responsible for activating cytokine genes causing a reduction in the production of TNF. Clearly, further study is required to determine if this is the case.

In summary, we have characterized a lunasin derived peptide (LN10) that can suppress TNF production and display antioxidant activity, indicating that it might have anti-inflammatory properties. Also, its suppression of neutrophil cells suggests that it might have some application as a lead molecule in asthma therapeutics. This region has previously been predicted to have a propensity to form helical structure, but here we show it does not form this structure in isolation. Further study is required to assess the mechanism of action of this peptide which might have implications for understanding the bioactivity and mechanism associated with the full-length lunasin peptide.

2.6. References

1. Hernandez-Ledesma B, C Hsieh C, O De Lumen B. Chemopreventive properties of Peptide Lunasin: a review. Protein Pept Lett. 2013;20(4):424-32.

2. Messina M. Impact of Soy Foods on the Development of Breast Cancer and the Prognosis of Breast Cancer Patients. Complement Med Res. 2016;23(2):75-80.

3. Seber LE, Barnett BW, McConnell EJ, Hume SD, Cai J, Boles K, et al. Scalable purification and characterization of the anticancer lunasin peptide from soybean. PLoS ONE. 2012;7(4):e35409.

4. Shidal C, Al-Rayyan N, Yaddanapudi K, Davis KR. Lunasin is a novel therapeutic agent for targeting melanoma cancer stem cells. Oncotarget. 2016;7(51):84128-41.

5. Gu L, Gong Y, Zhao C, Wang Y, Tian Q, Lei G, et al. Lunasin Improves the LDL-C Lowering Efficacy of Simvastatin via Inhibiting PCSK9 Expression in Hepatocytes and ApoE−/− Mice. Molecules. 2019;24(22):4140.

6. Dzirkale Z, Nakurte I, Jekabsons K, Muceniece R, Klusa V. Intra-Nasally Administered Oligopeptide Lunasin Acts as a Possible Anti-Psychotic Agent in Mice Models. Medicina. 2019;55(7):393.

7. Cruz-Huerta E, Fernández-Tomé S, Arques MC, Amigo L, Recio I, Clemente A, et al. The protective role of the Bowman-Birk protease inhibitor in soybean lunasin digestion: the effect of released peptides on colon cancer growth. Food Funct. 2015;6(8):2626-35.

8. Cam A, de Mejia EG. RGD-peptide lunasin inhibits Akt-mediated NF-κB activation in human macrophages through interaction with the αVβ3 integrin. Mol Nutr Food Res. 2012;56(10):1569-81.

9. Chang H-C, Lewis D, Tung C-Y, Han L, Henriquez SM, Voiles L, et al. Soypeptide lunasin in cytokine immunotherapy for lymphoma. Cancer Immunol Immunother. 2014;63(3):283-95.

10. Tung C-Y, Lewis DE, Han L, Jaja M, Yao S, Li F, et al. Activation of dendritic cell function by soypeptide lunasin as a novel vaccine adjuvant. Vaccine. 2014;32(42):5411-9.

11. Dia VP, Torres S, De Lumen BO, Erdman JJW, De Mejia EG. Presence of lunasin in plasma of men after soy protein consumption. J Agric Food Chem. 2009;57(4):1260-6.

12. Price SJ, Pangloli P, Krishnan HB, Dia VP. Kunitz trypsin inhibitor in addition to Bowman-Birk inhibitor influence stability of lunasin against pepsin-pancreatin hydrolysis. Food Res Int. 2016;90:205-15.

13. Ren G, Hao Y, Zhu Y, Shi Z, Zhao G. Expression of Bioactive Lunasin Peptide in Transgenic Rice Grains for the Application in Functional Food. Molecules (Basel, Switzerland). 2018;23(9):2373.

14. Hao Y, Fan X, Guo H, Yao Y, Ren G, Lv X, et al. Overexpression of the bioactive lunasin peptide in soybean and evaluation of its anti-inflammatory and anti-cancer activities in vitro. J Biosci Bioeng. 2020;129(4):395-404.

15. Hernández-Ledesma B, Hsieh C-C, Ben O. Lunasin, a novel seed peptide for cancer prevention. Peptides. 2009;30(2):426-30.

16. Jeong HJ, Lam Y, De Lumen BO. Barley lunasin suppresses ras-induced colony formation and inhibits core histone acetylation in mammalian cells. J Agric Food Chem. 2002;50(21):5903-8.

17. Hernández-Ledesma B, Hsieh C-C, De Lumen BO. Relationship between lunasin's sequence and its inhibitory activity of histones H3 and H4 acetylation. Mol Nutr Food Res. 2011;55(7):989-98.

18. Hsieh C-C, Hernández-Ledesma B, de Lumen BO. Lunasin, a novel seed peptide, sensitizes human breast cancer MDA-MB-231 cells to aspirin-arrested cell cycle and induced apoptosis. Chem Biol Interact. 2010;186(2):127-34.

19. Dia VP, de Mejia EG. Lunasin potentiates the effect of oxaliplatin preventing outgrowth of colon cancer metastasis, binds to α5β1 integrin and suppresses FAK/ERK/NF-κB signaling. Cancer letters. 2011;313(2):167-80.

20. Hsieh C-C, Chou M-J, Wang C-H. Lunasin attenuates obesity-related inflammation in RAW264. 7 cells and 3T3-L1 adipocytes by inhibiting inflammatory cytokine production. PLoS One. 2017;12(2):e0171969.

21. Fernández-Tomé S, Xu F, Han Y, Hernández-Ledesma B, Xiao H. Inhibitory Effects of Peptide Lunasin in Colorectal Cancer HCT-116 Cells and Their Tumorsphere-Derived Subpopulation. Int J Mol Sci. 2020;21(2):537.

22. Jiang Q, Pan YU, Cheng Y, Li H, Liu D, Li HUI. Lunasin suppresses the migration and invasion of breast cancer cells by inhibiting matrix metalloproteinase-2/-9 via the FAK/Akt/ERK and NF-κB signaling pathways. Oncol Rep. 2016;36(1):253-62.

23. Hsieh C, Hernández-Ledesma B, Jeong H, Park J, de Lumen B. Complementary roles in cancer prevention: protease inhibitor makes the cancer preventive peptide lunasin bioavailble. PloS one. 2010;5(1):e8890.

24. Dia VP, de Mejia EG. Lunasin promotes apoptosis in human colon cancer cells by mitochondrial pathway activation and induction of nuclear clusterin expression. Cancer Lett. 2010;295(1):44-53.

25. Dia VP, de Mejia EG. Potential of lunasin orally-administered in comparison to intraperitoneal injection to inhibit colon cancer metastasis in vivo. J Cancer Ther. 2013;4:34-43.

26. McConnell EJ, Devapatla B, Yaddanapudi K, Davis KR. The soybean-derived peptide lunasin inhibits non-small cell lung cancer cell proliferation by suppressing phosphorylation of the retinoblastoma protein. Oncotarget. 2015;6(7):4649-62.

27. Jeong HJ, Jeong JB, Kim DS, de Lumen BO. Inhibition of core histone acetylation by the cancer preventive peptide lunasin. J Agric Food Chem. 2007;55(3):632-7.

28. De Lumen BO. Lunasin: A novel cancer preventive seed peptide that modifies chromatin. J AOAC Int. 2008;91(4):932-5.

29. Hubert HB, Feinleib M, McNamara PM, Castelli WP. Obesity as an independent risk factor for cardiovascular disease: A 26-year follow-up of participants in the Framingham Heart Study. Circulation. 1983;67(5):968-77.

30. Galvez AF, Benito O. A soybean cDNA encoding a chromatin-binding peptide inhibits mitosis of mammalian cells. Nat Biotechno. 1999;17(5):495.

31. Lule VK, Garg S, Pophaly SD, Tomar SK. Potential health benefits of lunasin: a multifaceted soy-derived bioactive peptide. J Food Sci. 2015;80(3):R485-R94.

32. de Lumen BO. Lunasin: a cancer-preventive soy peptide. Nutr Rev. 2005;63(1):16-21.

33. Masotti AI, Buckley N, Champagne CP, Green-Johnson J. Immunomodulatory bioactivity of soy and milk ferments on monocyte and macrophage models. Food Res Int. 2011;44(8):2475-81.

34. Yoshikawa M, Takahashi M, Yang S. Delta opioid peptides derived from plant proteins. Curr Pharm Des. 2003;9(16):1325-30.

35. Mitchell RAC, Lovegrove A, Shewry PR. Lunasin in cereal seeds: What is the origin? J Cereal Sci. 2013;57(3):267-9.

36. Rizzello CG, Nionelli L, Coda R, Gobbetti M. Synthesis of the cancer preventive peptide lunasin by lactic acid bacteria during sourdough fermentation. Nutr Cancer. 2012;64(1):111-20.

37. Shidal C, Inaba J-I, Yaddanapudi K, Davis KR. The soy-derived peptide Lunasin inhibits invasive potential of melanoma initiating cells. Oncotarget. 2017;8(15):25525.

38. Aleksis R, Jaudzems K, Muceniece R, Liepinsh E. Lunasin is a redox sensitive intrinsically disordered peptide with two transiently populated α-helical regions. Peptides. 2016;85:56-62.

39. Kim DY, Park BS, Hong GU, Lee BJ, Park JW, Kim SY, et al. Anti-inflammatory effects of the R2 peptide, an inhibitor of transglutaminase 2, in a mouse model of allergic asthma, induced by ovalbumin. British journal of pharmacology. 2011;162(1):210-25.

40. Wishart DS, Bigam CG, Holm A, Hodges RS, Sykes BD. 1 H, 13 C and 15 N random coil NMR chemical shifts of the common amino acids. I. Investigations of nearest-neighbor effects. J Biomol NMR. 1995;5(1):67-81.

41. Brand-Williams W, Cuvelier ME, Berset C. Use of a free radical method to evaluate antioxidant activity. Lebensm-Wissu-Technol. 1995;28:25-30.

42. Yeshi K, Yangdon P, Kashyap S, Wangchuk P. Antioxidant activity and the polyphenolic and flavonoid contents of five high altitude medicinal plants used in Bhutanese sowa rigpa medicine. JBAPN. 2017;7(1):18-26.

43. Chanput W, Mes JJ, Savelkoul HF, Wichers HJ. Characterization of polarized THP-1 macrophages and polarizing ability of LPS and food compounds. Food Funct. 2013;4(2):266-76.

44. Lamiable A, Thévenet P, Rey J, Vavrusa M, Derreumaux P, Tufféry P. PEP-FOLD3: faster de novo structure prediction for linear peptides in solution and in complex. Nucleic Acids Res. 2016;44(W1):W449-W54.

45. Shen Y, Maupetit J, Derreumaux P, Tufféry P. Improved PEP-FOLD approach for peptide and miniprotein structure prediction. J Chem Theory Comput. 2014;10(10):4745-58.

46. Thevenet P, Shen Y, Maupetit J, Guyon F, Derreumaux P, Tuffery P. PEP-FOLD: an updated de novo structure prediction server for both linear and disulfide bonded cyclic peptides. Nucleic Acids Res. 2012;40(W1):W288-W93.

47. de Souza SMA, Fernandes TVA, Kalume DE, Lima LMT, Pascutti PG, de Souza TLF. Physicochemical and structural properties of lunasin revealed by spectroscopic, chromatographic and molecular dynamics approaches. Biochim Biophys Acta Proteins Proteom. 2020;1868(8):140440.

48. Wüthrich K. NMR with proteins and nucleic acids. Europhys News. 1986;17(1):11-3.

49. Koradi R, Billeter M, Wüthrich K. MOLMOL: a program for display and analysis of macromolecular structures. Journal of molecular graphics. 1996;14(1):51-5.

50. Kim J-H, Jang H-J, Cho W-Y, Yeon S-J, Lee C-H. In vitro antioxidant actions of sulfur-containing amino acids. Arabian Journal of Chemistry. 2020;13(1):1678-84.

51. Zhou N, Zhao Y, Yao Y, Wu N, Xu M, Du H, et al. Antioxidant Stress and Anti-Inflammatory Activities of Egg White Proteins and Their Derived Peptides: A Review. J Agric Food Chem. 2021;70(1):5-20.

52. Hernández-Ledesma B, Hsieh C-C, de Lumen BO. Antioxidant and anti-inflammatory properties of cancer preventive peptide lunasin in RAW 264.7 macrophages. Biochem Biophys Res Commun. 2009;390(3):803-8.

53. Agrawal PK, Agrawal S, Shrivastava R. Modern molecular approaches for analyzing microbial diversity from mushroom compost ecosystem. 3 Biotech. 2015;5(6):853-66.

54. Yagi A, Uchida R, Hamamoto H, Sekimizu K, Kimura K-i, Tomoda H. Anti-Mycobacterium activity of microbial peptides in a silkworm infection model with Mycobacterium smegmatis. J Antibiot. 2017;70(5):685-90.

55. Okujo N, Iinuma H, George A, Eim KS, Li TL, Ting NS, et al. Bispolides, novel 20-membered ring macrodiolide antibiotics from Microbispora. J Antibiot. 2007;60(3):216-9.

56. Indananda C, Igarashi Y, Ikeda M, Oikawa T, Thamchaipenet A. Linfuranone A, a new polyketide from plant-derived Microbispora sp. GMKU 363. J Antibiot. 2013;66(11):675-7.

57. Dunker AK, Lawson JD, Brown CJ, Williams RM, Romero P, Oh JS, et al. Intrinsically disordered protein. J Mol Graph Model. 2001;19(1):26-59.

58. Espinoza-Fonseca LM. Aromatic residues link binding and function of intrinsically disordered proteins. Molecular BioSystems. 2012;8(1):237-46.

59. Williams R, Obradovic Z, Mathura V, Braun W, Garner E, Young J, et al. The protein non-folding problem: amino acid determinants of intrinsic order and disorder. Biocomputing 2001: World Scientific; 2000. p. 89-100.

60. Radivojac P, Iakoucheva LM, Oldfield CJ, Obradovic Z, Uversky VN, Dunker AK. Intrinsic disorder and functional proteomics. Biophysical journal. 2007;92(5):1439-56.

61. Vacic V, Uversky VN, Dunker AK, Lonardi S. Composition Profiler: a tool for discovery and visualization of amino acid composition differences. BMC bioinformatics. 2007;8(1):211.

62. Dunker AK, Oldfield CJ, Meng J, Romero P, Yang JY, Chen JW, et al. The unfoldomics decade: an update on intrinsically disordered proteins. BMC genomics. 2008;9(2):1-26.

63. Dunker AK, Silman I, Uversky VN, Sussman JL. Function and structure of inherently disordered proteins. Curr Opin Struct Biol. 2008;18(6):756-64.

64. Uversky VN, Dunker AK. Understanding protein non-folding. Biochim Biophys Acta Proteins Proteom. 2010;1804(6):1231-64.

65. Dyson HJ, Wright PE. Intrinsically unstructured proteins and their functions. Nat Rev Mol Cell Biol. 2005;6(3):197-208.

66. Uversky VN. A decade and a half of protein intrinsic disorder: biology still waits for physics. Protein Sci. 2013;22(6):693-724.

67. Uversky VN. Unusual biophysics of intrinsically disordered proteins. Biochim Biophys Acta Proteins Proteom. 2013;1834(5):932-51.

68. Uversky VN, Dunker AK. The case for intrinsically disordered proteins playing contributory roles in molecular recognition without a stable 3D structure. F1000 Biol Rep. 2013;5.

69. Fink AL. Natively unfolded proteins. Curr Opin Struct Biol. 2005;15(1):35-41.

70. Ho SL, Wang AH-J. Structural bioinformatics analysis of free cysteines in protein environments. J Taiwan Inst Chem Eng. 2009;40(2):123-9.

71. Requejo R, Hurd TR, Costa NJ, Murphy MP. Cysteine residues exposed on protein surfaces are the dominant intramitochondrial thiol and may protect against oxidative damage. FEBS J. 2010;277(6):1465-80.

72. Rahal A, Kumar A, Singh V, Yadav B, Tiwari R, Chakraborty S, et al. Oxidative stress, prooxidants, and antioxidants: the interplay. BioMed research international. 2014;2014.

73. Vaziri ND, Rodríguez-Iturbe B. Mechanisms of disease: oxidative stress and inflammation in the pathogenesis of hypertension. Nature clinical practice Nephrology. 2006;2(10):582-93.

74. Birben E, Sahiner UM, Sackesen C, Erzurum S, Kalayci O. Oxidative stress and antioxidant defense. World allergy organization journal. 2012;5(1):9-19.

75. Kim J, Moon S, Ahn D, Paik H, Park E. Antioxidant effects of ovotransferrin and its hydrolysates. Poultry Science. 2012;91(11):2747-54.

76. Ru Z, Xu M, Zhu G, Tu Y, Jiang Y, Du H. Ovotransferrin exerts bidirectional immunomodulatory activities via TLR4-mediated signal transduction pathways in RAW264. 7 cells. Food Science & Nutrition. 2021;9(11):6162-75.

77. Majumder K, Chakrabarti S, Davidge ST, Wu J. Structure and activity study of egg protein ovotransferrin derived peptides (IRW and IQW) on endothelial inflammatory response and oxidative stress. J Agric Food Chem. 2013;61(9):2120-9.

78. Yang X, Li H, Ma Q, Zhang Q, Wang C. Neutrophilic asthma is associated with increased airway bacterial burden and disordered community composition. BioMed Research International. 2018;2018.

79. Takada Y, Singh S, Aggarwal BB. Identification of a p65 peptide that selectively inhibits NF-κ B activation induced by various inflammatory stimuli and its role in down-regulation of NF-κB-mediated gene expression and up-regulation of apoptosis. J Biol Chem. 2004;279(15):15096-104.

80. Schütze S, Wiegmann K, Machleidt T, Krönke M. TNF-induced activation of NF-κB. Immunobiology. 1995;193(2-4):193-203.

81. Gupta S, Yel L, Kim C, Chiplunkar S, Gollapudi S. Role of NF-kappaB signaling pathway in increased apoptosis of lymphocytes in aged humans. J Allergy Clin Immunol. 2004;113(2):S215.

CHAPTER 3: Characterisation of an anti-inflammatory motif based on the soybean protein lunasin

Reynold Philip, David T. Wilson, Roland Rusher, Kim Miles, Paramjit S. Bansal, Severine Navarro, Yan Lu , Alex Loukas and Norelle L. Daly

3.1. Abstract

Lunasin is a 43-residue bioactive soy peptide with potential in the treatment of cancer and obesity related diseases. The full-length peptide has an effect on inflammatory cytokines and extensive studies have shown that lunasin is involved with the acetylation-deacetylation process that leads to cell apoptosis of various cancer cells. Lunasin contains a region with sequence homology to chromatin binding proteins, and here we show that a truncated version containing this region (Glu23-Ile30), suppressed neutrophils in a mouse model of asthma, and potentially suppressed a range of inflammatory cytokines in human immune cells, in a donor specific manner. This truncated peptide appears to have the propensity to form hydrogen bonds in solution, an unusual property for such a small peptide. Interestingly, this sequence motif is present in several peptides and proteins previously shown to have anti-inflammatory activity. The bioactivity, sequence conservation across a wide range of proteins/peptides and stabilizing hydrogen bonds suggests this motif has significant potential in drug design.

3.2. Introduction

As introduced in Chapter 2, lunasin appears to be responsible for some of the beneficial effects of soy products, including anticancer (1, 2) and anti-inflammatory properties (3, 4), and is available as a supplement (5). The intrinsically disordered nature of lunasin suggests dissecting out individual bioactivities of lunasin might be useful in the design of novel drug leads. Following on from Chapter 2, this chapter explores the structure and bioactivity of the region within lunasin (residues 23-30) that has sequence similarity to chromatin binding proteins (6, 7). It was of interest to determine if this region also had potential anti-inflammatory effects, similar to that observed in Chapter 2 for LN10.

In this study, we have synthesised a peptide corresponding to (residues 23-30) of lunasin and have shown that it results in suppression of a range of cytokines in immune cells in a donor specific manner, has an effect on immune cells in a mouse model of asthma, and forms part of a conserved sequence motif in chromatin binding and anti-inflammatory proteins and peptides.

3.3. Experimental Procedures

3.3.1. Peptide synthesis and purification

Peptides were synthesised manually using Fmoc chemistry on a 0.1 mmole scale. Linear peptides were synthesised using 2-chlorotrityl chloride resin activated in dimethylformamide (DMF) before coupling with amino acids. The amino acids were activated with 10% diisopropylethylamine (DIPEA) and coupled to the resin followed by washing with 20% piperidine in DMF. Peptides were then cleaved from the resin using trifluoroacetic acid (TFA)/water/trisisopropylsilane (95:2.5:2.5) for 2-3 hours, precipitated with diethyl ether, dissolved in 50% acetonitrile, 0.05%TFA and subsequently lyophilized. The resulting crude peptides were purified with an Agilent RP-HPLC using a C-18 preparative column (Phenomenex Jupiter 250 x 21.2 mm) using a 1% gradient of solvent B (solvent A: 0.05% TFA; solvent B: 90% acetonitrile, 0.05% TFA). The mass was analysed using a 5800 MALDI TOF-TOF (SCIEX) mass spectrometer.

3.3.2. NMR spectroscopy

Lyophilized peptides were resuspended with 90% water:10% deuterium (D_2O) (500 µL:50 µL) to acquire 1D and 2D (TOCSY, NOESY) spectra at 290 K using a 600 MHz AVANCE III NMR spectrometer (Bruker, Karlsruhe, Germany). Random coil chemical shifts were used to calculate secondary shifts for the peptides based on the experimental alpha proton shifts (8). Three-dimensional structures were calculated for peptides that have chemical shifts indicative of structure and sufficient NOEs in the NOESY spectra. The program CYANA was not used

since the linear peptide has less than 10 residues. However, slowly exchanging amide protons were detected from a series of one-dimensional and TOCSY spectra recorded over 24 hours after dissolution of the peptide in 100% D_2O. Peptide solutions were pH 4 prior to lyophilisation for the exchange experiment.

3.3.3. Cytokine assay on human peripheral blood mononuclear cells (PBMCs)

The human blood used for this project was donated by healthy volunteers. Written informed consent was obtained from each donor at the time of blood draw. Ethical approval for this research was obtained from the James Cook University Human Ethics Committee (Australia). PBMCs were isolated from whole blood by density gradient centrifugation using Ficoll-Paque media. For induction of T cell cytokines, PBMCs were activated with a cell stimulation cocktail of 50 ng/ml of phorbol 12-myristate 13-acetate (PMA) and 1 µg/ml of ionomycin (eBioscience). PMA + ionomycin-stimulated cells were treated with 0.1-100 µg/ml of soybean derived peptide or remained untreated. For stimulation of myeloid-associated cytokines, PBMCs were activated with 10 ng/ml lipopolysaccharide (LPS) (Sigma-Aldrich). LPS-stimulated PBMCs were treated with 0.1-100 µg/ml of soybean derived peptide or remained untreated. The cell culture plates were incubated overnight at 37°C and 6.5% CO_2. After incubation, the samples were centrifuged at 1,500 x g for 5 minutes and the culture supernatants were collected for cytokine analysis using a LEGENDplex (BioLegend) kit. Toxicity assays were performed with the LIVE/DEAD Cell Viability Assay (Thermo Fisher Scientific) and readout using flow cytometry. This dye binds to amines in cells with compromised cell membranes but cannot enter healthy cells.

3.3.4. THP-1 derived M1 macrophages cell assay

M1 macrophages derived from the human THP-1 monocyte cell line were obtained as described elsewhere (9) with some modifications. THP-1 cells were resuspended in R-10 medium containing 200 nM phorbol 12-myristate 13-acetate (PMA) (Sigma) and cultured at 1×10^5 cells per 100 µL per well in flat-bottom 96-well plates. After 48 hours the cells were washed with PBS and the medium replaced with R-10 (without PMA). After 24 hours of PMA starvation, the resulting M0 macrophages were polarized by replacing the medium with R-10 containing 20 ng/mL human recombinant IFNγ and 2 ng/mL human recombinant TNF-α (PeproTech). Forty-eight hours later the cells were washed, and the media replaced with R-10 containing either 100 µg/mL LN10 or an equivalent volume of PBS (vehicle control). The cells were stimulated with 10 ng/mL LPS (Sigma) and soups were collected 24 hours later and analysed using an ELISA kit as per the manufacturer's instructions.

3.3.5. Allergic asthma house dust mite (HDM) model

HDM extract (Citeq Biologics, Groningen, Netherlands) was resuspended in a sterile Dulbecco's phosphate-buffered saline (DPBS) with Ca^{2+} Mg^{2+} (ThermoFisher Scientific) and administered via intratracheal instillation (i.t.) in 23 male BALB/c mice. The treatment groups contained five mice and three mice were placed in the naïve group. Mice were treated with 10 µg HDM *(D. pteronyssinus*) dissolved in 30 µL DPBS+Ca^{2+} Mg^{2+} buffer saline on days 0-7 and day 14, 15 and 16. No treatment was given for days 8-11. On day 12 and 13, 20 µg of the peptides (LN10 or scrambled peptides), dissolved in 200 µL DPBS+Ca^{2+} Mg^{2+} saline, was administered with intraperitoneal (i.p) injection. On days 14, 15 and 16, the negative control

mice continued to receive the HDM dose, while the peptide treated mice received HDM in the morning and peptide in the evening. On day 17 mice were culled. Mice were euthanized with ketamine (K)/xylazine (X) to reduce red blood cells (RBC) in the bronchoalveolar lavage fluid (BALF). Blood was collected from inferior vena cava, put in the z-gel serum tube, spun at 10,000 g for 10 min, and stored at -80°C. BALF from trachea was collected after flushing the lungs with 1 mL DPBS 3 times at room temperature and placed immediately on ice. Lung tissue was snap frozen in liquid nitrogen, the superior lobe in a separate tube for RNA extraction and the rest with trachea and mediastinal lymph node (MdLN) in nitrogen for cytokine analysis. The BALF tubes were spun at 360 g for 5 minutes at 4°C. Supernatants were removed and ammonium chloride potassium (ACK) pellets collected and those that appeared red were neutralized with DPBS and centrifuged again and the supernatant subsequently removed. Cells were counted during the staining process and 5 µL of cells from each purified cell tubes were taken as control tube for voltage/gating setup. The cells were stained with a monoclonal antibody (mAb) cocktail for 30 minutes at 4°C in the dark (5 µl x 25 =125 µL = 37.5 mAb +87.5 FACS). Cells were further washed with FACS buffer and reading were acquired on the flow cytometry.

The experiment was repeated in dose response at 20 µg/mL, 100 µg/mL and 200 µg/mL of LN9 including S2 peptide as a control.

3.4. Results

3.4.1. Peptide synthesis

Three peptides were synthesised to provide insight into the structure/function relationships of the chromatin binding sequence motif (E/DXXXXXEK#) within lunasin. The sequences of the peptides are shown in Table 3.1. The peptide corresponding to 9 residues (Glu23-Ile31) of lunasin is referred to as lunasin 9 (LN9). Two mutants of LN9 were synthesised to analyse the structural effects of the conserved EK motif in LN9.

Table 3.1: Sequences of lunasin derived peptides

Peptide	Sequence	Description
Lunasin 9 (LN9)	EKHIMEKIQ	Residues 23-31 of lunasin
LN9-E6A	EKHIMAKIQ	LN9-mutant 1
LN9-K7A	EKHIMEAIQ	LN9-mutant 2

3.4.2. Structural studies using NMR spectroscopy

The structures of the synthetic peptides were analysed in aqueous solution using NMR spectroscopy. Similar to the LN10 peptide analysed in Chapter 2, the LN9 peptides displayed sharp peaks in the one-dimensional spectra indicating that the peptide had not aggregated. Analysis of the two-dimensional spectra allowed assignment of the majority of the resonances and the secondary chemical shifts are shown in Figure 3.1. The majority of the secondary shifts in LN9 are within +/- 0.1 ppm indicating that the structure does not contain regular secondary structure in aqueous solution. In addition, the secondary shift analysis on the mutants shown in Figure 3.1 indicates only minor chemical shift changes result from the mutations, but the shifts are also generally within +/- 0.1 ppm. The NOESY spectra for LN9 and the two mutants (E6A and K7A) all had limited medium or long-range NOEs consistent with a lack of regular secondary structure.

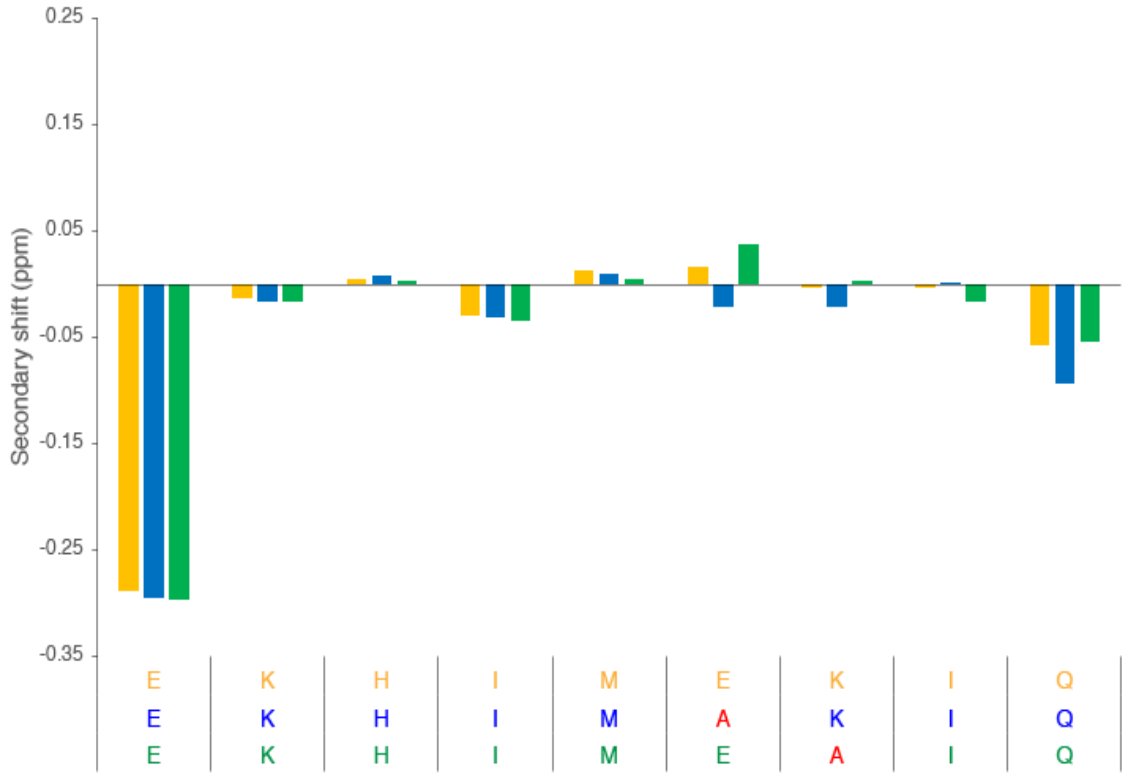

Figure 3.1: Secondary chemical shifts of the synthetic peptides. LN9 is shown in orange colour and the two mutants (E6A and K7A) in blue and green colour respectively, with the substituting alanine residue highlighted in red. The secondary shifts were determined by subtracting the random coil shifts from the alpha proton shifts. The random coil shifts were taken from Wishart *et al* (1995) (8). The large negative shift observed for the N-terminal residues are presumably due to effects of positive charge at the N terminal.

While the lack of structure of LN9 was not unexpected for such a small peptide with no additional covalent constraints such as disulfide bonds or a cyclic backbone, the amide exchange rates indicate that the peptide is not completely unstructured. The amide protons of nine residues were present after 30 minutes of resuspension of LN9 in D_2O. Two of these residues (Glu 6 and Ile 8) were still evident after 2.5 hours and sufficient data was collected to

allow exchange rates to be calculated (Table 3.2). Based on previous studies, amide protons with exchange rates > 4.16 min^{-1} are considered in fast exchange, those with exchange rates between 4.16 and 0.1 min^{-1} in intermediate exchange, those between 0.1 and 0.002 min^{-1} in slow exchange, and those less than 0.002 min^{-1} are non-exchangeable (10). The most common reason for slow exchange of amide protons in small peptides is hydrogen bonding. Consequently, the slow exchange of Glu 6 and Ile 8 in LN9 suggests that they have a propensity to form hydrogen bonds in solution and given the small size of the peptide are most likely to be involved in a helix or turn.

The amide exchange rates determined for the two mutants (K7A and E6A) showed that mutation of Lys 7 to an alanine resulted in similar exchange rates to LN9 with Glu 6 and Ile 8 still displaying slow exchange. However, when Glu 6 was mutated to an alanine residue, the alanine residue was in fast exchange, indicating that the glutamic acid has an important structural role. Despite these differences in exchange rates there are limited changes in the chemical shifts. Such effects have been observed for previous mutations studies (11).

Table 3.2: Amide proton exchange rates

Peptide	Residue	Exchange rate	Comments
LN9	Glu 6	0.0748	H-bonding
	Ile 8	0.0354	H-bonding
E6A	Ala 6	Fast*	No H-bonding
	Ile 8	0.0227	H-bonding
K7A	Glu 6	0.0440	H-bonding
	Ile 8	0.0332	H-bonding

*Exchange rate could not be measured as the peak was not present in the first spectrum recorded following dissolution in D_2O.

3.4.3. Biological activities

3.4.3.1. *In vitro* assays

Cytokine assays using fresh PBMCs derived from two different healthy donors showed reduction of several cytokines. Specifically, LN9 reduced TNF, IL12p70, IL-23, IFNγ, IL-1β and MCP-1 in donor 1 but only TNF in donor 2 (Appendix A). The reduction of TNF, an inflammatory cytokine, in both donors, is an indication that LN9 potentially has anti-inflammatory activity (Figure 3.2) but more research would be required to determine the reasons for donor specific differences. To provide additional structure/function data LN9 and the two mutants were also tested in a macrophage (M-1) cell assay. This assay was chosen to for several reasons including the ability to test multiple samples and to ascertain if there was less variation given the cells are not directly derived from human donors. Cytokines TNF, IL-1β, IL-6, IL-8 and IL-33 were all supressed by LN9 and its mutants (Figure 3.3).

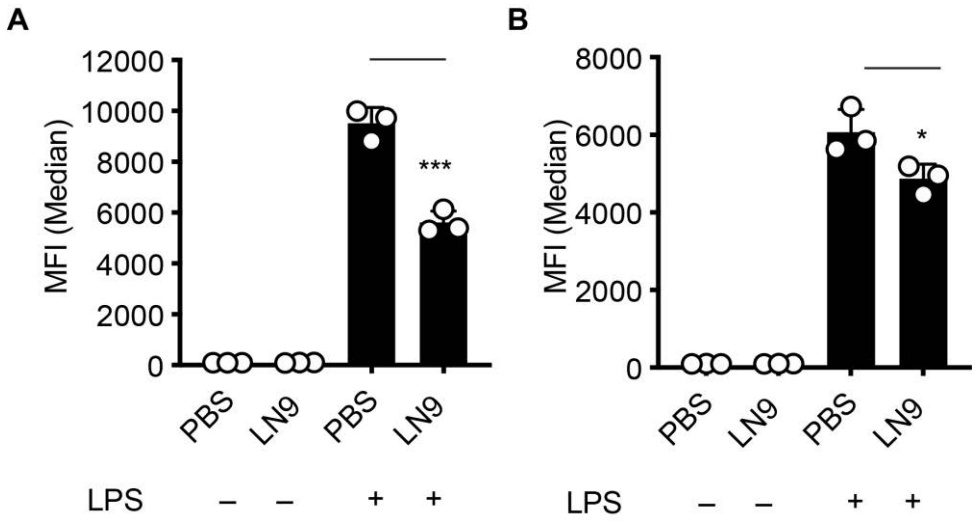

Figure 3.2: LN9 suppression of TNF secretion in human cells. The median fluorescence intensity (MFI) of TNF analysed in fresh PBMCs of two different human donors (A and B) using a Legendplex Kit, in the presence or absence of LPS. The peptide was administered at a concentration of 75 µg/mL concentration in both donors A and B. Other cytokines suppressed by LN9 are listed in the supplementary section. Phosphate buffered salt (PBS) was used as positive control. Data was generated using unpaired t-test in GraphPad Prism 9 displaying two-tailed P values (*P≤0.05, ***P≤0.001). All results reported represent means ± standard deviation (SD).

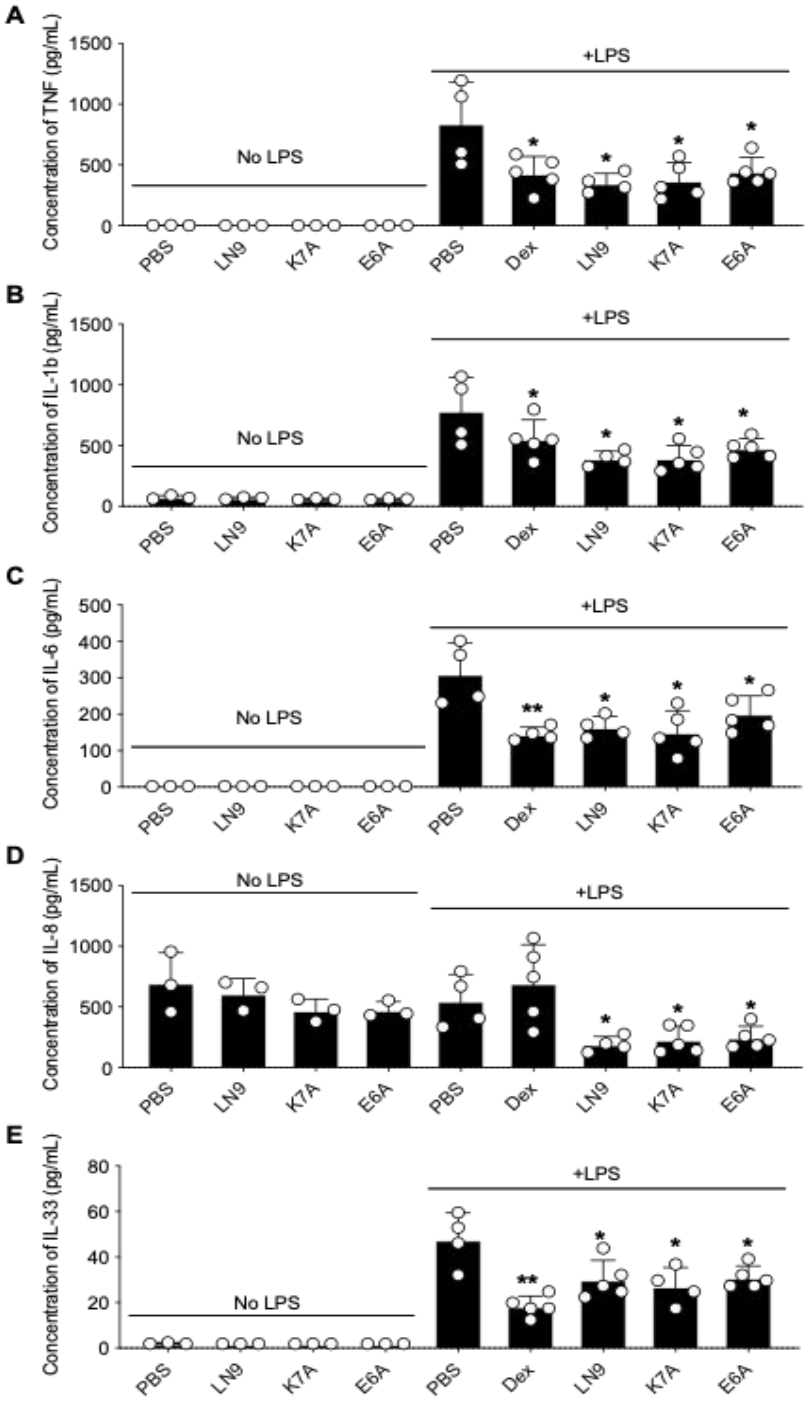

Figure 3.3: Influence of LN9 and mutants on cytokine expression in human macrophage (M1) cells derived from THP-1 monocytes. The cytokines analyzed were TNF (A), IL-1b (B), IL-6 (C), IL-8 (D) and IL-33 (E). 10 µg/mL of LN9 and mutants shows no production of cytokine in M-1-macrophage without lipopolysaccharide (LPS), whereas LPS induced

cytokines – TNF, IL-1β, IL-6, IL-8 and IL-33 were suppressed. PBS and Dexamethasone (Dex) are used as a positive and negative controls respectively. Results were analysed using Unpaired t test in GraphPad Prism 9 displayed by a two-tailed P values (*P≤0.05, **P≤0.01).

The initial results on LN9 and the mutants showed some promising effects. However, significant challenges were faced in reproducing the results. For example, in a repeat PBMC experiment, significant variation in the levels of TNF expressed as a result of LPS was observed between two additional donors, and there was no significant effect following the addition of LN9 (Figure 3.4). This highlights the complications of using different human donors for such an experiment. Further, a repetition of the macrophage (M-1) assay analysing only TNF in the presence of LN9 and the mutants showed significant variations in the results (Figure 3.5). Mutant E6A showed a reduction of TNF but LN9 and K7A did not show significant effects in contrast to the original macrophage assay (Figure 3.3). The peptides used in the assay had not degraded based on mass spectrometry and the experiment was carried out using the same protocol. Consequently, it was not clear where the inconsistency was coming from.

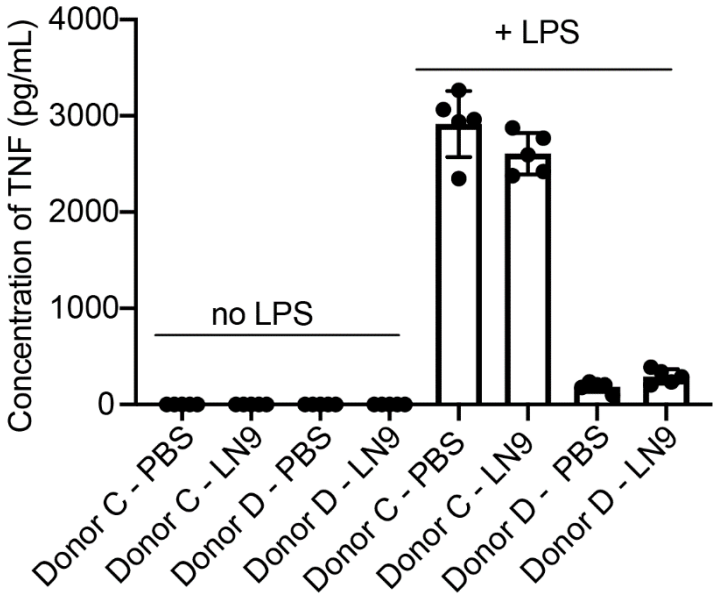

Figure 3.4: LN9 does not reproducibly influence TNF secretion in human cells. Multifunction cytokine TNF analyses in fresh PBMCs in the presence of 75 µg /mL of LN9**.** TNF was not produced in either donor without LPS present. In the presence of LPS, donor D had significantly lower TNF expression compared to donor C but no TNF suppression was observed for either donor and this could be related to the issues of cell viability. Data was analysed using an unpaired t-test in GraphPad Prism 9.

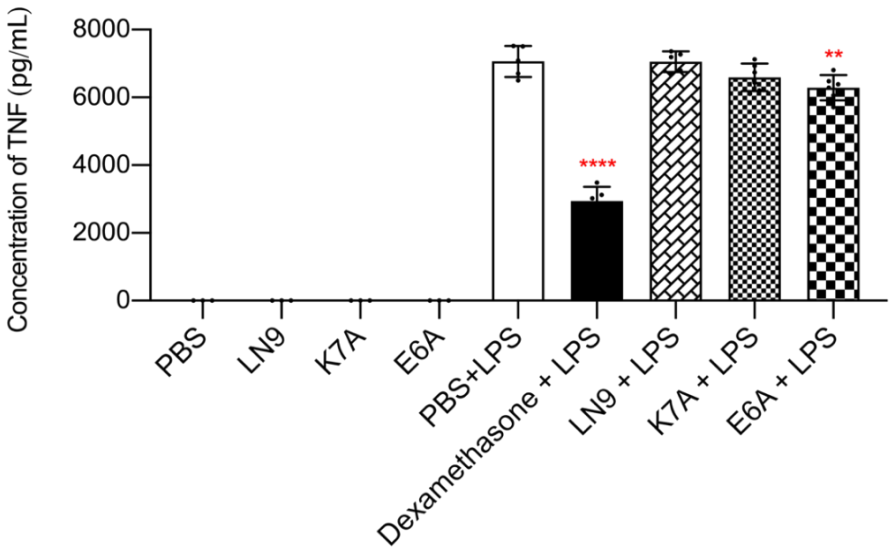

Figure 3.5: Variation in the effect of LN9 peptides in human macrophage (M1) cells derived from THP-1 monocytes. TNF was analysed in the absence and presence of LPS tested with 10 μg/mL peptides (LN9 and mutants) using ELISA kit. No cytokine was induced without LPS, cytokine induced showed no reduction in LN9 and K7A, except E6A compared to positive control (dexamethasone). Data analysed using ordinary one-way ANOVA in GraphPad Prism 9.

The *in vitro* assays suggested that LN9 might have anti-inflammatory effects by suppressing inflammatory cytokines, however given the challenges with the *in vitro* assays, the use of *in vivo* assay could be alternate approach to further explore the potential anti-inflammatory effects of LN9. An allergic asthma mouse model was chosen as anti-inflammatory peptides are known to be bioactive in this model. This model used allergens derived from house dust mite (*Dermatophagoides pteronyssinus*) to induce asthma in mice and, LN9 and a scrambled version (IMEKIQHIEK) were administered to the mice via intraperitoneal (i.p) injection. LN9 had no significant effects on eosinophils, and lymphocytes (T+B-cells), however significant reduction

of neutrophils after administration of 20 μg/mL LN9 peptide. Interestingly the control peptide (scrambled LN9) also showed an effect on neutrophils (Figure 3.6).

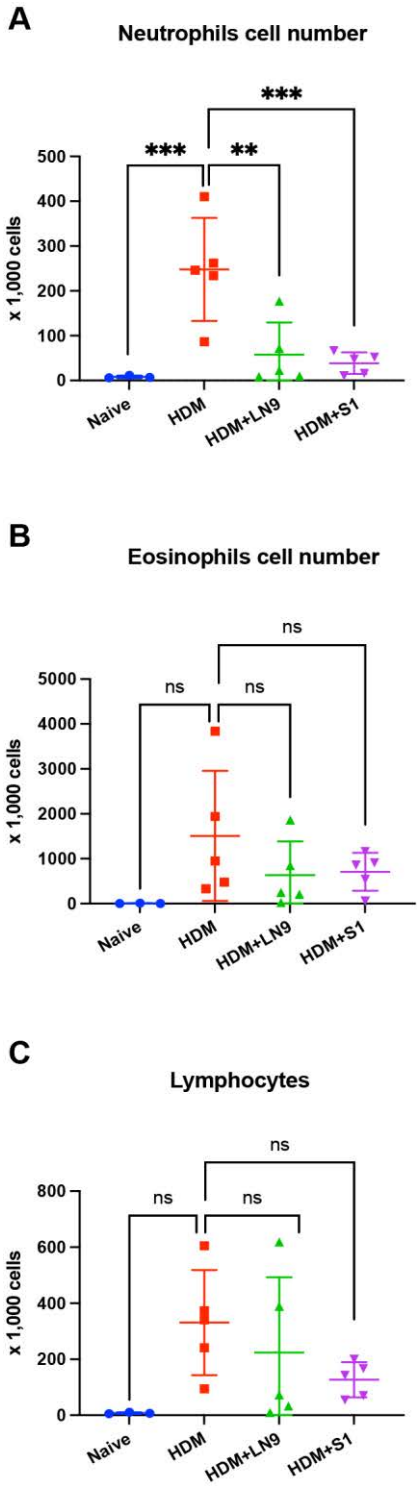

Figure 3.6: Effects of LN9 in a house dust mite (HDM) induced allergic asthma assay in mice. Analyses showed significant reduction of (A) neutrophils cells by LN9 and scramble LN9 (S1), while (B) eosinophils and (C) lymphocytes cells did not show suppression at a concentration of 20μg/mL. Data are shown as mean±SD in GraphPad Prism9. Differences between groups were analysed by one-way ANOVA with multiple comparison (* $p<0.05$, ** $p<0.01$, ***$p<0.0007$).

A repetition of the assay with a new control peptide, S2-scramble (GVLDGGDP), which has previously used as a negative control in an asthma model (12) was utilized in a dose response analysis of the LN9 peptide. Consistent with the first experiment eosinophils, and lymphocytes were not suppressed in the presence of LN9 (Figure 3.7). Neutrophils were again inhibited, but only at a concentration of 100 μg/mL. The variability of results compared to the first assay could be related to age of mice during the time of injection. In the first HDM assay mice were immunized when 4 weeks old while in the repeat assay, immunization occurs at 5 weeks old. Age variability may likely have slight impact on the results. The LN9 mutants were not able to be tested in the *in vivo* assay because of time constraints.

A

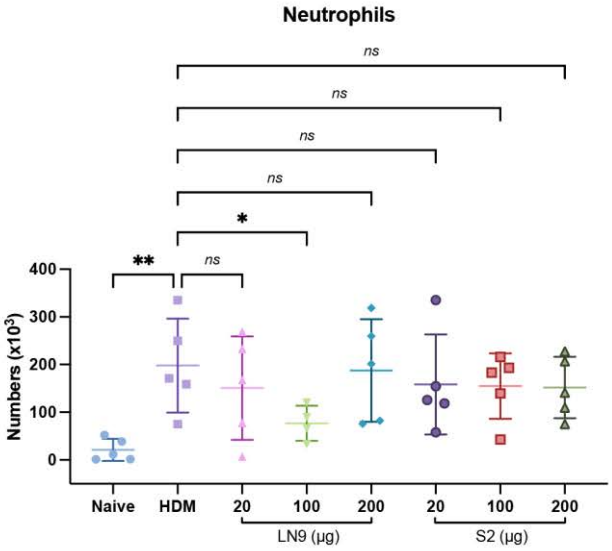
Neutrophils
ns
ns
ns
ns
*
**
ns
Numbers (x10³)
400
300
200
100
0
Naive
HDM
20
100
200
20
100
200
LN9 (µg)
S2 (µg)

B

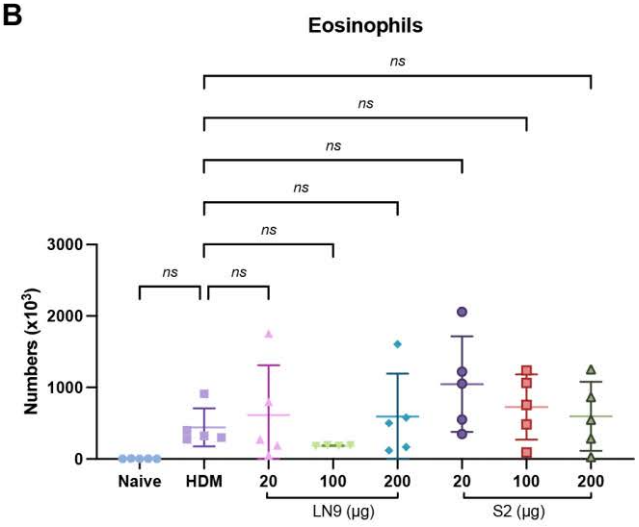
Eosinophils
ns
ns
ns
ns
ns
ns
ns
3000
2000
1000
0
Numbers (x10³)
Naive
HDM
20
100
200
20
100
200
LN9 (µg)
S2 (µg)

C

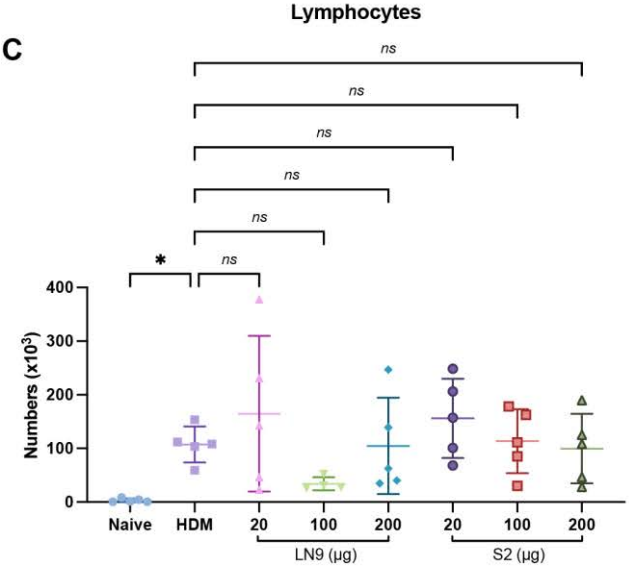
Lymphocytes
ns
ns
ns
ns
ns
*
ns
400
300
200
100
0
Numbers (x10³)
Naive
HDM
20
100
200
20
100
200
LN9 (µg)
S2 (µg)

Figure 3.7: Effects of LN9 on house dust mite induced asthma model in mice. Neutrophils (A) were suppressed at 100 μg/mL, but not at 20 or 200 μg/mL, and eosinophils (B) and lymphocytes (C) were also not affected following treatment with LN9. The control (S2) showed no significant effects to all cells analysed. Data are displayed as mean±SD using GraphPad Prism 9. Differences between groups were analysed by one-way ANOVA with multiple comparison (* $p<0.05$, ** $p<0.01$).

3.4.4. Identification of the conserved sequence motif in non-chromatin binding proteins

Suppression of cytokines is a hallmark of peptides/proteins involved in autoimmune/inflammatory diseases and led us to compare the sequences of proteins that attenuate the effects of in autoimmune disease models such as colitis and asthma, with the LN9 sequence. Intriguingly, a range of proteins/peptide were identified based on literature searches and results from the laboratory, as shown in Table 3.3. These proteins include hookworm proteins (AIP proteins), antrum mucosal proteins (AMP) and a human filarial protein. Fragments of hookworm AIP proteins have also been shown to have anti-inflammatory activity (13) and the sequences are included in the table. The sequences of chromatin binding proteins, which have previously been identified as having homology to lunasin, are also shown. The conserved residues are highlighted in bold and suggest a consensus motif of E/DXXXXEKXI/L/V.

Table 3.3. Proteins and peptides containing a potential anti-inflammatory motif

Protein name	Sequence	Assay/Functions	Residue numbers	Reference
Lunasin	**E**KH-IM**EK-I**Q	Various	(23-31)	(4)
HuHP1	**E**EEYVV**EK-V**L	Chromatin binding	(17-26)	(14)
DmPc	**D**LVYAA**EK-I**I	Chromatin binding	(23-32)	(6, 15)
DMHP1A	**E**EEYAV**EK-I**I	Chromatin binding	(21-30)	(16)
Ac-AIP-1	**D**VSGE-**EK**K**L**L	Colitis	(114-123)	(17)
Ac-AIP-2	**D**VTPE-**E**HD**L**L	Asthma	(110-119)	(18)
AIP2-20	TPEEHDLLMDLMGDPKKAEE	Colitis	(115-134)	(13)
AIP1-13	PSKEKADLGKYKA	Colitis	(125-137)	(13)
ES2-10	SQKEKDLLKE	Colitis	(93-102)	(13)
AMP-18	**D**ALVK-**EK**K**L**Q	T-cell-transfer colitis	(112-121)	(19)
BmALT2	**E**MVVDV**EK**D**V**L	T-cell-transfer colitis	(381-391)	(20)
WbL2	**E**KAQY-**EK-I**H	T-cell-transfer colitis	(87-95)	(21)

3.5. Discussion

Lunasin has a range of potential applications for treating chronic disorders but there is limited understanding of the structure/function relationships, primarily because the peptide is intrinsically disordered. Here we show a nine-residue peptide from lunasin, corresponding to the region with homology to chromatin binding proteins, has a potential role in the anti-inflammatory activity of lunasin.

Our *in vitro* studies suggest that LN9 can reduce inflammatory cytokine production, at least in some human blood donors. Previous studies have shown that genetic variations among donors can affect cytokine production in PBMCs (22, 23). In addition, studies on non-heritable factors such as age, gender and lifestyle also showed variations in the baseline cytokines (24, 25). This donor variation is likely to account for the lack of reproducibility in the PBMC *in vitro* assays. However, further study, including the analysis of dose response is required to determine the reasons for the variation in the macrophage cell line assays.

The indication that LN9 results in suppression of TNF and elevation of IL-10, at least in some donors, suggests the peptide has an anti-inflammatory effect. The *in vivo* asthma study also supports this suggestion with a reduction in neutrophils. There is emerging evidence that neutrophilic asthma is a distinct endotype (26), characterised by high levels of neutrophils in the lungs and airway. The reduction of neutrophils observed in the mouse study in the presence of LN9 suggests the peptide might provide insight into novel approaches for treating this class of asthma.

The combination of LN9 sequence homology with chromatin binding proteins and its apparent effect on neutrophils is intriguing. It has been previously shown that histone proteins, the primary protein components of chromatin, have direct pathogenic effects on neutrophil activation, which induces systematic autoimmune diseases (27, 28). It is possible LN9 is interacting with chromatin and preventing neutrophil activation, but this is only speculation at this stage. Suppression of neutrophils by LN9 might also be related to inhibition of proinflammatory cytokines. Overall, our data suggest LN9 might have potential as an anti-inflammatory therapeutic agent for treating neutrophil-related asthma and autoimmune diseases.

Although reproducibility issues for the *in vitro* assays prevented reliable data on structure/function relationships of LN9, the LN9 scrambled peptide (S1) used in the asthma studies inadvertently provided a suggestion of a key sequence involved in bioactivity. Significant suppression of neutrophils was observed with the scrambled LN9 peptide. As this peptide maintains the IMEK sequence, it is possible these charged residues are important for bioactivity.

Structural analysis of LN9 with NMR spectroscopy indicates it is disordered/unstructured in solution, consistent with the intrinsically disordered nature of the full-length peptide. However, several amide protons, including Glu6, Lys7 and Ile8 were evident in the LN9 NMR spectra following dissolution in D_2O, indicating the presence of hydrogen bonds. Glu6 and Ile8 showed the slowest exchange making it possible to determine the exchange rates. This region of the full-length lunasin peptide has previously been shown to have a propensity to form a helical structure and the presence of these slowly exchanging amide protons, suggests that the nine

residue LN9 peptide also has this propensity. The apparent stabilization by hydrogen bonds is unusual for a small peptide, particularly in the absence of additional covalent restraints such as disulfide bonds. However, ES2-10 and AIP1-13, AIP-derived peptides (Table 3.3) also show the presence of slowly exchanging amide protons (13) despite showing no regular secondary structure in solution. Our mutational studies indicate that Glu6 in LN9 has a role in the formation of hydrogen bonds and given that the side chain of this residue can adopt a negative charge it is possible that a salt bridge is important in this role. By contrast, mutating the conserved lysine residue (Lys7 in LN9) did not influence the slow exchange properties significantly.

A previous study relating to chromatin binding in *Drosophila* heterochromatin protein - DmHP1A, revealed that mutating isoleucine 30 to phenylalanine (highlighted in bold in the sequence in Table 3.3), resulted in the loss of chromatin targeting activity (16). In the sequence analysis in Table 3.3, this position is invariably an Ile/Leu/Val residue and this conservation is consistent with this residue/position having an important role in bioactivity. Determining whether this residue is important in the cytokine suppression observed for LN9 requires more study. Furthermore, the relationship between chromatin binding and anti-inflammatory activity is as yet unclear but some studies have suggested a link with the conformation of chromatin and auto-inflammatory disease (29).

The conservation of the sequence motif present in LN9 with chromatin binding proteins and proteins with anti-inflammatory activity suggests the possibility of a similar biological target. The mechanism of action for the AIP proteins and the other peptides/proteins with activity in

the T-cell transfer colitis model (Table 3.3) have not been determined and a possible link with chromatin binding has not been explored, but the sequence similarity warrants further study.

To summarise, the chromatin binding region in lunasin has an influence on cytokine expression, appears to be stabilized by hydrogen bonds and it is conserved in not only chromatin binding proteins but other anti-inflammatory peptides and proteins. The insights gained from these studies indicates we have identified a conserved anti-inflammatory sequence motif, prevalent throughout nature, and has potential in developing novel lead molecules against anti-inflammatory and autoimmune related diseases.

3.6. References

1. Davis K, Inaba J-i. Lunasin—a multifunctional anticancer peptide from soybean. International Journal of Cancer Therapy and Oncology. 2016;4(2):4218.

2. de Mejia EG, Dia VP. The role of nutraceutical proteins and peptides in apoptosis, angiogenesis, and metastasis of cancer cells. Cancer and Metastasis Reviews. 2010;29(3):511-28.

3. Hsieh C-C, Chou M-J, Wang C-H. Lunasin attenuates obesity-related inflammation in RAW264. 7 cells and 3T3-L1 adipocytes by inhibiting inflammatory cytokine production. PLoS One. 2017;12(2):e0171969.

4. de Mejia EG, Dia VP. Lunasin and lunasin-like peptides inhibit inflammation through suppression of NF-κB pathway in the macrophage. Peptides. 2009;30(12):2388-98.

5. Wealth thru nutirtion. Reliv Australia Products 2021 [Available from: https://www.wealththrunutrition.com/au/reliv-products/#lunarichx.

6. Assland R, stewart F. The chromo shadow domain, a second chromo domain in heterochromatin-binding protein 1, HP1. Nucleic Acids Res. 1995;23(16):3168-73.

7. Furuta K, Chan EK, Kiyosawa K, Reimer G, Luderschmidt C, Tan EM. Heterochromatin protein HP1 Hsβ (p25β) and its localization with centromeres in mitosis. Chromosoma. 1997;106(1):11-9.

8. Wishart DS, Bigam CG, Holm A, Hodges RS, Sykes BD. 1 H, 13 C and 15 N random coil NMR chemical shifts of the common amino acids. I. Investigations of nearest-neighbor effects. J Biomol NMR. 1995;5(1):67-81.

9. Chanput W, Mes JJ, Savelkoul HF, Wichers HJ. Characterization of polarized THP-1 macrophages and polarizing ability of LPS and food compounds. Food Funct. 2013;4(2):266-76.

10. Yan X, Zhang H, Watson J, Schimerlik MI, Deinzer ML. Hydrogen/deuterium exchange and mass spectrometric analysis of a protein containing multiple disulfide bonds: Solution structure of recombinant macrophage colony stimulating factor-beta (rhM-CSFβ). Protein Sci. 2002;11(9):2113-24.

11. Daly NL, Craik DJ. Acyclic permutants of naturally occurring cyclic proteins: characterization of cystine knot and β-sheet formation in the macrocyclic polypeptide Kalata B1. Journal of Biological Chemistry. 2000;275(25):19068-75.

12. Kim DY, Park BS, Hong GU, Lee BJ, Park JW, Kim SY, et al. Anti-inflammatory effects of the R2 peptide, an inhibitor of transglutaminase 2, in a mouse model of allergic asthma, induced by ovalbumin. British journal of pharmacology. 2011;162(1):210-25.

13. Cobos C, Bansal PS, Wilson DT, Jones L, Zhao G, Field MA, et al. Peptides derived from hookworm anti-inflammatory proteins suppress inducible colitis in mice and inflammatory cytokine production by human cells. Frontiers in Medicine. 2022:2743.

14. Saunders WS, Chue C, Goebl M, Craig C, Clark RF, Powers JA, et al. Molecular cloning of a human homologue of Drosophila heterochromatin protein HP1 using anti-centromere autoantibodies with anti-chromo specificity. Journal of cell science. 1993;104(2):573-82.

15. Epstein H, James TC, Singh PB. Cloning and expression of Drosophila HP1 homologs from a mealybug, Planococcus citri. Journal of cell science. 1992;101(2):463-74.

16. Messmer S, Franke A, Paro R. Analysis of the functional role of the Polycomb chromo domain in Drosophila melanogaster. Genes & development. 1992;6(7):1241-54.

17. Ferreira IB, Pickering DA, Troy S, Croese J, Loukas A, Navarro S. Suppression of inflammation and tissue damage by a hookworm recombinant protein in experimental colitis. Clinical & translational immunology. 2017;6(10):e157.

18. Navarro S, Pickering DA, Ferreira IB, Jones L, Ryan S, Troy S, et al. Hookworm recombinant protein promotes regulatory T cell responses that suppress experimental asthma. Science translational medicine. 2016;8(362):362ra143-362ra143.

19. Chen P, Bakke D, Kolodziej L, Lodolce J, Weber CR, Boone DL, et al. Antrum mucosal protein-18 peptide targets tight junctions to protect and heal barrier structure and function in models of inflammatory bowel disease. Inflammatory bowel diseases. 2015;21(10):2393-402.

20. Khatri V, Amdare N, Yadav RS, Tarnekar A, Goswami K, Reddy MVR. Brugia malayi abundant larval transcript 2 protein treatment attenuates experimentally-induced colitis in mice. 2015.

21. Togre NS, Bhoj PS, Khatri VK, Tarnekar A, Goswami K, Shende MR, et al. SXP–RAL Family Filarial Protein, rWbL2, Prevents Development of DSS-Induced Acute Ulcerative Colitis. Indian Journal of Clinical Biochemistry. 2018;33(3):282-9.

22. Li Y, Oosting M, Smeekens SP, Jaeger M, Aguirre-Gamboa R, Le KT, et al. A functional genomics approach to understand variation in cytokine production in humans. Cell. 2016;167(4):1099-110. e14.

23. Li Y, Oosting M, Deelen P, Ricano-Ponce I, Smeekens S, Jaeger M, et al. Inter-individual variability and genetic influences on cytokine responses to bacteria and fungi. Nature medicine. 2016;22(8):952-60.

24. Brodin P, Jojic V, Gao T, Bhattacharya S, Angel CJL, Furman D, et al. Variation in the human immune system is largely driven by non-heritable influences. Cell. 2015;160(1-2):37-47.

25. Ter Horst R, Jaeger M, Smeekens SP, Oosting M, Swertz MA, Li Y, et al. Host and environmental factors influencing individual human cytokine responses. Cell. 2016;167(4):1111-24. e13.

26. Crisford H, Sapey E, Rogers GB, Taylor S, Nagakumar P, Lokwani R, et al. Neutrophils in asthma: the good, the bad and the bacteria. Thorax. 2021;76(8):835-44.

27. Smith CK, Vivekanandan-Giri A, Tang C, Knight JS, Mathew A, Padilla RL, et al. Neutrophil extracellular trap–derived enzymes oxidize high-density lipoprotein: an additional proatherogenic mechanism in systemic lupus erythematosus. Arthritis & rheumatology. 2014;66(9):2532-44.

28. Silvestre-Roig C, Braster Q, Wichapong K, Lee EY, Teulon JM, Berrebeh N, et al. Externalized histone H4 orchestrates chronic inflammation by inducing lytic cell death. Nature. 2019;569(7755):236-40.

29. Mirlekar B, Gautam D, Chattopadhyay S. Chromatin remodeling protein SMAR1 is a critical regulator of T helper cell differentiation and inflammatory diseases. Frontiers in immunology. 2017;8:72.

CHAPTER 4: Effects of cyclization on an anti-inflammatory peptide

Reynold Philip, David T. Wilson, Roland Rusher, Kim Miles, Paramjit S. Bansal, Alex Loukas, Norelle L. Daly

4.1. Abstract

Hookworms produce a myriad of Excretory/Secretory (ES) Products (lipids, carbohydrates, proteins and secondary metabolites) that enable them to survive throughout their different life stages. Several ES products have shown potential as anti-inflammatory drugs for conditions such as IBD and asthma. A 10-residue peptide (ES2-10) derived from *Ace*ES2, a protein secreted by *Ancylostoma ceylanicum*, displayed anti-inflammatory activity *in vitro* and *in vivo*. However, ES2-10 was degraded in human serum within 4 hours. Here, we engineered two analogues (a cyclic and extended form of ES2-10) that promoted structural stability in solution and also demonstrated a greater stability in serum compared to ES2-10. However, conformational changes to the cyclic version of ES2-10 caused a decrease in the bioactivity. The extended variant maintains the structure of the ES2-10 peptide, but further study is required to determine the bioactivity of this peptide.

4.2. Introduction

Hookworm infections affect almost 500 million people worldwide, predominantly in the tropical regions of South America, Africa and Asia (1). Most of these infections are caused by *Necator americanus*, *Ancylostoma ceylanicum* and *A. duodenale* species (2), and can result in iron deficiency anaemia, which is a clinical hallmark of hookworm infection (3, 4).

Despite the pathogenic effects of hookworm infection, several studies have indicated that the coexistence of hookworms with humans plays a significant role in reducing autoimmune diseases (5, 6). Autoimmune diseases/conditions such as asthma and inflammatory bowel disease (IBD) have a significant impact on healthcare systems and with the limited treatment options (7), there is great need for new drug leads for therapeutic development.

Recent studies on live helminth therapy in low subclinical doses have demonstrated promising levels of success in managing autoimmune conditions (8, 9). For instance, human trials with anthropophilic and zoonotic (pig) hookworm have efficaciously treated a number of patients with chronic inflammatory conditions such as IBD, multiple sclerosis, allergies and celiac disease (8, 9, 10, 11, 12). Although the therapy is promising, it has challenges especially in apprehension of patients to accept live helminths, safety and regulatory problems. To overcome these challenges several studies have involved characterizing the bioactive components within the helminth secretions. Analysis of the hookworm secretome has identified several molecules with anti-inflammatory activities. Several metabolites have been identified in the secretions of *A. caninum* (13), and the tapeworm *Dipylidium caninum* (14) that display protection against TNBS induced acute colitis and cytokine suppression in PBMC assays (13). In addition, the *A.*

caninum proteins *Ac*-AIP 1 and *Ac*-AIP-2 have been shown to have activity in mouse models of colitis (15, 16) and asthma (17) respectively. Recombinant forms of these proteins significantly alleviate the disease symptoms, reduce immunopathology and suppress expression of inflammatory cytokines.

The promising activities of hookworm AIP proteins has led to structure/function relationship analyses. In particular, a "reductionist" approach, which involves determining the bioactive regions of larger proteins (18, 19), has been applied. This approach can be valuable for designing peptide-based drug leads that have lower immunogenicity, greater tissue penetration, and are cheaper to manufacture than larger proteins (20, 21). Although selecting a bioactive segment in proteins is not necessarily straightforward, we have recently identified a conserved sequence motif in hookworm AIP proteins with anti-inflammatory activity. In the *Ace*ES-2 protein this region corresponds to a 10-residue sequence that has a helical structure in the full-length protein (22). NMR experimental data on hydrogen/deuterium exchange rates indicated the presence of hydrogen bonds but the peptide does not appear to have a defined structure in solution. The peptide displays significant protective effects in a TNBS mouse model of colitis and supresses pro-inflammatory cytokines in PBMC assays but is degraded in human serum. This sequence motif has similarity to the lunasin LN9 peptide described in Chapter 3.

Several approaches have been used to enhance the stability of peptides including the introduction of covalent constraints as well as stabilizing elements of secondary structure (23, 24, 25, 26, 27). In this study, we examined the influence of disulfide-linked cyclization, and extension of the helical region on the structural stability and bioactivity of ES2-10 variants.

4.3. Experimental procedures

4.3.1. Peptide synthesis and purification

Peptides were synthesised, purified and the masses analysed using the methods described in Chapter 2. The purified linear peptide containing cysteine residues was oxidised in 0.1 M ammonium bicarbonate (pH 8.5) for 48 hours. After 24-hours, the native mass was reduced by 2 Da indicating disulfide bond formation had occurred.

4.3.2. NMR spectroscopy

Lyophilized peptides were resuspended to a final concentration of ~0.2 mM in 90%H2O:10%D_2O. 2D^{1}H-^{1}H TOCSY, ^{1}H-^{1}H NOESY, ^{1}H-^{1}H DQF-COSY, ^{1}H-^{15}N HSQC, and ^{1}H-^{13}C HSQC spectra were acquired at 290 K using a 600 MHz AVANCE III NMR spectrometer (Bruker, Karlsruhe, Germany) equipped with a cryogenically cooled probe. All spectra were recorded with an interscan delay of 1 s. NOESY spectra were acquired with mixing times of 200-300 ms, and TOCSY spectra were acquired with isotropic mixing periods of 80 ms. Standard Bruker pulse sequences were used with an excitation sculpting scheme for solvent suppression. Slowly exchanging amide protons were detected by acquiring a series of one-dimensional and TOCSY spectra over a 24-hour period, following dissolution of the peptides in D_2O. Exchange rates were calculated as previously described for comparison of acyclic and cyclic peptides (33).

The 2D NOESY spectra of ES2-10-cyc and DGL-ES2-10 were automatically assigned and an ensemble of structures calculated using the program CYANA (34). Torsion-angle restraints from TALOS+ were used in the structure calculations. Final structures were visualized using MOLMOL (37).

4.3.3. Cytokine assay (THP-1 derived M1 macrophages)

Macrophage cells derived from THP-1 were used to induce cytokines against peptides to assess its inhibitory effects. With the method described in section 3.5 of Chapter 2, cell assay was performed and data was interpreted using a statistical method in GraphPad Prism 9.

4.3.4. Assay on PBMCs derived from frozen blood

Among different cell used for cytokine assay, PBMCs was generated from frozen blood to assess inhibition of cytokines by peptides using the method described in Chapter 3. Generated data were analysed using unpaired T - test Statistical methods in Prism 9.

4.3.5. Serum stability assay

The serum stability of the peptides was tested using human male AB plasma (Sigma-Aldrich) following methods previously described (28). Peptides were tested at each time point in triplicate. Human serum was prepared by centrifugation at 17,000g for 10 min to remove the lipid component. Supernatant was incubated for 15 min at 37°C prior to the assay. 200 μM stock solution of each peptide was diluted (1:10) in 100% human serum or PBS and incubated

at 37°C. 30 µL aliquots were taken at 0 h, 3 h, 8 h and 24 h. The aliquots of serum were denatured by quenching with 30 µL of 3 M urea and incubated for 10 minutes at 4°C. Serum proteins were precipitated with the addition of 30 µL of 7% trichloroacetic acid for 10 min at 4ºC. PBS received the same treatment as serum. Subsequently, the samples were centrifuged at 17000 g for 10 min. 90 µL of supernatant was analysed by RP-HPLC at a flow rate of 0.4 mL/min using a Phenomenex Jupiter Proteo C12 analytical column (150 x 2.00 mm, 4 µm, 90 Å). A linear 1% min^{-1} acetonitrile gradient (0-50% B) was used for the analysis. The elution time for each peptide was determined by the PBS control for that time point. The absorbance of the eluent was observed using a dual wavelength UV detector set to 215nm and 280nm. The stability at each time point was calculated as the amplitude/area of the serum treated peptide peak on RP-HPLC at 214 nm as percentage of the amplitude/area of the 0 hour PBS treated control peptides.

4.4. Results

4.4.1. Peptide design and synthesis

To determine if cyclization or helical stabilization enhances the stability of ES2-10, two variants referred to as ES2-10-cyc and DGL-ES2-10 were synthesised using Fmoc chemistry. ES2-10-cyc has cysteine residues at the N- and C-termini which were oxidised to form a cyclic peptide. Oxidation occurred effectively within 48 hours and the final oxidized mass of the peptide was decreased by 2Da indicating the peptide had cyclised. DGL-ES2-10 is an extended version with three additional residues, corresponding to the residues present in the full-length protein. The sequences of the synthetic peptides, and the location of the helical region corresponding to ES2-10 in the protein structure are shown in Figure 4.1.

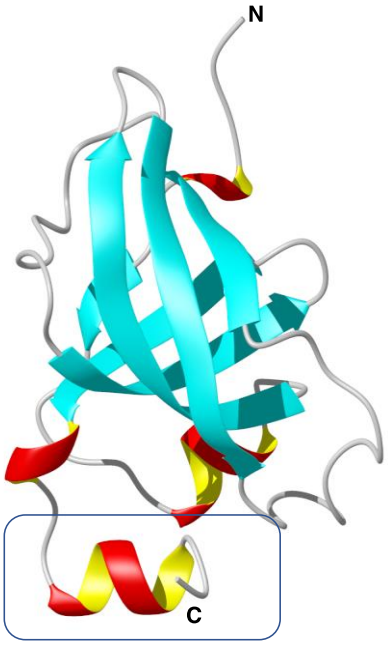

(A) ES2-10 (*Aes*ES2 protein)

ES2-10 : SQKEKDLLKE

DGL-ES2-10: DGLSQKEKDLLKE

ES2-10-cyc: CSQKEKDLLKEC

(B) Sequence of ES2-10 and analogues

Figure 4.1: *Ace*ES2 Protein structure and its derived ES2-10 peptide and analogues. (A) *Ace*ES2 protein with boxed helical region corresponding to native ES2-10 peptide, (B) shows sequence of ES2-10 and variants. The cyclic variant (ES2-10-cyc) involves a disulfide bond between the N- and C-termini. The extended variant has three residues (DGL) added to ES2-10 sequence.

4.4.2. Structural analyses using NMR spectroscopy

The structures of the ES2-10 analogues were analysed in aqueous solution using NMR spectroscopy. Both peptides displayed significant dispersion in the amide region, and a single set of resonances for each residue. Analysis of the TOCSY and NOESY spectra of ES2-10-cyc

and-DGL-ES2-10 allowed assignment of the majority of the proton resonances. The secondary chemical shifts (secondary shifts) were determined by subtracting random-coil chemical shifts from the α-H chemical shifts (29). A comparison of the secondary shifts of ES2-10-cyc, and DGL-ES2-10 with ES2-10 is given in Figure 4.2.

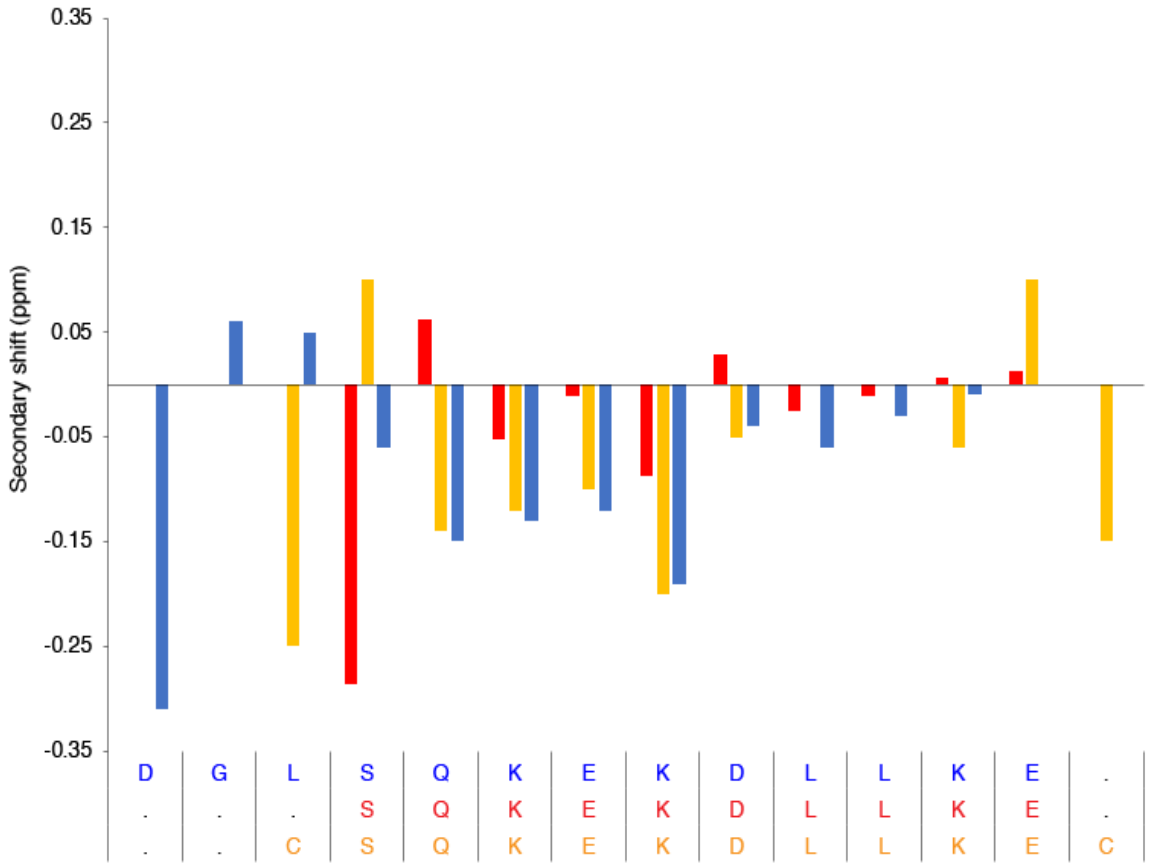

Figure 4.2: Secondary shifts of ES2-10 and variants. The sequences and secondary shifts are shown in red for ES2-10, orange for ES2-10-cyc and blue for DGL-ES2-10.

As published previously, the majority of the secondary shifts for ES2-10 are between +/- 0.1 ppm indicating no regular secondary structure. The lack of secondary structure was consistent with the lack of non-sequential NOEs in the NOESY spectra, which prevented determination of the three-dimensional structure (30). However, ES2-10 had several slowly exchanging amide protons, indicating the presence of hydrogen bonds. Hydrogen bonds are usually found in regular elements of secondary structure which appears inconsistent with the NOE data, but this might be related to the dynamics of the peptide structure.

In contrast to ES2-10, both ES2-10-cyc and DGL-ES2-10 had several consecutive secondary shifts more negative than -0.1 ppm suggesting the presence of helical structure from residues 3-6 and 5-8 respectively (QKEK). The residues with slowly exchanging amide protons in these peptides are displayed in Table 4.1.

Table 4.1: Slow exchanging amide protons in residues of ES2-10, ES2-10-cyc and DGL-ES2-10 peptides.

Peptide	Residue	Exchange rate (k_{ex}) (min^{-1})
ES2-10	Leu 7	0.0022
	Leu 8	0.0003
ES2-10-cyc	Leu 8	0.008
	Leu 9	0.036
DGL-ES2-10	Lys 6	0.0248
	Glu 7	0.0330
	Lys 8	0.0329
	Leu 10	0.0232
	Leu 11	0.0146
	Lys 12	0.0267
	Glu 13	0.0371

The residues undergoing slow exchange are listed with their exchange rates (K_{ex}) values that fall within $0.1>k_{ex}>0.002min^{-1}$ reflecting slow exchanging rates of amide protons with 100% deuterium (D_2O).

Both of the adjacent leucine residues in ES2-10 and ES2-10-cyc have slow exchanging amide protons, indicative of hydrogen bonds. The extended variant had seven slowly exchanging amide protons, consistent with a well-defined three-dimensional structure.

The structures of ES2-10-cyc and DGL-ES2-10 were calculated based on distance restraints derived from the NOESY spectra, angle restraints based on TALOS+ and hydrogen bond restraints based on the slow exchange data and preliminary structures. The structural statistics are given in Table 4.2A and 4.2B respectively for ES2-10-cyc and DGL-ES2-10. Despite the small size of the peptides they displayed relatively well-defined structures.

Table 4.2A: Structural statistics for the ES2-10-cyc ensemble

Experimental restrains	
Interproton distance restraints	99
Intraresidue, | *i-j* |=0	47
Sequential, |*i-j* |= 1	31
Medium range, 1<|*i-j*|< 5	21
Dihedral angle restraints	9
Hydrogen bond restraints	
(2 restraints per bond)	2
R.m.s deviations from mean coordinate Structure (Å)	
Backbond atoms	0.26±0.09
All heavy atoms	1.41±0.24
Ramachandran statistics	
% in most favoured region	96
% in additionally allowed region	4

Table 4.2B: Structural statistics for the DGL-ES2-10 ensemble

Experimental restrains	
Interproton distance restraints	142
Intraresidue, | *i-j* |=0	56
Sequential, |*i-j* |= 1	45
Medium range, 1<|*i-j*|< 5	41
Dihedral angle restraints	12
Hydrogen bond restraints	
(2 restraints per bond)	10
R.m.s deviations from mean coordinate Structure (Å)	
Backbond atoms	1.42±0.61
All heavy atoms	2.17±0.57
Ramachandran statistics	
% in most favoured region	93.3
% in additionally allowed region	6.7

Despite the similar secondary shifts for DGL-ES2-10 and ES2-10-cyc and NOE patterns, the helical regions in the three-dimensional structures do not superimpose well, with an RMSD of 2.314 Å, over the backbone atoms of residues Q5-L10 and K6-E11 respectively. MOLMOL identifies a helical structure from residues Q5-K12 in DGL-ES2-10 and residues K6 to E11 in ES2-10-cyc. Structural comparison with the *Ace*ES-2 protein structure indicates that the DGL-ES2-10 peptide has maintained the fold of the native protein (Figure 4.3). An RMSD of 0.270 Å was calculated for the backbone atoms of the helical regions (Q94-L99) and (Q5-L10) for DGL-ES2-10 and *Ace*ES2 respectively. The distinct helical structure of ES2-10-cyc conformation could not be superimposed with the *Ace*ES-2 protein structure.

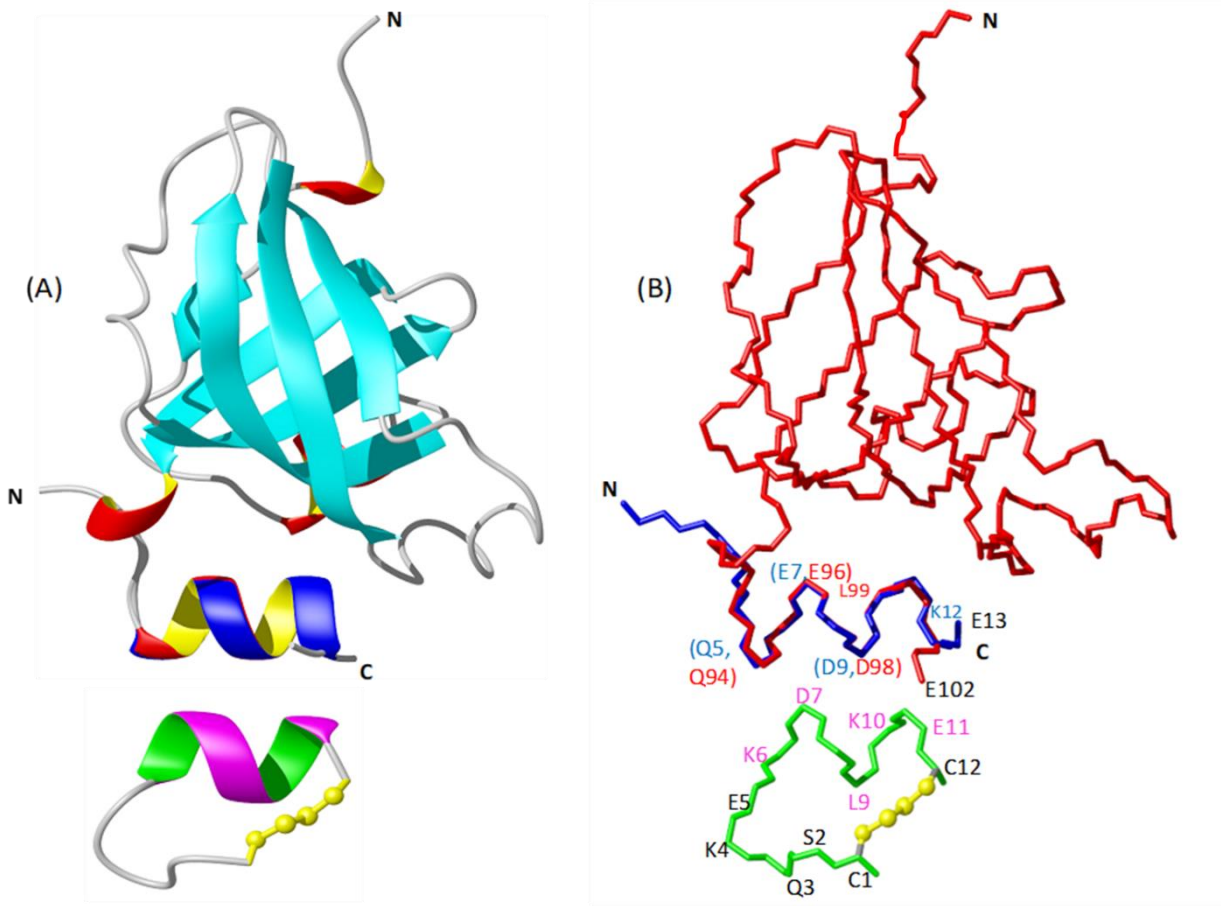

Figure 4.3: Structural comparison of the ES2-10 region in *Ace*ES2 protein with peptide variants. Panel (A) shows the structure of the full-length protein in ribbon format with DGL-ES2-10 superimposed over the corresponding region and in Panel (B), the backbone is shown in stick format. DGL-ES2-10, shown in blue, overlays well with the ES2-10 region in the protein structure (RMSD 0.270 Å). By contrast, superimposing residue 5-9 of ES2-10-cyc shown at the bottom of panels A and B has an RMSD of 2.314 Å as the helix is shifted in this peptide with respect to the helix in the protein structure. The residues within the helical regions are colour coded in red, blue and green representing ES2-10, DGL-ES2-10 and ES2-10-cyc respectively. A great contrast is observed in ES2-10-cyc helical region compared to ES2-10 and DGL-ES2-10. The figure was prepared using MOLMOL (31).

4.4.3. Serum Stability Assay

The serum stability assay was carried out over a 24-hour timeframe and showed both cyclization and N-terminal extension enhanced the stability of ES2-10 (Figure 4.4). Cyclisation of ES2-10 with a disulfide bond showed the greatest enhancement, and although DGL-ES2-10 was completely degraded at the end of the experiment more than 50% remained at the 8 hour time point.

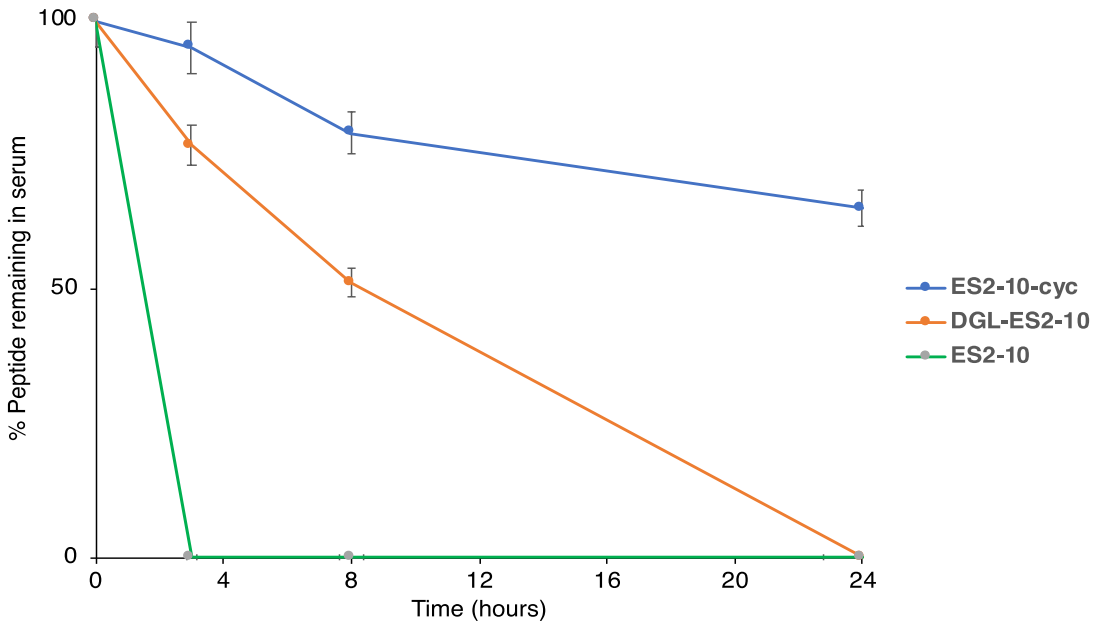

Figure 4.4: Comparison of serum stability of ES2-10, ES2-10-cyc and DGL-ES2-10 peptide. A high percentage of ES2-10-cyc was remaining at 24 hours, indicating that the peptide is quite stable. DGL-ES2-10 remains above 50% in serum at 8 hours, which is significantly more stable peptide than ES2-10 which was not detected at the 3 hour time point.

4.4.4. Cytokine analysis using macrophage cells and PBMCs

Having shown that the ES2-10 peptide could be stabilized in human serum it was of interest to determine if the bioactivity was maintained. Challenges with the *in vitro* assays, outlined in Chapter 3, also plagued these studies and only preliminary data could be obtained. A cytokine assay was conducted in a macrophage (M-1) cells derived from THP-1 human monocyte cells. Cells without LPS treatment showed no sign of cytokine production when incubated with ES2-10 or ES2-10-cyc (Figure 4.5). However, M-1 cells in the presence of LPS induced cytokines, which were reduced by ES2-10 for all the cytokines tested. By contrast, ES2-10-cyc did not show a reduction of cytokine expression. The assays were repeated on macrophages and additional assay on PBMC were also carried out, but overall the results were inconsistent preventing solid conclusions being drawn. Further validation of the assays is required.

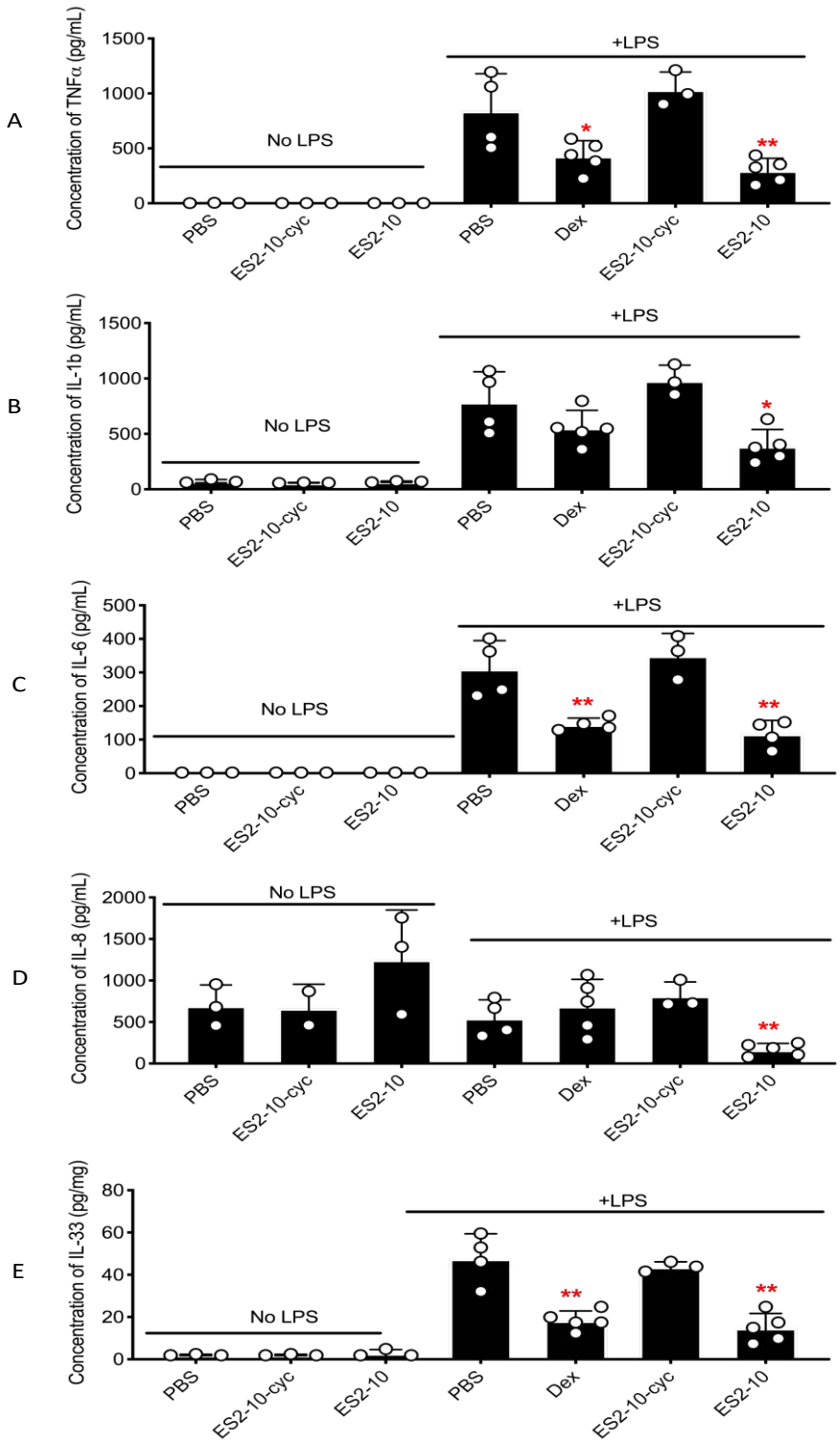

Figure 4.5: Cytokine results of ES2-10 and ES2-10-cyc in Macrophage (M-1) cells treated with and without LPS. Panels 4A, 4B, 4C,4D and 4E represent concentration of cytokines - TNF, IL-1b, IL-6, IL-8 and IL-33 respectively. Cells treated with LPS induce cytokines that are reduced by ES10, but not ES2-10-cyc. No activity in ES2-10-cyc could be linked to

structural conformation. Dexamethasone (Dex) was used as a positive control. Data analysed using unpaired t-test in Prism 9 indicate two-tailed P-value (*$p<0.05$, **$p<0.01$)

4.5. Discussion

ES2-10 shows protective effects in a TNBS mouse model of colitis and supresses pro-inflammatory cytokines in PBMC assays but does not form a well-defined structure in solution and is not stable in the human serum (30). Here we show that the serum stability can be enhanced through cyclization and N-terminal extension of the peptide sequence. Preliminary *in vitro* assays suggest relatively minor structural changes might be having a significant influence on bioactivity but further study is required to assess the effect of these changes on bioactivity.

Cyclization of the ES2-10 sequence had a significant impact on the three-dimensional structure. The effects of cyclising ES2-10 with a disulfide bond caused a shift in the helical region from its native position in the *Ace*ES-2 protein (residues Q94-L99) to K6-E11 in ES2-10-cyc (Figure 4.3). By contrast, N-terminal extension maintained the native structure. Addition of residues to the ES2-10 sequence appears to have allowed additional hydrogen bonds to form leading to a well-defined helical structure in solution. Two additional residues (Leu 11 and Lys12) form part of helical region of DGL-ES2-10 compared to the ES2-10 region in the protein structure.

Although the ES2-10 peptide is not structured in solution it is likely it can adopt an appropriate conformation upon binding to a biological target. The apparent lack of activity of ES2-10-cyc in the macrophage assay could be related to the disulfide bond constraining the peptide into a non-native conformation and preventing it from forming an appropriate conformation. Based on this line of thought, we would hypothesise that DGL-ES2-10 would maintain activity given

the similarity in structure to the native protein. Furthermore, it would potentially have enhanced potency as a result of the enhanced stability. Similar effects have been observed in other studies which have aimed to enhance the stability of bioactive peptides. For example, Cobos Caceres et al (30) showed that grafting a tripeptide into a cyclic framework not only enhanced the stability of the peptide in human serum but also improved the potential in a mouse model of colitis.

In summary, cyclisation of ES2-10 significantly affected the structure of ES2-10, enhanced the stability but possibly at the expense of the bioactivity. However, it is promising to observe that an extended version of ES2-10 has a defined helical structure in solution similar to the full-length protein, with improved stability in human serum compared to ES2-10 that may require further activity assay. It is of interest to examine the effect of both analogues in *in vivo* models of colitis and HDM allergic asthma which could give a clear indication of structure-function relationships of the ES2-10 analogues.

4.6. Reference

1. Pullan RL, Smith JL, Jasrasaria R, Brooker SJ. Global numbers of infection and disease burden of soil transmitted helminth infections in 2010. Parasites & vectors. 2014;7(1):37.

2. Farthing MJ, Keusch GT. Enteric Infection: Mechanisms, Manifestations, and Management: Chapman & Hall; 1989.

3. Traub RJ. Ancylostoma ceylanicum, a re-emerging but neglected parasitic zoonosis. International journal for parasitology. 2013;43(12-13):1009-15.

4. George S, Levecke B, Kattula D, Velusamy V, Roy S, Geldhof P, et al. Molecular identification of hookworm isolates in humans, dogs and soil in a tribal area in Tamil Nadu, India. PLoS neglected tropical diseases. 2016;10(8).

5. Weinstock JV, Elliott DE. Helminths and the IBD hygiene hypothesis. Inflammatory bowel diseases. 2009;15(1):128-33.

6. Helmby H. Human helminth therapy to treat inflammatory disorders-where do we stand? BMC immunology. 2015;16(1):12.

7. To T, Stanojevic S, Moores G, Gershon AS, Bateman ED, Cruz AA, et al. Global asthma prevalence in adults: findings from the cross-sectional world health survey. BMC public health. 2012;12(1):204.

8. Loukas A, Hotez PJ, Diemert D, Yazdanbakhsh M, McCarthy JS, Correa-Oliveira R, et al. Hookworm infection. Nature Reviews Disease Primers. 2016;2:16088.

9. Summers RW, Elliott DE, Urban Jr JF, Thompson RA, Weinstock JV. Trichuris suis therapy for active ulcerative colitis: a randomized controlled trial. Gastroenterology. 2005;128(4):825-32.

10. Maizels RM. Parasitic helminth infections and the control of human allergic and autoimmune disorders. Clinical Microbiology and Infection. 2016;22(6):481-6.

11. Fleming J, Hernandez G, Hartman L, Maksimovic J, Nace S, Lawler B, et al. Safety and efficacy of helminth treatment in relapsing-remitting multiple sclerosis: results of the HINT 2 clinical trial. Multiple Sclerosis Journal. 2019;25(1):81-91.

12. Croese J, Giacomin P, Navarro S, Clouston A, McCann L, Dougall A, et al. Experimental hookworm infection and gluten microchallenge promote tolerance in celiac disease. J Allergy Clin Immunol. 2015;135(2):508-16. e5.

13. Wangchuk P, Shepherd C, Constantinoiu C, Ryan RY, Kouremenos KA, Becker L, et al. Hookworm-derived metabolites suppress pathology in a mouse model of colitis and inhibit

secretion of key inflammatory cytokines in primary human leukocytes. Infection and immunity. 2019;87(4).

14. Wangchuk P, Constantinoiu C, Eichenberger RM, Field M, Loukas A. Characterization of tapeworm metabolites and their reported biological activities. Molecules. 2019;24(8):1480.

15. Ferreira IB, Pickering DA, Troy S, Croese J, Loukas A, Navarro S. Suppression of inflammation and tissue damage by a hookworm recombinant protein in experimental colitis. Clinical & translational immunology. 2017;6(10):e157.

16. Mulvenna J, Hamilton B, Nagaraj SH, Smyth D, Loukas A, Gorman JJ. Proteomics analysis of the excretory/secretory component of the blood-feeding stage of the hookworm, Ancylostoma caninum. Molecular & Cellular Proteomics. 2009;8(1):109-21.

17. Navarro S, Pickering DA, Ferreira IB, Jones L, Ryan S, Troy S, et al. Hookworm recombinant protein promotes regulatory T cell responses that suppress experimental asthma. Science translational medicine. 2016;8(362):362ra143-362ra143.

18. Harrison RS, Shepherd NE, Hoang HN, Ruiz-Gómez G, Hill TA, Driver RW, et al. Downsizing human, bacterial, and viral proteins to short water-stable alpha helices that maintain biological potency. Proceedings of the National Academy of Sciences of the United States of America. 2010;107(26):11686-91.

19. Reid RC, Yau M-K, Singh R, Hamidon JK, Reed AN, Chu P, et al. Downsizing a human inflammatory protein to a small molecule with equal potency and functionality. Nature Communications. 2013;4(1):2802.

20. Fosgerau K, Hoffmann T. Peptide therapeutics: current status and future directions. Drug discovery today. 2015;20(1):122-8.

21. Sachdeva S. Peptides as 'Drugs': The Journey so Far. International Journal of Peptide Research and Therapeutics. 2017;23(1):49-60.

22. Kucera K, Harrison LM, Cappello M, Modis Y. Ancylostoma ceylanicum excretory–secretory protein 2 adopts a netrin-like fold and defines a novel family of nematode proteins. Journal of molecular biology. 2011;408(1):9-17.

23. Li Y, Bi T, Camarero JA. Chemical and biological production of cyclotides. Advances in botanical research. 76: Elsevier; 2015. p. 271-303.

24. Harris KS, Durek T, Kaas Q, Poth AG, Gilding EK, Conlan BF, et al. Efficient backbone cyclization of linear peptides by a recombinant asparaginyl endopeptidase. Nature communications. 2015;6(1):1-10.

25. Dawson PE, Muir TW, Clark-Lewis I, Kent S. Synthesis of proteins by native chemical ligation. Science. 1994;266(5186):776-9.

26. Arnison PG, Bibb MJ, Bierbaum G, Bowers AA, Bugni TS, Bulaj G, et al. Ribosomally synthesized and post-translationally modified peptide natural products: overview and recommendations for a universal nomenclature. Natural product reports. 2013;30(1):108-60.

27. Camarero JA, Pavel J, Muir TW. Chemical synthesis of a circular protein domain: evidence for folding-assisted cyclization. Angewandte Chemie International Edition. 1998;37(3):347-9.

28. Chan LY, Gunasekera S, Henriques ST, Worth NF, Le S-J, Clark RJ, et al. Engineering pro-angiogenic peptides using stable, disulfide-rich cyclic scaffolds. Blood. 2011;118(25):6709-17.

29. Wishart DS, Bigam CG, Holm A, Hodges RS, Sykes BD. 1 H, 13 C and 15 N random coil NMR chemical shifts of the common amino acids. I. Investigations of nearest-neighbor effects. J Biomol NMR. 1995;5(1):67-81.

30. Cobos C, Bansal PS, Wilson DT, Jones L, Zhao G, Field MA, et al. Peptides derived from hookworm anti-inflammatory proteins suppress inducible colitis in mice and inflammatory cytokine production by human cells. Frontiers in Medicine. 2022:2743.

31. Koradi R, Billeter M, Wüthrich K. MOLMOL: a program for display and analysis of macromolecular structures. Journal of molecular graphics. 1996;14(1):51-5.

CHAPTER 5: Characterization of an *Na*-APR-2 derived peptide as a vaccine target

Reynold Philip, Paramjit Bansal, Guangzu Zao, David T. Wilson, Luke Becker, Darren Pickering, Bemnet Tedla, Alex Loukas and Norelle L. Daly

5.1. Abstract

Human helminth infections cause devastating morbidity and mortality in developing countries, yet there are no vaccines against these complex multicellular pathogens. Several compounds have been identified with potential in vaccine development, including an epitope derived from the human hookworm, *Necator americanus*, *Na*-APR-1 protein. Given that helminths have several developmental stages expressing unique antigens, it is of interest to explore epitopes from a range of hookworm proteins. *Na*-APR-2 is a pepsin-like aspartic protease from *N. americanus* that is distinct from *Na*-APR-1 and is primarily expressed in the L3 stage of development in contrast to *Na*-APR-1 which is more abundant in the adult stage. In the current study an epitope ($G_{350}Y$) from *Na*-APR-2 was designed based on the *Na*-APR-1 epitope, and antibodies shown to be produced when the synthetic peptide was administered with intraperitoneal injection. By contrast, no antibodies were generated in mice when the peptide was administered orally, most likely because $G_{350}Y$ is not structurally well-defined based on NMR analysis and could have fragmented by the digestive enzymes. To assess the bioactivity of the synthetic $G_{350}Y$ peptide in inhibiting *Na*-APR-2, recombinant *Na*-APR-2 was bacterially expressed, and purified from inclusion bodies but was not bioactive based on an *in vitro* haemoglobin assay displayed by evidence of hemoglobin bands on the SDS-PAGE gel. It appears likely the protein did not refold correctly. Alternate folding conditions, or recombinant protein expression systems may be required to produce correctly folded *Na*-APR-2 and further explore the potential of $G_{350}Y$ as a potential vaccine antigen.

5.2. Introduction

Human helminth (worm) infections cause devastating morbidity and mortality in developing countries (1, 2), yet there are no vaccines against these complex multicellular pathogens. Efforts are underway to develop vaccines against infections with the human hookworm, *Necator americanus*. Hookworm infection affects almost 500 million people in developing tropical regions (3). The hookworm parasites primarily feed on intestinal blood and establish chronic infections that can last for decades. Heavy intensity infections can led to iron-deficiency anaemia, which drastically affects intellectual development and weakens the neurological functions in children, can reduce productivity in adults and have a significant impact during pregnancy (4, 5). Chemotherapy using benzimidazole drugs such as albendazole is used to treat the adult parasites, but the efficacy is limited in some studies and reinfection rapidly occurs after treatment (6, 7). The development of a vaccine holds significant promise for inducing immunologic resistance to hookworm infections.

Several potential vaccine antigens have been found in the different developmental stages of mammalian hookworms (8, 9), and among them is *Na*-APR-1 (10). *Na*-APR-1 is a 45 kDa cathepsin-D-like aspartic protease found in the gut of adult *N. americanus* and is responsible for initiating the haemoglobin digestive cascade (11). Inhibiting *Na*-APR-1 proteolytic activity kills the parasites by preventing it from obtaining nutrients. Antibodies raised to a recombinant form of *Na*-APR-1 have been shown to inhibit its ability to digest haemoglobin, and the recombinant protease confers protection in canine and hamster models of human hookworm infection (12, 13). For example, recombinant *Na*-APR-1 used in vaccination trials in dogs effectively reduced the adult parasite loads and blood loss compared to unchallenged dogs

(control) (10, 12). However, expressing this protein on a large scale has been challenging (14), which is likely to limit its potential as a subunit vaccine. It is unclear why the yields of this protein have been low in the expression but mutational studies might provide insight into the factors of the protein that are responsible for this effect.

Elucidating the epitopes involved in the protective antibody response might provide an alternative source of vaccine candidates, and this approach has been applied to *Na*-APR-1. Using a series of overlapping fragments from *Na*-APR-1, Pearson and co-workers (15) mapped out an epitope region which corresponds to residues 291 to 303. This peptide was termed $A_{291}Y$ (AGPKAQVEAIQKY), and is the target of monoclonal antibodies that neutralise the proteolytic activity of *Na*-APR-1, consequently inhibiting its ability to cleave synthetic and natural substrates (15).

$A_{291}Y$ requires adjuvants to induce an antibody response, but Skwarczynski et al., 2012 (14), introduced a self-adjuvating lipid core peptide (LCP) system that effectively triggered a strong immune response when incorporated with the $A_{291}Y$ peptide. Upon vaccination of mice, the new chimeric LCP construct induced effective production of antibodies that inhibit the proteolytic activity of *Na*-APR-1. The LCP system has also been used in a recent study involving three chimeric peptides (p1, p2 and p3) derived from the $A_{291}Y$ epitope. A β sheet peptide (p1) conjugated to LCP was developed that demonstrated the potential of inducing antibodies that blocked the enzymatic activity of the native hookworm protease (16, 17). Recently, oral delivery of *Na*-APR-1 combined with chimeric peptide -p3 incorporated with lipids, liposomes and polymers has demonstrated 98% reduction of intestinal rodent hookworms *(Nippostrongylus brasiliensis*) and 99% egg burdens effectively in immunized

mice (18). These studies show that the LCP system has significant potential for subunit vaccine development and can drive protective antibody responses (19, 20).

Given that helminths have several developmental stages expressing unique antigens, it is of interest to explore epitopes from a range of antigens. *Na*-APR-2 is a pepsin-like aspartic protease from *N. americanus* that is distinct from *Na*-APR-1 and is primarily expressed in the L3 stage of development in contrast to *Na*-APR-1 which is more abundant in the adult stage (21). The sequences of *Na*-APR-1 and *Na*-APR-2 have only 30% sequence identity and distinct activities (21). *Na*-APR-1 can neutralise haemoglobin proteolysis at an optimum pH of 5.5. It is regarded as an upstream protease because it can cleave and expose other sites to cascading proteolysis by other proteases such as cystine proteases, metalloproteases or aspartic proteases (11, 21). However, recombinant *Na*-APR-2 is capable of digesting complete haemoglobin *in vitro* and is most active at a much lower pH, and cleaves at multiple distinct sites compared to *Na*-APR-1 (21). Therefore, it is of interest to explore epitopes from *Na*-APR-2, that could neutralise the recombinant form of *Na*-APR-2, as potential vaccine candidates.

Here we produced a fragment from *Na*-APR-2 comprising 14 residues and termed it $G_{350}Y$ (GAPRGILRSIARQY). Based on the sequence alignment between *Na*-APR-1 and *Na*-APR-2, $G_{350}Y$ is equivalent to $A_{291}Y$ (AGPKAQVEAIQKY) from *Na*-APR-1. Antibodies raised using the epitope $G_{350}Y$ could be a potential vaccine antigen against human hookworm, and we have carried out preliminary studies aimed at achieving this goal.

5.3. Experimental procedures

5.3.1. Peptide Synthesis and Purification

Peptide $G_{350}Y$, truncated from *Na*-APR-2, was synthesised manually using Fmoc chemistry on a 0.1 mmole scale. The peptide was synthesised using 2-chlorotrityl chloride resin, which was swelled in dimethylformamide (DMF) before amino acid coupling. The amino acids were activated with 10% DIEPA and coupled to the resin followed by washing with 20% piperidine in DMF. The peptide was cleaved from the resin using trifluoroacetic acid (TFA)/water/trisisopropylsilane (95:2.5:2.5) for 2-3 hours, precipitated with diethyl ether, dissolved in 50% acetonitrile, 0.05% TFA and subsequently lyophilized. The resulting crude peptide was purified with an Agilent RP-HPLC using a C-18 preparative column (Phenomenex Jupiter 250 x 21.2mm) using a 1% gradient of solvent B (solvent A: 0.05% TFA; solvent B: 90% acetonitrile, 0.05% TFA). The mass was analysed using a 5800 MALDI TOF-TOF (SCIEX) mass spectrometer.

5.3.2. NMR Spectroscopy

Lyophilized peptide $G_{350}Y$ was resuspended with 90% water:10% deuterium (D_2O) (500 µL:50 µL) to acquire 1D and 2D (TOCSY, NOESY) spectra at 290 K using a 600 MHz AVANCE III NMR spectrometer (Bruker, Karlsruhe, Germany). Secondary shifts were calculated by subtracting random coil chemical shifts (22) from the experimental alpha proton shifts, which

can indicate if peptides have secondary structure or not. Slowly exchanging amide protons were analysed from a series of one-dimensional and TOCSY spectra recorded over 24 hours after dissolution of the peptide in 100% D_2O. The peptide solution was pH 4 prior to lyophilisation for the exchange experiment. No three-dimensional structure calculations were done for this peptide as the chemical shifts, lack of non-sequential NOEs in the NOESY spectra, and slowly exchanging amide protons were consistent with a random coil structure.

5.3.3. Ethics Statement

All experimental procedures performed on animals in this study were approved by the James Cook University animal ethics committee (A2391). All experiments were performed in accordance with the 2007 Australian Code of Practice for the Care and Use of Animals for Scientific Purposes and the 2001 Queensland Animal Care and Protection Act.

5.3.4. Intraperitoneal (IP) Immunization of BALB/c mice

A group of five male BALB/c mice (8-10 week-old) were intraperitoneally immunized with 50 μg of $G_{350}Y$ per mouse. Naïve (natural/unaffected) sera via tail bleeding was collected from each mouse two days prior to immunization, with sera diluted 10-fold (10 μL:90 μL). Peptide was mixed with an equal volume of Imject alum adjuvant (Thermo Fisher Scientific), each formulated with 5 μg of CpG ODN1826 (InvivoGen, San Diego, CA, USA) and administered four times, two weeks apart. Two weeks after the final immunization, mice were sacrificed, and blood was collected via cardiac puncture. Blood from the five mice was pooled and serum was separated by centrifugation at 3500 g for 20 minutes after clotting and stored at -30°C.

5.3.5. Oral Immunization of BALB/c mice

A group of four (8-10 week-old) male BALB/c mice (Animal Resources Centre, Perth, WA, Australia) were employed for the study. Naïve (natural/unaffected) sera via tail bleeding was collected from each mouse with sera diluted 10-fold (10 µL:90 µL) in PBS two days prior to immunization. The mice were orally immunized via oral gavage with cholera toxin subunit B (CTB) mixed with the peptide. Vaccine doses contained 100 µg of antigen in 100 µL of PBS formulated with 10 µg CTB. Four immunizations were given to a group of four mice, with two-week intervals between doses. Two weeks after the final immunization, mice were sacrificed, and blood was collected via cardiac puncture. Blood from the four mice were separated by centrifugation after clotting and stored at -30°C.

5.3.6. Antibody detection using Enzyme-linked immunosorbent assays (ELISA)

Enzyme-linked immunosorbent assays (ELISA) were used to evaluate antibody titers of $G_{350}Y$ peptide using 96-well, flat bottom and high binding affinity plates (Greiner Bio-One, Germany). The plates were coated with 100 µL of solution in carbonate buffer (pH 9.6) with $G_{350}Y$ peptide (5 µg/mL per well) and incubated overnight at 4°C. PBS containing 0.05% tween 20 (PBST) was used as wash buffer. The plate was washed three times using PBST, then dried by tapping. The plates were blocked with 200 µL PBST containing 5% skim milk, incubated overnight or at room temperature for 2 hours and then washed with PBST. PBST with 0.5% skim milk was added to the plates at a volume of 90 µL to the wells in the first column, and 50 µL to all remaining wells. Then, 10 µL of neat serum from each mouse was added to first-

column wells, and the plates were mixed and serially diluted (2-fold) along plate rows using a multichannel pipette (Biotools Pty Ltd, Australia). The plates were incubated at room temperature for 2 hours or 37°C for 90 minutes, then washed using wash buffer, and dried by tapping. Secondary antibody solution (100 µL, 1/4000 diluted in PBST with 0.5% skim milk) of either goat anti-mouse IgG-(H+L) (62-6520, InvivoGen, San Diego, CA, USA), goat anti-mouse IgA Cross Adsorbed (62-6720, InvivoGen, San Diego, CA, USA) was added to the wells depending on antibody isotype or subclass of interest. The plates were incubated again at room temperature for 2 hours or 37°C for 90 min, then washed three time with wash buffer, and dried by tapping. Finally, horseradish peroxidase tertramethylbenzidine substrate was applied and kept in dark for 30 mins. The reaction was stopped using 100 µL of 2 N sulfuric acid and the absorbance of each well was measured at 450 nm using a Polarstar Omega microplate reader (BMG Labtech).

5.3.7. *Na*-APR-2 Recombinant Protein expression

5.3.7.1. Cloning of cDNA and molecular modelling

A codon optimised gene construct covering full-length matured *Na*-APR-2 sequence was ordered from Genscript and cloned into pET41a expression vector (Novagen) such that the N-terminal GST tag was removed. The plasmid construct is shown in Figure 5.1.

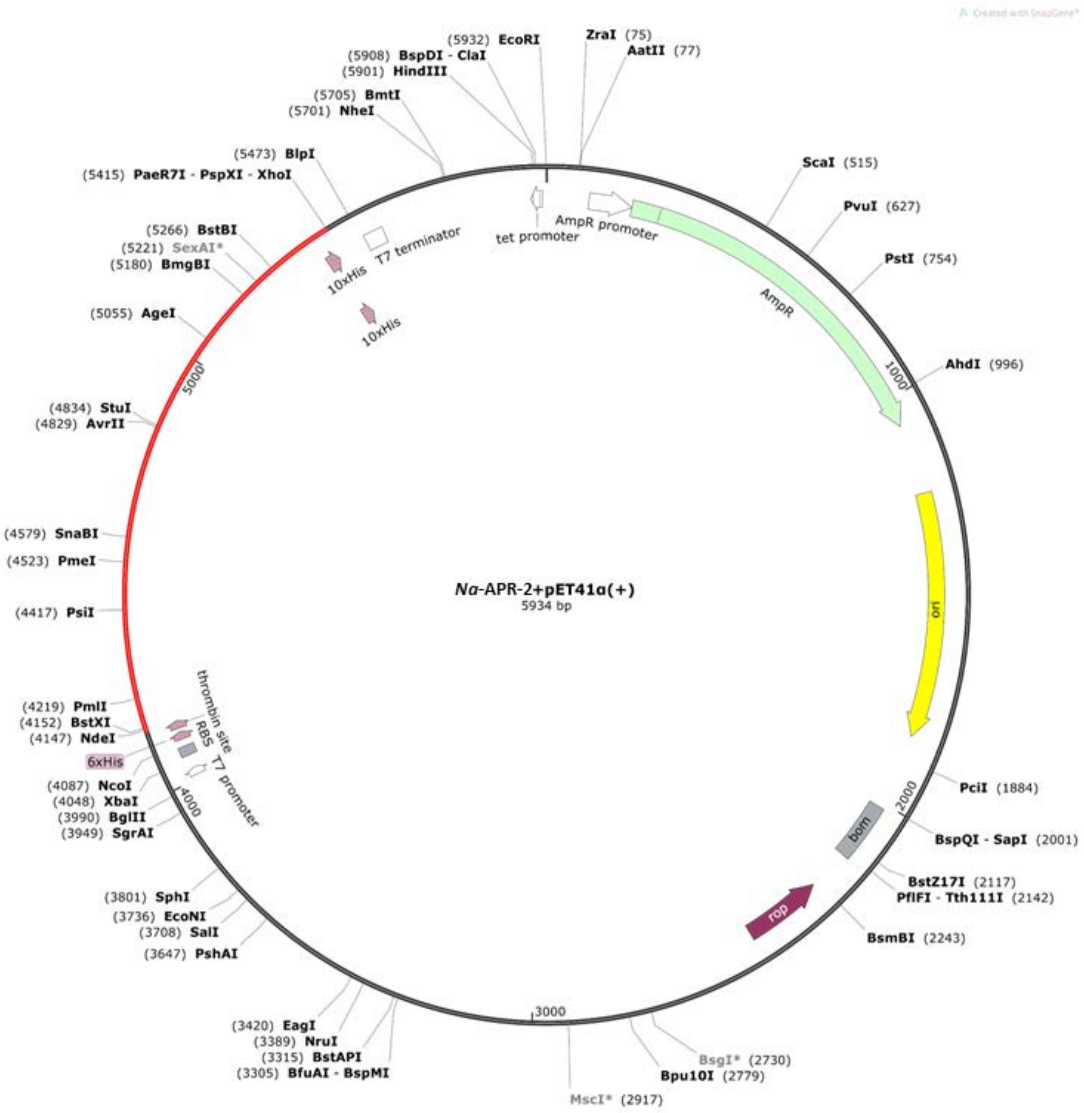

Figure 5.1: Circular plastid map of *Na*-APR-2 clones in pET41a(+) expression vector with Ndel and XhoI restriction enzyme sites and *Na*-APR-2 transcription sense shown in red.

Note: the GST fusion tag was removed from the multicloning site (MCS).

5.3.7.2. Expression of *Na*-APR-2 in bacteria (*E. coli*)

Aspartic protease expression was induced for 24 h in *E. coli* BL21 (DE3) at 4°C by the addition of 1 mM isopropyl beta-D-1-thiogalactopyranoside (IPTG) using standard methods. Cultures were harvested by centrifugation (8000 *g* for 20 min at 4°C), re-suspended in 50 mL lysis buffer (50 mM sodium phosphate, pH 8.0, 300 mM NaCl, 40 mM imidazole) and stored at -80°C . Cell pellets were lysed by three freeze-thaw cycles at -80°C and 42°C, followed by sonication on ice (10 x 5 s pulses [70% amplitude] with 30 s rest periods between each pulse) with a Qsonica Sonicator. Triton X-100 was added to the lysate at a final concentration of 3% and incubated for 1 h at 4°C with end-over-end mixing. Insoluble material (containing *Na*-APR-2) was pelleted by centrifugation at 20,000 *g* for 20 min at 4°C. The supernatant was discarded, and inclusion bodies (IBs) were washed twice by resuspension in 30 mL of lysis buffer, followed by centrifugation at 20,000 *g* for 20 min at 4°C. IBs were then solubilized sequentially by resuspension in 25 mL lysis buffers containing either 2, 4, or 8 M urea; end-over-end mixing overnight at 4°C; and centrifugation at 20,000 *g* for 20 min at 4°C.

5.3.7.3. Purification of denatured aspartic proteases

The supernatant containing solubilized IBs was diluted 1:4 in lysis buffer containing 8 M urea and filtered through a 0.22 μm membrane (Millipore). Solubilized IBs were purified by immobilized metal affinity chromatography (IMAC) by loading onto a prepacked 1 mL His-Trap HP column (GE Healthcare) equilibrated with lysis buffer containing 8 M urea at a flow rate of 1 mL/min using an AKTA-pure-25 FPLC (GE Healthcare). After washing with 20 mL

lysis buffer containing 8 M urea, bound His-tagged proteins were eluted using the same buffer with a stepwise gradient of 50-250 mM imidazole (50 mM steps). Fractions containing *Na*-APR-2 (as determined by SDS-PAGE) were pooled and concentrated using Amicon Ultra-15 centrifugal devices with a 3 kDa molecular weight cut off and quantified using the Pierce BCA Protein Assay kit. The final concentration of each *Na*-APR-2 was adjusted to 1 mg/mL and proteins were aliquoted and stored at -80°C.

5.3.7.4. Refolding of purified *Na*-APR-2

Aliquots of purified, denatured recombinant *Na*-APR-2 (1.0 mg/mL) were refolded at a concentration of 10 µg/mL in 0.1 M Tris (pH 8.0) with different concentrations (0-1.0 M) of L-arginine with and without 5.0 mM/0.5 mM reduced and oxidized glutathione (GSH/GSSG) for 16 h at 4°C with gentle stirring. After removal of urea, protein solutions were dialyzed against two changes of PBS (pH 7.4) at 4°C using 10-kDa cutoff dialysis tubing. The first dialysis was for 3 h, and the final dialysis was overnight. Refolded *Na*-APR-2 protein was concentrated to volumes approximating the starting volume similar to that of denatured *Na*-APR-1 (reported in study by Pearson et, al., 2010 (15)) using Amicon Ultra-15 centrifugal concentration devices, followed by centrifugation at 16,000 g for 10 min at 4°C to remove any precipitate. The yield of refolded protein was determined by comparative gel densitometry with bovine serum albumin (BSA) standards, and catalytic activity was assessed by cleavage of a fluorogenic peptide substrate (see below).

5.3.7.5. Determination of catalytical activity of *Na*-APR-2

The ability of recombinant *Na*-APR-2 to cleave haemoglobin (Hb) was determined by incubation of 1.0 µg of each recombinant protein with 1.0 µg of human Hb in 50 mM sodium acetate (NaAc) (pH 3.5) at 37°C in a final reaction volume of 100 µL. Hydrolysates were collected at hourly intervals from 1 to 6 h and after 16 h, and analysed by SDS-PAGE for evidence of Hb hydrolysis. Control reactions without enzyme and with the addition of 1.0 µM pepstatin A were also performed and analysed after 16 h.

5.4. Results

5.4.1. Peptide Synthesis

The synthetic G_{350}Y(GAPRGILRSIARQY) *Na*-APR-2 derived peptide was purified to purified >95% purity using RP-HPLC, and subsequently used for NMR and analysis and antibody studies.

5.4.2. NMR Structural analysis

The structure of G_{350}Y was analysed in aqueous solution using NMR spectroscopy. The peptide displayed sharp peaks in the one-dimensional spectra indicating the presence of monomeric structures. Resonance assignments were primarily done using two-dimensional TOCSY and NOESY spectra (24). Analysis of the secondary chemical shifts is shown in Figure 5.2. The secondary shifts of G_{350}Y were less than +/- 0.1 ppm for the majority of residues, indicating G_{350}Y is unstructured. No amide proton signals were detected in the slow exchange experiment, indicating that all the amide protons in G_{350}Y were in fast exchange with deuterium. Both the secondary shifts and the amide exchange experiments were consistent with the peptide being unstructured. Consecutive secondary shifts more positive than 0.1 ppm are indicative of β-sheet structures, whereas consecutive secondary shifts more negative than 0.1 ppm are indicative of helical structures.

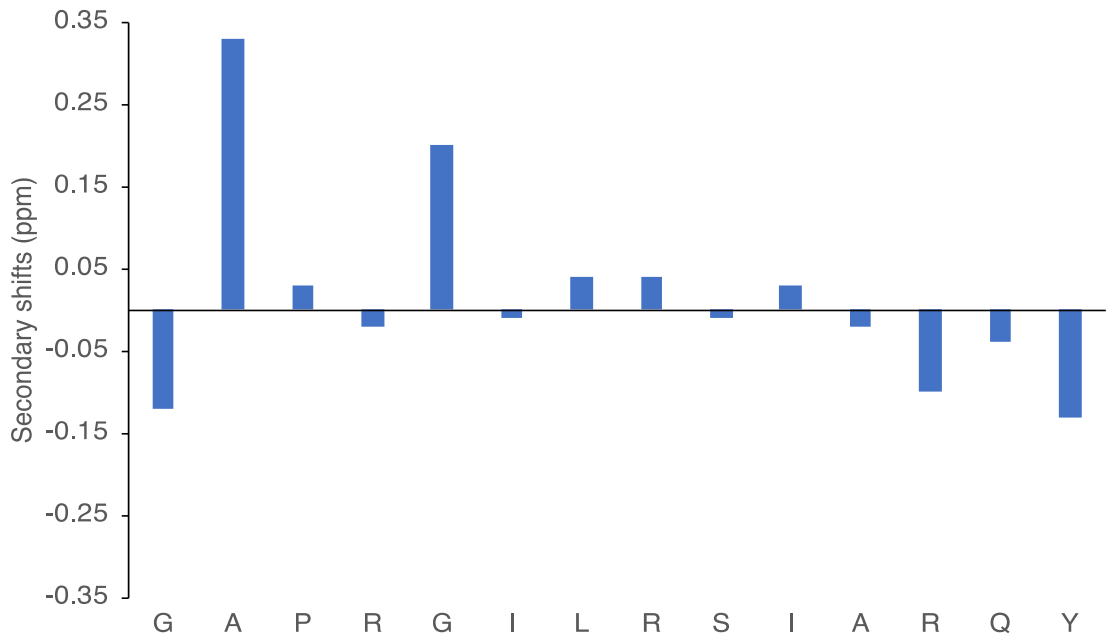

Figure 5.2: Secondary shifts of $G_{350}Y$. The secondary shifts were determined by subtracting the random coil shifts from the alpha proton shifts. The random coil shifts were taken from Wishart et al (1995) (22).

5.4.3. Antibody sera

Mice intraperitoneally injected with $G_{350}Y$ and alum adjuvant produced antibodies in their serum, in contrast to mice where the peptide was orally administered in the presence of CTB adjuvant. Secondary antibodies for IgG and IgA were used with serum obtained from IP and oral administered mice respectively in ELISA tests. ELISA on IP serum showed the presence of IgG antibodies but nothing was observed from the serum obtained from orally administered mice for IgA antibodies. Figure 5.3 shows the antisera titer from IP serum.

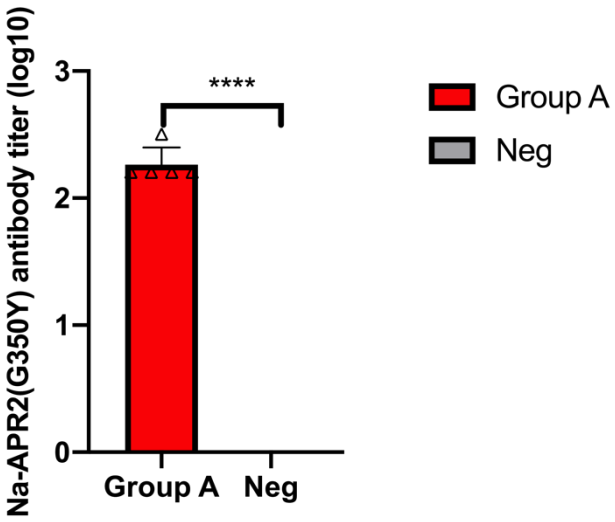

Figure 5.3: Mean specific antibody titer from $G_{350}Y$. An unpaired T-test in Prism 9 shows a significant IgG-monoclonal antibody (IgG-mAb) production (****p<0.0001) from the IP administered mice (Group A) indicated by red bar. The negative (Neg) control is the baseline serum before first IP injection. No IgA-mAb was detected in serum obtained from the orally administered mice using the gavage (results not shown).

5.4.4. Recombinant expression of *Na*-APR-2 using bacteria *(E. coli*)

Recombinant *Na*-APR-2 was successfully cloned and expressed in bacteria. The product was fractionated with immobilized metal affinity chromatography (IMAC) and analysis of the fractions with SDS-PAGE indicated that fractions 3 to 8 contained *Na*-APR-2 in purified form.

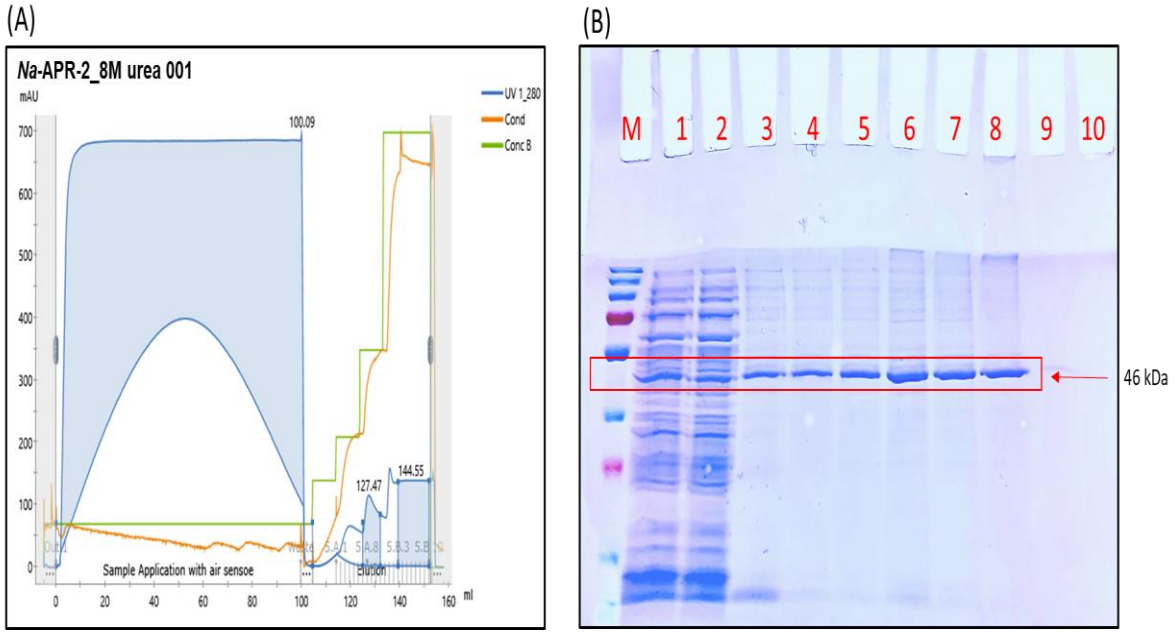

Figure 5.4: Overview of *Na*-APR-2 purification results. (A) Chromatogram illustrating the step-by-step purification procedure applied to *Na*-APR-2 cell lysate solution using HisTrap HP column in an AKTA FPLC system. Absorbance at 280 nm is shown as a blue peak in the spectrum. (B) SDS–PAGE examination of the IMAC data presented in (A) fractions were analysed using 12% SDS-PAGE followed by Coomassie Brilliant Blue staining. Protein marker (lane M), sample lysate (lane 1), flow through (lane 2), eluted fractions (lanes 3-10). Eluted fractions 3-8 shows pure *Na*-APR-2 (46 kDa).

5.4.4.1. Refolded Na-APR-2

The eluted fractions containing *Na*-APR-2 were pooled and refolded with oxidized/reduced glutathione using dialysis. The glutathione solution was exchanged with PBS overnight resulting in final PBS-refolded protein mixture in the dialysis tubing, which was concentrated using an Amicon Ultra-15 centrifuging tube. A concentrate of 1.2 mL refolded *Na*-APR-2 showed a concentration of 1.1 mg based on a BSA assay. The refolded aspartic protease was aliquoted (50 μL) and stored at -80ºC.

5.4.4.2. Catalytic cleavage of recombinant-*Na*-APR-2

The *Na*-APR-2 enzyme was incubated with hemoglobin (Hb), but no cleavage was observed within a 16-hour timeframe. As expected, no cleavage was observed in the presence of the protease inhibitor pepstatin or when Hb was incubated in isolation for 16 hours at 37°C. Figure 5.5 shows bands of non-cleavage hemoglobin from lysate A incubated with recombinant *Na*-APR-2 protein at different times displayed in the SDS-PAGE gel. This result indicates that the recombinant *Na*-APR-2 is not active, as hemoglobin was not cleaved. The lack of activity suggests that the enzyme did not refold into the native conformation.

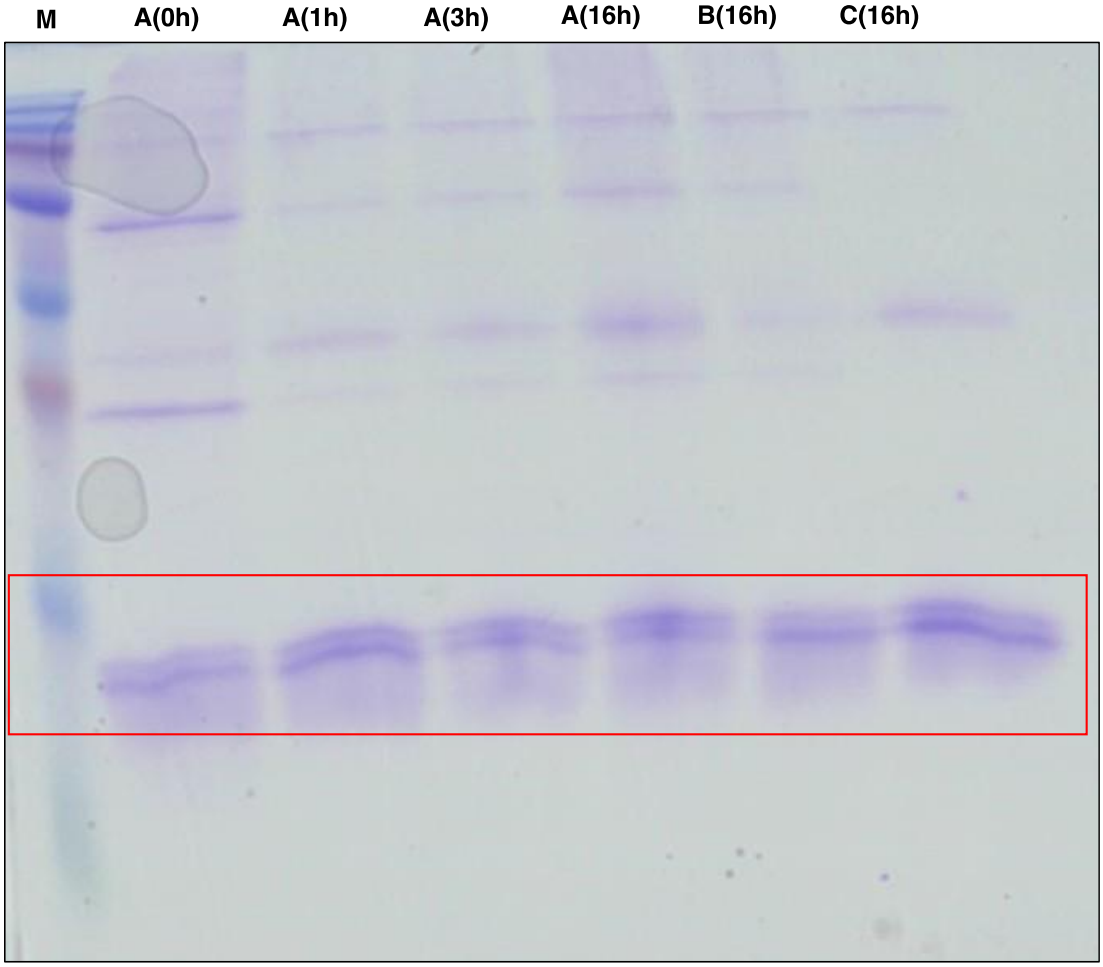

Figure 5.5: SDS–PAGE examination of incubated hydrolysates. Analysis using 12% SDS-PAGE followed by Coomassie Brilliant Blue staining. Protein marker (lane M), sample lysate A (composed of recombinant *Na*-APR-2, Hb, NaAc) shown in lane A: (0 h, 1 h, 3 h, 16 h), sample B lysate (recombinant *Na*-APR-2, Pepstatin A, Hb, NaAC) in lane B: (16 h) and sample lysate C (Hb and NaAC) in lane C: (16 h). Boxed in red is the human hemoglobin present in all incubated lysates analyses, an indication that the refolded protease (*Na*-APR2) was catalytically inactive.

5.5. Discussion

Here we show that the peptide $G_{350}Y$ from *Na*-APR-2 has potential as a hookworm vaccine candidate. The peptide induced antibody response when administered intraperitoneally combined with Imject alum adjuvant. By contrast, the peptide did not induce an antibody response when administered orally, suggesting that the peptide was degraded in the gut by digestive proteases. This lack of stability is likely to be related to the lack of secondary structure observed in the NMR analysis and is not uncommon for such as small peptide.

Structural stability is essential for peptide-based oral vaccines to avoid degradation and this generally requires a delivery system that can induce an antibody response and provide protection against digestive proteases. Studies on the *Na*-APR-1 epitope, $A_{291}Y$, with different delivery systems have been promising (14, 16). These vaccine delivery systems could be applied to $G_{350}Y$ in future for developing effective vaccine candidates against human hookworm infections.

To assess the bioactivity of the $G_{350}Y$ peptide as an inhibitor of *Na*-APR-2, the protein was recombinantly expressed. However, an enzymatic assay of recombinant *Na*-APR-2 did not show signs of Hb cleavage. This indicates *Na*-APR-2 is inactive, suggesting that the protein did not refold correctly. This could be related to unfavourable conditions experienced by the bacteria during the experiment. Previous studies have indicated that disruptions such as reduction of bacterial cytosol, lack of eukaryotic chaperones and post-translational machinery can contribute to the formation of inclusion bodies (25). Other possible contributing factors

such as temperature, inducer concentration and translational rate can affect the bacterial protein quality system leading to protein aggregation (26). The conditions used in the refolding process might also be impacting the folding of the protein and exploring a range of different buffers and additives might enhance the folding of the correct conformation. The conditions chosen in this study for refolding were based on previous studies on *Na*-APR-1 (15). The sequence differences between the two proteins appear to be having an influence of the refolding properties. Exploring a different non-mammalian expression system such as insect cells is also a possibility to solve the issue of correct folding of *Na*-APR-2 and that would be a suggestion for this project in future.

To summarize, in this study we demonstrated that a 14-residue peptide (epitope $G_{350}Y$) downsized from *Na*-APR-2 produced antibodies in mice and might have potential in the development of a vaccine against hookworm infection. The lack of antibody production when the peptide was orally administered could potentially be influenced by the use of conjugates such as those used for the *Na*-APR-1 derived peptide. Further study is also required to determine the bioactivity of the antibodies raised against the G350Y epitope of *Na*-APR-2, and understand the *in vitro* folding of *Na*-APR-2.

5.6. Acknowledgment

This work was supported by the Australian Research Council and National Health and Medical Research Council via a Future Fellowship to NLD (110100226), and a senior principal research fellowship to AL (1117504).

5.7. Reference

1. Hotez PJ, Brooker S, Bethony JM, Bottazzi ME, Loukas A, Xiao S. Hookworm infection. New England Journal of Medicine. 2004;351(8):799-807.

2. Hotez PJ, Molyneux DH, Fenwick A, Ottesen E, Ehrlich Sachs S, Sachs JD. Incorporating a rapid-impact package for neglected tropical diseases with programs for HIV/AIDS, tuberculosis, and malaria: a comprehensive pro-poor health policy and strategy for the developing world. PLoS medicine. 2006;3(5):e102.

3. Loukas A, Hotez PJ, Diemert D, Yazdanbakhsh M, McCarthy JS, Correa-Oliveira R, et al. Hookworm infection. Nature Reviews Disease Primers. 2016;2:16088.

4. Tolentino K, Friedman JF. An update on anemia in less developed countries. The American journal of tropical medicine and hygiene. 2007;77(1):44-51.

5. Jones BF, Cappello M. Hookworm infection: molecular mechanisms of disease and targets for control. Drug Discovery Today: Disease Mechanisms. 2004;1(2):217-22.

6. Albonico M, Smith PG, Ercole E, Hall A, Chwaya HM, Alawi KS, et al. Rate of reinfection with intestinal nematodes after treatment of children with mebendazole or albendazole in a highly endemic area. Transactions of the Royal Society of Tropical Medicine and Hygiene. 1995;89(5):538-41.

7. Keiser J, Utzinger J. Efficacy of current drugs against soil-transmitted helminth infections: systematic review and meta-analysis. Jama. 2008;299(16):1937-48.

8. Hotez PJ, Bethony JM, Diemert DJ, Pearson M, Loukas A. Developing vaccines to combat hookworm infection and intestinal schistosomiasis. Nature Reviews Microbiology. 2010;8(11):814.

9. Seid CA, Curti E, Jones RM, Hudspeth E, Rezende W, Pollet J, et al. Expression, purification, and characterization of the Necator americanus aspartic protease-1 (Na-APR-1 (M74)) antigen, a component of the bivalent human hookworm vaccine. Human vaccines & immunotherapeutics. 2015;11(6):1474-88.

10. Pearson MS, Bethony JM, Pickering DA, de Oliveira LM, Jariwala A, Santiago H, et al. An enzymatically inactivated hemoglobinase from Necator americanus induces neutralizing antibodies against multiple hookworm species and protects dogs against heterologous hookworm infection. The FASEB Journal. 2009;23(9):3007-19.

11. Williamson AL, Brindley PJ, Abbenante G, Prociv P, Berry C, Girdwood K, et al. Cleavage of hemoglobin by hookworm cathepsin D aspartic proteases and its potential contribution to host specificity. The FASEB Journal. 2002;16(11):1458-60.

12. Loukas A, Bethony JM, Mendez S, Fujiwara RT, Goud GN, Ranjit N, et al. Vaccination with recombinant aspartic hemoglobinase reduces parasite load and blood loss after hookworm infection in dogs. PLoS medicine. 2005;2(10):e295.

13. Xiao S, Zhan B, Xue J, Goud GN, Loukas A, Liu Y, et al. The evaluation of recombinant hookworm antigens as vaccines in hamsters (Mesocricetus auratus) challenged with human hookworm, Necator americanus. Experimental parasitology. 2008;118(1):32-40.

14. Skwarczynski M, Dougall AM, Khoshnejad M, Chandrudu S, Pearson MS, Loukas A, et al. Peptide-based subunit vaccine against hookworm infection. PLoS One. 2012;7(10):e46870.

15. Pearson MS, Pickering DA, Tribolet L, Cooper L, Mulvenna J, Oliveira LM, et al. Neutralizing Antibodies to the Hookworm Hemoglobinase Na-APR-1: Implications for a Multivalent Vaccine against Hookworm Infection and Schistosomiasis. The Journal of Infectious Diseases. 2010;201(10):1561-9.

16. Fuaad AAHA, Pearson MS, Pickering DA, Becker L, Zhao G, Loukas AC, et al. Lipopeptide Nanoparticles: Development of Vaccines against Hookworm Parasite. ChemMedChem. 2015;10(10):1647-54.

17. Skwarczynski M, Dougall AM, Khoshnejad M, Chandrudu S, Pearson MS, Loukas A, et al. Peptide-based subunit vaccine against hookworm infection. PloS one. 2012;7(10):e46870-e.

18. Bartlett S, Eichenberger RM, Nevagi RJ, Ghaffar KA, Marasini N, Dai Y, et al. Lipopeptide-based oral vaccine against hookworm infection. The Journal of Infectious Diseases. 2020;221(6):934-42.

19. Zhong W, Skwarczynski M, Toth I. Lipid core peptide system for gene, drug, and vaccine delivery. Australian journal of chemistry. 2009;62(9):956-67.

20. Moyle PM, Toth I. Self-adjuvanting lipopeptide vaccines. Current medicinal chemistry. 2008;15(5):506-16.

21. Williamson AL, Brindley PJ, Abbenante G, Datu BJ, Prociv P, Berry C, et al. Hookworm aspartic protease, Na-APR-2, cleaves human hemoglobin and serum proteins in a host-specific fashion. The Journal of infectious diseases. 2003;187(3):484-94.

22. Wishart DS, Bigam CG, Holm A, Hodges RS, Sykes BD. 1 H, 13 C and 15 N random coil NMR chemical shifts of the common amino acids. I. Investigations of nearest-neighbor effects. J Biomol NMR. 1995;5(1):67-81.

23. Daly NL, Craik DJ. Acyclic permutants of naturally occurring cyclic proteins Characterization of cystine knot and β-sheet formation in the macrocyclic polypeptide kalata B1. J Biol Chem. 2000;275(25):19068-75.

24. Wüthrich K. NMR with proteins and nucleic acids. Europhys News. 1986;17(1):11-3.

25. Carrió MM, Cubarsi R, Villaverde A. Fine architecture of bacterial inclusion bodies. FEBS letters. 2000;471(1):7-11.

26. Carrió MM, Villaverde A. Localization of chaperones DnaK and GroEL in bacterial inclusion bodies. Journal of bacteriology. 2005;187(10):3599-601.

CHAPTER 6: Conclusions and Future Directions

6.1. Conclusions

There has been a recent increase in studies aiming to explore the potential of peptides for the development of new treatments and prevention of diseases. In particular, naturally occurring peptides are providing inspiration for these studies. This thesis highlights new information regarding anti-inflammatory peptides sourced from plants and hookworms, with strategies to harness them as potential anti-inflammatory therapeutics. In addition to the anti-inflammatory peptides from hookworms, an epitope from a hookworm protein, with potential as a vaccine candidate against human hookworm infection is described in this thesis.

A major theme of this thesis was to truncate or downsize proteins to study the structure and bioactivity of the resultant peptides. This approach has previously been shown to be useful in the design of novel drug leads and vaccine candidates (1, 2, 3, 4, 5, 6) The hypotheses for Chapters 2 and 3 were based on such evidence that certain regions in a protein contribute to the function of the entire protein and truncating them could provide insight into lead molecules. The specific aims of these chapters were to design peptides and identify residues responsible for bioactivity through structure/function studies. The potential lead molecule could then be pursued in developing anti-inflammatory drugs.

The studies in Chapters 2 and 3 were successfully completed with insights gained into the structure/function relationships on lunasin derived peptides based on *in vitro* and *in vivo* assays. The downsized fragment described in Chapter 2, displayed both anti-inflammatory and

antioxidant activities. In Chapter 3, we identified a conserved sequence motif (EK Motif) present in chromatin binding proteins that appears to be responsible for anti-inflammatory activities. In addition, the lunasin derived peptides have potential for the development of novel therapeutics against neutrophils in systematic autoimmune diseases.

Interestingly, the epitope identified in Chapter 3 as potentially having anti-inflammatory activity is conserved in a family of hookworm proteins. A hookworm derived-peptide (termed ES2-10 as it is a 10-residue peptide from the hookworm protein *Ace*-ES2) containing this motif has recently been shown to mitigate the effects of colitis in a mouse model (3). However, this peptide is readily degraded in human serum. Chapter 4 explored the implications of using cyclization to stabilize ES2-10. Although the stability could be improved via cyclization with a disulfide bond, this appears to be at the expense of bioactivity. Analysis of the three-dimensional structure using NMR spectroscopy indicated that the helical region had been altered as a result of the introduction of the disulfide bond and this structural change presumably prevents binding to a biological target. We also showed that a linear extended version of ES2-10 (referred to as DGL-ES2-10) displayed a well-defined helical structure in solution with greater stability in human plasma compared to the native ES2-10. The structure of this analogue is similar to the equivalent region in the full-length protein and is likely to demonstrate activity in colitis or asthma assays. Our *in vitro* assay did not show activity probably due to storage effects on PBMCs that may have affected the cells and/or since the PBMCs derived are from different donors, the peptide might be donor specific. Nonetheless, we have designed DGL-ES2-10 with a well-defined helical structure that is stable in human serum compared to native ES2-10. This looks promising as a potential candidate for anti-inflammatory drug development but additional in vitro and in vivo assays are required.

Chapter 5 describes an epitope $G_{350}Y$ truncated from an aspartic protease (*Na*-APR-2) derived from the Excretory/Secretory (ES) products of *Necator americanus*. The objective was to downsize, synthesise and carry out structure-function analyses for a potential vaccine candidate against human hookworm. The results indicated that the epitope chosen can produce IgG-antibodies when injected IP but not generate IgA-antibodies with oral administration based on an ELISA assay. IgG are most common antibodies that are induced in the blood and other body fluids after an infection or immunisation that protects against bacterial and viral infections (7), while IgA are found in the linings of the respiratory tract and digestive system as well as in saliva (spit) and tears (7). Since the $G_{350}Y$ peptide is unstructured, it may not be able to withstand digestive proteases and therefore no IgA-antibody production would be induced via the orally administered pathway. The recombinant form of *Na*-APR-2 did not fold properly based on an enzymatic cleavage assay with human haemoglobin. Neutralisation or blocking experiments involving refolded *Na*-APR-2 with antisera or purified antibody raised from IP were not performed in this chapter due to the nonactive enzymatic activity of *Na*-APR-2.

The main outcome from Chapter 5 was that a 14-residue peptide induced antibody production following IP injection in the presence of an adjuvant. Enhancing antibody production may require structural engineering to form a more stable epitope that could generate antibodies in greater titre and also can withstand digestive proteases for orally administered epitopes.

6.2. Future Directions

The most obvious direction for future studies is to address lack of information on biological targets and mode of action of the anti-inflammatory peptides (Chapters 2-5). Studies have shown that lunasin is anti-inflammatory, but the mode of action has not been characterised. Similarly, the mechanism of action for the hookworm derived peptide (ES2-10) has also yet to be identified.

A range of approaches could be used to understand the mode of action of peptides such as LN10, including the use of alanine scanning and inflammatory disease models such as colitis, and asthma and subsequent assessment of the influences on different cells types using cytometry and other cell diagnostic tools. In particular, replacing the single cysteine may impact the activities. Similar studies could also be applied to LN9 and ES2-10. Protein arrays are also a useful for approach for identifying biological targets (8) but a screen for the ES2-10 peptide did not result in any potential hits (Daly et al, unpublished results). Consequently, other approaches such as pull-down experiments and mass spectrometry approaches might be required (9, 10). Chromatin binding studies could also be carried out for the LN9 and ES2-10 peptides based on the sequence similarity to chromatin binding proteins.

The challenges in the *in vitro* PMBC assays appear to be related, at least to some extent, to variation in donors. Although having a consistent donor supply of PBMCs could possibly improve consistency in the cytokine studies, the donor specific effects could be a limitation for future drug design studies and suggests that such peptides would only be useful for certain populations. However, this lack of consistency of drug across human populations is not unusual and is a limitation of many drugs and drug leads. The use of so called “dirty mice” (11) might be useful in subsequent studies, since these mice have more robust immune systems and this

might reflect the human population more so than the pathogen free mice often used in animal models.

Peptide stability is often a limitation in peptide drug development. This thesis demonstrated stabilisation with cyclization and extension of helical structure but highlighted implications for bioactivity. Alternative approaches such as grafting bioactive sequences into stable scaffolds is another approach that could be applied to improve the stability of the peptides studied in this thesis. This approach has been successfully used for a range of bioactive peptides through grafting into scaffolds such as the sunflower trypsin inhibitor or cyclotides (12, 13, 14). There are also a range of other approaches that can also be used to further enhance the stability of peptides such as the incorporation of non-natural amino acids, N- methylation, albumin binding tags and synthesising the mirror-image peptides. Stabilization of the *Na*-APR-2 epitope could be achieved by incorporating an LCP moiety as shown previously for the epitope $A_{291}Y$ derived from *Na*-APR-1 protein. In addition to *Na*-APR-2 epitope stability, adjustment of buffer pH and compositions to a more preferred optimal pH condition such as pH 5.0 that could potentially confirm whether the recombinant protein is active or not.

These possible future directions might help develop therapeutic peptides against various inflammatory conditions and aid in the development of a hookworm vaccine.

6.3. Reference

1. Craik DJ, Fairlie DP, Liras S, Price D. The future of peptide-based drugs. Chemical biology & drug design. 2013;81(1):136-47.

2. Carstens BB, Berecki G, Daniel JT, Lee HS, Jackson KA, Tae HS, et al. Structure–Activity Studies of Cysteine-Rich α-Conotoxins that Inhibit High-Voltage-Activated Calcium Channels via GABAB Receptor Activation Reveal a Minimal Functional Motif. Angewandte Chemie International Edition. 2016;55(15):4692-6.

3. Cobos C, Bansal PS, Wilson DT, Jones L, Zhao G, Field MA, et al. Peptides derived from hookworm anti-inflammatory proteins suppress inducible colitis in mice and inflammatory cytokine production by human cells. Frontiers in Medicine. 2022:2743.

4. Jain S, Baranwal M. Conserved peptide vaccine candidates containing multiple Ebola nucleoprotein epitopes display interactions with diverse HLA molecules. Medical Microbiology and Immunology. 2019;208:227-38.

5. Blanco E, Guerra B, Beatriz G, Defaus S, Dekker A, Andreu D, et al. Full protection of swine against foot-and-mouth disease by a bivalent B-cell epitope dendrimer peptide. Antiviral research. 2016;129:74-80.

6. Shah M, Moon SU, Woo HG. Pharmacophore-based peptide biologics neutralize SARS-CoV-2 S1 and deter S1-ACE2 interaction in vitro. bioRxiv. 2020:2020.12. 30.424801.

7. Janeway Jr CA, Travers P, Walport M, Shlomchik MJ. The distribution and functions of immunoglobulin isotypes. Immunobiology: The Immune System in Health and Disease 5th edition: Garland Science; 2001.

8. Hartmann M, Roeraade J, Stoll D, Templin MF, Joos TO. Protein microarrays for diagnostic assays. Analytical and bioanalytical chemistry. 2009;393:1407-16.

9. Louche A, Salcedo SP, Bigot S. Protein–protein interactions: pull-down assays. bacterial Protein secretion systems: methods and protocols. 2017:247-55.

10. Fletcher S, Bowden S, Marrion N. False interaction of syntaxin 1A with a Ca2+-activated K+ channel revealed by co-immunoprecipitation and pull-down assays: implications for identification of protein–protein interactions. Neuropharmacology. 2003;44(6):817-27.

11. Kuypers M, Despot T, Mallevaey T. Dirty mice join the immunologist's toolkit. Microbes and Infection. 2021;23(6-7):104817.

12. Lesner A, Legowska A, Wysocka M, Rolka K. Sunflower trypsin inhibitor 1 as a molecular scaffold for drug discovery. Current pharmaceutical design. 2011;17(38):4308-17.

13. Colgrave ML, Korsinczky MJ, Clark RJ, Foley F, Craik DJ. Sunflower trypsin inhibitor-1, proteolytic studies on a trypsin inhibitor peptide and its analogs. Peptide Science. 2010;94(5):665-72.

14. de Veer SJ, White AM, Craik DJ. Sunflower trypsin Inhibitor-1 (SFTI-1): sowing seeds in the fields of chemistry and biology. Angewandte Chemie International Edition. 2021;60(15):8050-71.

Appendices

Appendix A

Chapter 3

LN9 peptide showed inhibition of various selected cytokines in PBMCs derived from two fresh donors. The results are shown as donor 1 and donor 2.

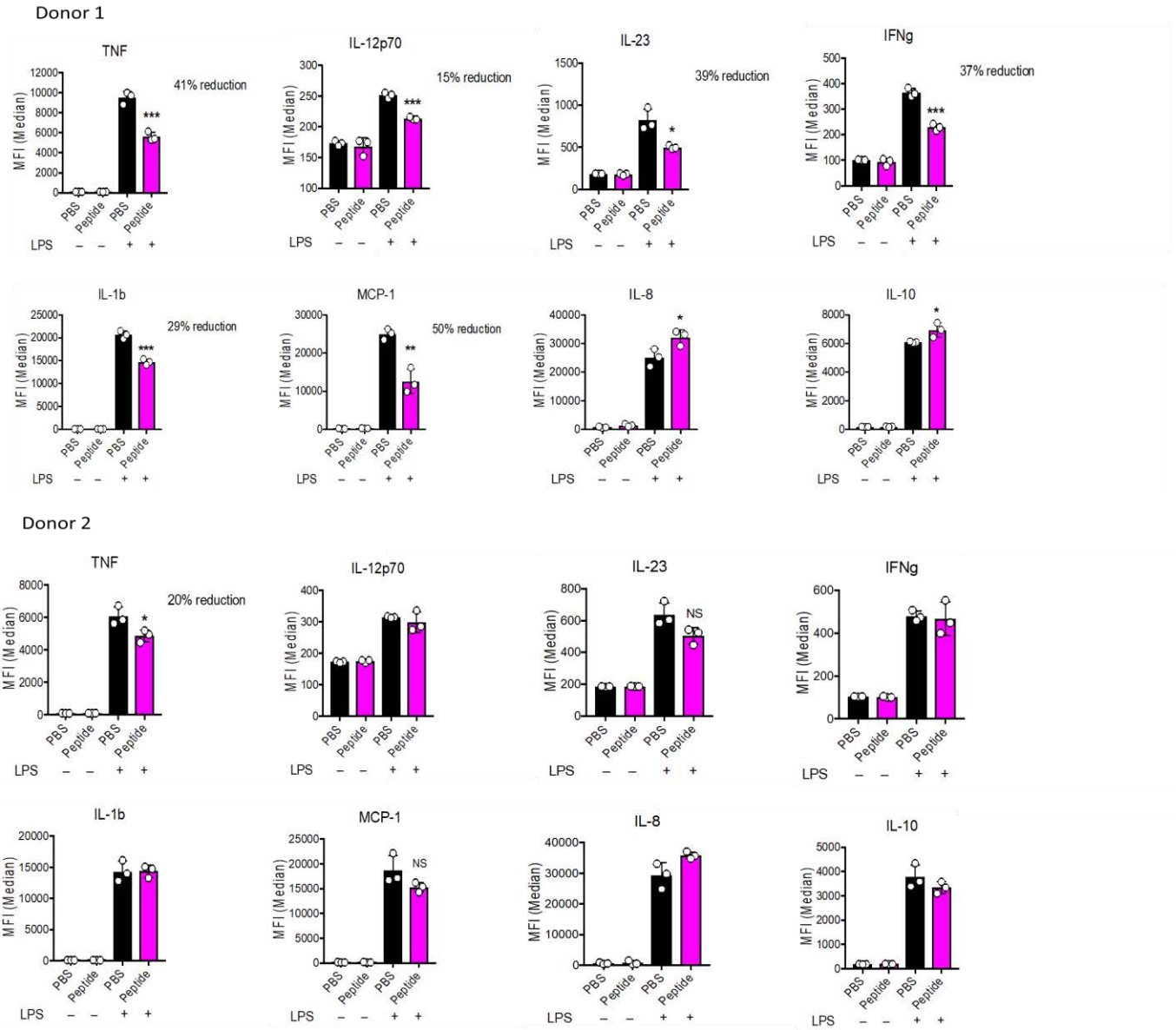

Figure B1: Reduction of cytokine released from fresh PBMCs derived from two human donors analysed using Lengendplex Kit. Donor 1 displayed a good number of cytokines being suppressed by LN9, however not donor 2 except for TNF at 75 μg/mL. TNF is reduced in both donors. Data was generated using unpaired t-test 9 displayed a two-tailed P value (***P<0.05, **P<0.01, ***P<0.0009) in GraphPad Prism 9.